Influence of Oxygen Vacancies on Oxygenate Reactions over SnO_2(110) Single Crystal Surfaces

by

Victoria A. Gercher

Dissertation submitted to the faculty of the

Virginia Polytechnic Institute and State University

in partial fulfillment of the requirements for the degree of

Doctor of Philosophy

in

Chemical Engineering

APPROVED:

David F. Cox, Chairman

Richey M. Davis

John G. Dillard

Mark R. Anderson

Brian E. Hanson

August, 1994

Blacksburg, Virginia

Influence of Oxygen Vacancies on Oxygenate Reactions over SnO_2(110) Single Crystal Surfaces

by

Victoria A. Gercher

Committee Chairman: David F. Cox

Chemical Engineering

(ABSTRACT)

The adsorption of a number of Brønsted acids of differing strengths has been studied on stoichiometric and defective SnO_2(110) surfaces. The extent of dissociation of these acids depends on the surface composition and the strength of the acid. Two crystallographically inequivalent types of oxygen vacancies can be introduced onto SnO_2(110) surfaces, and the kinetics of the reactions of Brønsted acids is influenced by the number and type of oxygen vacancies present on each surface.

The site requirement for dissociation of Brønsted acids has been described as a coordinatively unsaturated cation and an available anion. On the SnO_2(110) surfaces studied, this site requirement was seen to be a necessary but not sufficient condition for dissociation. In contradiction to the generally accepted idea that the presence of defects increases reactivity, the most defective SnO_2(110) surface considered showed the lowest activity for dissociation for all adsorbates studied.

ACKNOWLEDGEMENTS

I would like to thank my advisor, David F. Cox, for his encouragement, guidance and unfailing patience over the last four years.

I would like to thank my parents, John and Kate Gercher, and all my friends, without whom life would have been livable but not bearable.

I would like to thank the members of my committee for their time and effort.

I would like to thank DOE and the Charles M. Minor Fellowship program for financial support of my work.

I would like to thank Professor Jean-Marie Gilles, Facultés Universitaires Notre-Dame de la Paix, Namur, Belgium for providing the SnO_2(110) single crystal used in this study.

TABLE OF CONTENTS

CONTENTS

CONTENTS

LIST OF FIGURES

LIST OF FIGURES

LIST OF TABLES

Chapter 1

Introduction

1.1 Background

The use of metal oxides as heterogeneous catalysts for the selective oxidation of hydrocarbons has stimulated interest in the pathways and intermediates involved in these oxidation reactions. Various types of surface intermediates (carbonates, carboxylates, alkoxides and allylic species) in many catalytic systems have been identified. The sensitivity of these reactions to catalyst structure has been documented, with differences in reactivity for rutile and anatase forms of TiO_2 [1-3], and differences between polar and non-polar single crystal surfaces of ZnO [4,5].

Numerous studies indicate the important role of surface lattice oxygen in a reaction pathway. The degree of surface oxidation and the presence of reduced surface sites has been shown to influence both the activity and selectivity of oxide catalysts. Due to the structural sensitivity which oxide catalysts can exhibit, the details of the local structure and electronic properties of defects such as oxygen vacancies can be quite important.

SnO_2 is a component of many multi-metal oxide oxidation catalysts. One well-known use is in tin/antimony and tin/molybdenum oxide catalysts for the oxidation of propene to acrolein, the ammoxidation of propene to acrylonitrile and the oxidative dehydrogenation of butenes to 1,3-butadiene [6-11]. SnO_2 has also been used as a component for the selective isomerization of 1-butene to *cis*-2-butene [12], benzaldehyde oxidation to

benzoic acid [13], CO oxidation [14-17] and NO reduction [17-19].

The SnO_2(110) single crystal surface is a useful model system for the study of oxidation reaction pathways. Previous characterization work on SnO_2(110) [20] has shown that the surface may be manipulated by oxidation/reduction treatments to selectively introduce two types of crystallographically inequivalent oxygen vacancies. This allows a characterization of (1) anion vacancies, (2) the importance of surface cation coordination and (3) adsorption sites for hydrocarbon oxygenate reactions over SnO_2. It also allows the study of acid/base properties of the surface and the importance of local surface properties in controlling the acid/base interaction of adsorbates with the surface. Hydrocarbon oxygenate molecules are used to increase understanding of the interactions of the potential intermediates in oxidation reactions.

The focus of this dissertation is on the interaction of a variety of C_1-C_3 hydrocarbons and oxygenates with four SnO_2(110) surfaces which can be easily prepared. The oxygenates used are seen to dissociate to species which range over the types of intermediates observed in oxidation reactions. The objectives of the work were (1) to study reaction pathways on SnO_2(110) surfaces, (2) to determine the effect of anion vacancies on activity and selectivity, (3) to study the dependence of the reactions on surface structure, and, to a lesser extent, (4) to understand the role of two inequivalent forms of lattice oxygen in the formation of surface intermediates.

Methanol dissociation and oxidation was studied to monitor alkoxide formation and decomposition, and to test site requirements for the

reaction of this Brønsted acid. This study is presented in Chapter 2 [21]. Formic acid decomposition was studied to observe carboxylate formation and reaction, and to contrast its behavior with methanol, a weaker acid. This study is presented in Chapter 3 [22]. Water adsorption was studied for several reasons. There is a general interest in the interaction of water with oxide surfaces [3,23] due to the generally observed phenomenon of hydroxylation. Also, water is often seen as a product of oxidation reaction on oxides, including the methanol and formic acid reactions on SnO_2 mentioned above. Also, it was desired to compare a molecule with a similar acidity to methanol. This study is presented in Chapter 4 [24].

The reaction of isopropanol with $SnO_2(110)$ was studied to test higher alkoxide formation and decomposition, and to compare the behavior of a secondary alcohol with methanol. Also, isopropanol is traditionally used as an acid/base probe reaction [25-28]. This study is presented in Chapter 5 [29]. Propene adsorption was studied to observe olefin functionality and also to find the desorption-limited behavior. This study is presented as Chapter 6 [30].

1.2 Surfaces Investigated

SnO_2 has the cassiterite (rutile) structure. The ideal, stoichiometric $SnO_2(110)$ surface is illustrated in Figure 1.1(a). This ideal surface is nonpolar and exposes five-coordinate Sn^{4+} cations in the second atomic layer (one coordination vacancy). All second layer "in-plane" O^{2-} anions are fully (three) coordinate. The outer atomic layer is composed of two-coordinate anions (one coordination vacancy) which occupy bridging

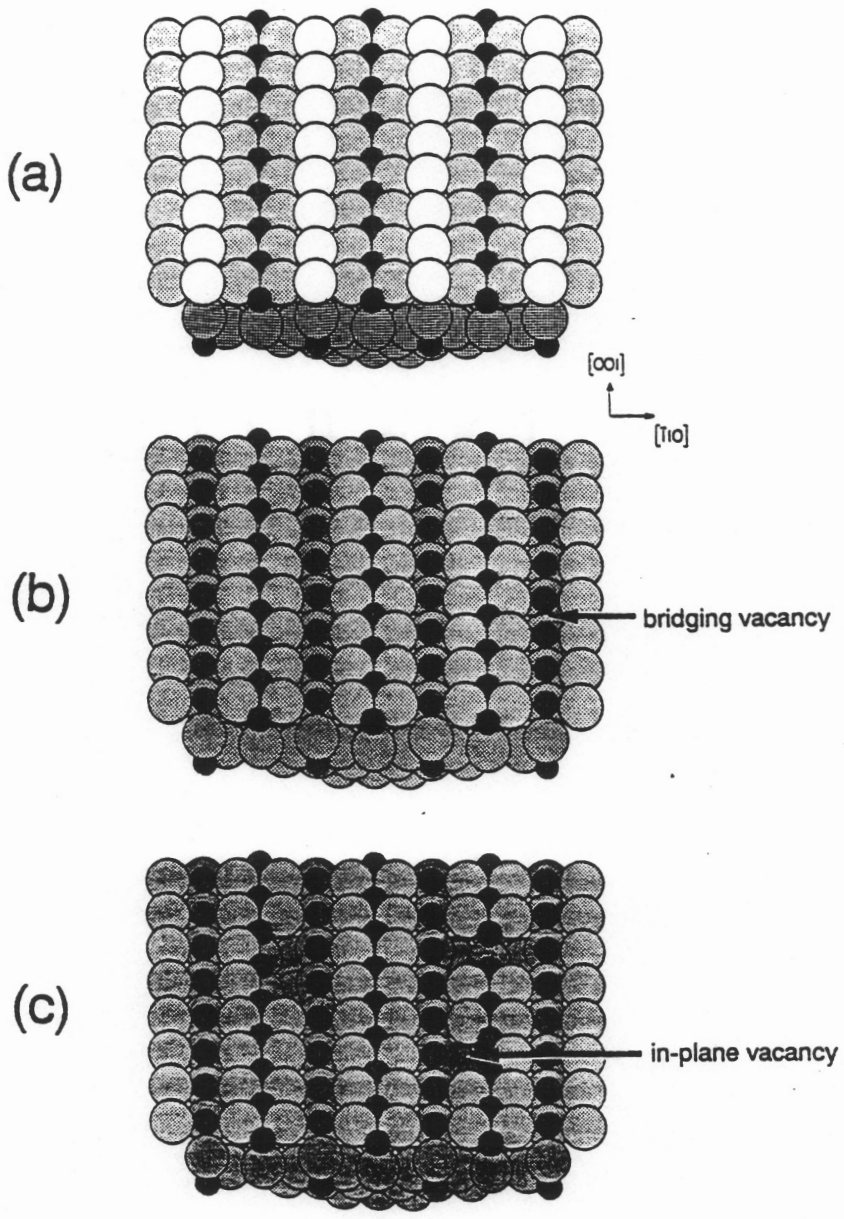

1.1 Ball model illustrations of: (a) the ideal, stoichiometric $SnO_2(110)$ surface, (b) the "reduced" surface missing all bridging oxygen anions and (c) the "defective" surface with in-plane oxygen vacancies. The small solid circles represent Sn cations while the large open circles represent O^{2-} anions. Increased shading of the oxygen anions represents increased depth away from the surface. The illustrations assume no relaxation.

positions between otherwise inaccessible, fully (six) coordinate, second layer Sn^{4+} cations. It was shown previously that a well-oxidized, nearly stoichiometric (110) surface can be reproducibly prepared from an oriented crystal by oxidation at 700 K in 1.0 Torr O_2 [20].

Heating the stoichiometric surface (Fig. 1.1(a)) in vacuum to anions as illustrated in Fig. 1.1(b) and leaves two in-plane oxygen anions per surface unit cell. This was demonstrated using ion-scattering spectroscopy (ISS) [20]. The coordination of the newly exposed tin cations associated with the "bridging" oxygen vacancies drops from six to four, with an apparent change in oxidation state from Sn^{4+} to Sn^{2+} [20,31,32]. Tight-binding, total-energy calculations for this surface suggest that the removal of the bridging oxygen anions is accompanied by a small "rumple" of the surface layer with the surface tin cations remaining in approximately their bulk positions [33]. The predicted relaxation is small because the surface topology forbids bond-length-conserving motions of the surface atoms [33]. For notational convenience this surface condition will be referred to as the "reduced" surface as in Ref. [33].

Further heating to temperatures above 700 K removes some in-plane oxygen anions from what was initially the second atomic layer as illustrated in Fig. 1.1(c) [20], again demonstrated by ISS. This treatment reduces the coordination of the neighboring cations from five and four coordinate to four and three coordinate, respectively. This condition will be referred to as the "defective" surface for notational convenience. [Note that the "reduced" and "defective" designations for the different surface

conditions are inexact since the two surface conditions are, in fact, both reduced and defective in comparison to the stoichiometric surface.] The temperatures up to 700 K removes only the top-layer, bridging oxygen concentration of in-plane vacancies (as in Fig 1.1(c)) is strongly dependent on the immediate sample history. Oxidation prior to high temperature (950 K) annealing produces a less oxygen-deficient surface than ion bombardment and high temperature annealing alone as demonstrated clearly in a previous ISS study [34]. Work to date to find a reasonable method of quantifying in-plane oxygen vacancies (e.g. titration with gas-phase probe molecules such as CO [35]) has been ineffective. As discussed previously [20,34], electron spectroscopies have not proven to be particularly useful in this endeavor.

All the compositional changes described above occur with no change in the surface periodicity from the (1x1) LEED pattern expected and observed for the stoichiometric surface. Full details of the surface characterization are given elsewhere [20].

1.3 Experimental

All experiments were conducted in a turbopumped, dual-chamber stainless steel ultrahigh vacuum system. The analysis chamber is equipped with a Leybold EA-II hemispherical analyzer, a dual anode Mg/Al x-ray source for x-ray photoelectron spectroscopy (XPS) and a differentially-pumped DC discharge lamp for ultraviolet photoelectron spectroscopy (UPS). All XPS spectra are referenced to a Sn $3d_{5/2}$ binding energy of 486.4 eV for SnO_2 [36]. The reported binding energies are

determined with a precision of ±0.1 eV typical for XPS. UPS data were collected at an analyzer resolution (ΔE) of 0.15 eV, an incident angle of 55° with respect to the surface normal for unpolarized HeI and HeII radiation, and normal emission. The preparation chamber is equipped with Vacuum Generators 3-grid reverse view LEED optics, and an Inficon Quadrex 200 mass spectrometer for thermal desorption spectroscopy (TDS).

Gas exposures were performed by backfilling the chamber through a variable leak valve. For TDS experiments, a 2 K/s linear temperature ramp was used. This low heating rate was used to reduce the possibility of thermal fracture of the ceramic SnO_2 sample. The mass spectrometer was equipped with a quartz skimmer to minimize the sampling of desorption products from the crystal support hardware. Six mass numbers were monitored simultaneously. All desorption traces have been corrected for the mass spectrometer sensitivity [procedure described in Appendix 1], and all doses have been corrected for ion gauge sensitivity. The background pressure between doses was less than 2×10^{-10} Torr. During TDS experiments, no H_2 desorption was detected; however, the background of hydrogen in the vacuum system was such that some H_2 desorption may have gone undetected. Several TDS runs were done for each molecule studied on each surface; the results were reproducible to within 10%.

The sample used in this study was cut from the side of a hollow, needle-shaped SnO_2 single crystal grown by the vapor-phase transport method of Thiel and Helbig [37]. The crystal was oriented by Laue

backreflection and mechanically polished to within 1° of the (110) surface. The resulting sample was approximately 7x3x½ mm^3. The sample was mounted on a tantalum holder which provided mechanical stability and acted as an indirect heating and cooling source. The holder was supported by two 1 mm tantalum wires connected to LN_2-cooled copper electrical feed-throughs in a sample rod manipulator. Sample temperature was monitored by a type K thermocouple. The thermocouple was bonded directly to the back of the SnO_2 crystal with Aremco #569 ceramic cement through a small hole in the tantalum holder, thus allowing a direct measure of the sample temperature. Ion bombardment performed on the sample was done using 3 keV Ar ions for 30 minutes.

Oxidation treatments for this study have been performed using N_2O (Matheson SCF purity, 99.995%) as an oxidant [21] rather than O_2 as used in the previous studies [20]. The stronger oxidant N_2O allows us to produced a stoichiometric surface at a reduced pressure (from 1.0 Torr with O_2 to 0.1 Torr with N_2O) while maintaining the same 700 K oxidation temperature. The primary benefit is a much faster pump-down time: 10 min. to $3x10^{-9}$ Torr for N_2O versus greater than 1 hour to reach the low 10^{-8} Torr range with O_2. The less than 1 ppm level of water typically found in research grade oxygen (which represents a greater than 100 L dose of H_2O in the vacuum system after an O_2 oxidation at 1.0 Torr for several minutes) is responsible for the different pump-down times. Note that the major contaminants from N_2O are N_2, O_2, CO, CO_2 and CH_4, all of which are more easily pumped than water. Hence, N_2O is a "cleaner" oxidant for use with vacuum systems.

Of the high pressure oxidation treatments, neither N_2O nor O_2 is compatible with cold hardware at LN_2 temperatures. Because N_2O is easily condensed (it is purchased as a liquid at room temperature and 745 psig), it collects in large amounts on any LN_2-cooled surfaces during the 0.1 Torr oxidation treatment. We found that an LN_2-cooled cryopanel or manipulator hardware exposed during the oxidation treatment would collect sufficient N_2O that the system would outgas in the 10^{-4} Torr range for several hours until the cold hardware warmed to near room temperature. Hence, to reduce the pressure for thermal desorption runs to reasonable levels (low to mid 10^{-10} Torr range) and in reasonable times (~30 min.) following an oxidation treatment, typically only one oxidation treatment could be run per day. Similar problems were encountered when using O_2 as an oxidant, presumably because of the uptake of water. Cryopanels and sample cooling hardware were always cooled with LN_2 *following* sample oxidation and chamber evacuation.

A typical oxidation treatment was performed as follows: a previously ion bombarded and 1000 K annealed (1x1) surface initially at room temperature was exposed to 0.1 Torr of N_2O, the sample was heated to 710 K at a rate of 2 K/s, held for 2 min., then cooled back to a maximum temperature of 310 K (approximately 15 min.) before the chamber was evacuated. After the chamber pressure decreased to $3x10^{-9}$ Torr (about 10 min.), LN_2 was admitted to the chamber cryopanel which reduced the pressure to about $4x10^{-10}$ Torr in approximately 10 min.

No water desorption traces are reported from stoichiometric

surfaces because of interference on this surface from the uptake of background water. The initial cool down time to 170 K following an oxidation treatment is typically about 30 min. TDS blank runs (no dose) indicate that the surface uptakes an amount of water equivalent to about a 1/8 L (L = Langmuir = 10^{-6}Torr·sec) H_2O dose at 170 K (i.e., less than or equal to 0.13 ML (ML = monolayer) of water, assuming a unity sticking coefficient) [24]. The total coverage of contaminant water is small, and has little effect on the adsorption and reaction of dosed molecules, as indicated by the lack of influence of the total amount of water evolution on the TDS behavior in repeated runs for the molecules studied. However, this uptake makes a significant contribution to the total water signal observed, from 1/3 to 1/2, after the formation of water during reaction of dosed molecules.

1.4 References

1. G. Ramis, G. Busca and V. Lorenzelli, *J. Chem. Soc. Farad. Trans. 1,* **83**(1987)1591.
2. G.C. Bond, A.J. Sarkany and G.D. Parfitt, *J. Catal.,* **57**(1979)476.
3. V.E. Henrich, *Reports on Progress in Physics,* **48**(1985)1481.
4. K. Lui, S. Akhter and H.H. Kung, *Solid State Chemistry in Catalysis,* **12**(1985)206.
5. J.M. Vohs and M.A. Barteau, *J. Phys. Chem.,* **95**(1991)297.
6. D.J. Hucknall, Selective Oxidation of Hydrocarbons, (Academic Press, New York, 1974).
7. S. Tan, Y. Moro-oka and A. Ozaki, *J. Catal.,* **17**(1970)125, 132.
8. J. Buiten, *J. Catal.,* **10**(1968)188.
9. V.I. Lazukin, M.Y. Rubanik, Y.V. Zhigailo, A.A. Kurganov and Z.F.

9. V.I. Lazukin, M.Y. Rubanik, Y.V. Zhigailo, A.A. Kurganov and Z.F. Buteiko, *Katal. Katal., Akad. Nauk. SSR, Resp. Mezhvedom. Sb.,* **No. 2**(1966)50.

10. V.I. Lazukin, V.M. Belousov and M.Y. Rubanik, *Ukr. Khim.,* **32**(1966)231.

11. G.W. Godin, C.C. McCain and E.A. Porter, In *Proceedings of the 4th International Congress on Catalysis,* Moscow, 1968, D.A. Kazanaskii, ed. (Akademiai Kaido, Budapest, 1971).

12. M. Itoh, H. Hattori and K. Tanabe, *J. Catal.,* **43**(1976)192.

13. W.M.H. Sachtler, *Catal. Rev.,* **4**(1970)27.

14. M.J. Fuller and M.E. Warwick, *J. Catal.,* **29**(1973)441.

15. G.C. Bond, L.R. Molloy and M.J. Fuller, *J.C.S. Chem. Commun., 1975* 796.

16. G.C. Bond, M.J. Fuller and L.R. Molloy, *Proc. Int. Congr. Catal. 6th,* **1**(1977)356.

17. B. Hori, N. Takezawa and H. Kobayashi, *J. Catal.,* **80**(1983)437.

18. M. Niwa, T. Minami, H. Kodama, T. Hattori and Y. Murakami, *J. Catal.,* **53**(1978)198.

19. F. Solymosi and J. Kiss, *J. Catal.,* **41**(1976)202.

20. D.F. Cox, T.B. Fryberger and S. Semancik, *Phys. Rev. B,* **38**(1988) 2072.

21. V.A. Gercher, D.F. Cox and J.-M. Themlin, *Surf. Sci.,* **306**(1994) 279.

22. V.A. Gercher and D.F. Cox, *Surf. Sci.,* **312**(1994)106.

23. J.M. McKay and V.E. Henrich, *Phys. Rev. B,* **32**(1985)6764.

24. V.A. Gercher and D.F. Cox, *Surf. Sci.,* SUBMITTED.

25. K. Tanabe, Solid Acids and Bases (Academic Press, New York, 1970).

26. M. Ai, *Bull. Chem. Soc. Jpn.,* **50**(1977)2579.

27. M. Bowker, R.W. Petts and K.C. Waugh, *J. Catal.,* **99**(1986)53.

28. J.M. Vohs and M.A. Barteau, *Surf. Sci.,* **221**(1989)590.

29. V.A. Gercher and D.F. Cox, *J. Phys. Chem.,* MANUSCRIPT IN PREPARATION.

30. V.A. Gercher and D.F. Cox, unpublished propene TDS results on SnO_2(110).

31. P.A. Cox, R.G. Egdell, C. Harding, W.R. Patterson and P.J. Tavener, *Surf. Sci.,* **123**(1982)179.

32. J.-M. Themlin, R. Sporken, J. Darville, R. Caudano, J.-M. Gilles and R.L. Johnson, *Phys. Rev. B,* **42**(1990)11914.

33. T.J. Godin and J.P. LaFemina, *Phys. Rev. B,* **47**(1993)6518.

34. D.F. Cox, T.B. Fryberger and S. Semancik, *Surf. Sci.,* **224**(1989) 121.

35. V.A. Gercher and D.F. Cox, unpublished CO TDS data for SnO_2(110).

36. C.D. Wagner, W.M. Riggs, L.E. Davis, J.F. Moulder and G. G. Muilenberg, Handbook of X-ray Photoelectron Spectroscopy (Perkin-Elmer, Eden Prairie, 1979).

37. B. Thiel and R. Helbig, *J. Cryst. Growth,* **32**(1976)259.

Chapter 2

Oxygen-Vacancy-Controlled Chemistry on a Metal Oxide Surface: Methanol Dissociation and Oxidation on SnO_2(110)

2.1 Introduction

Recent studies of the reactions of Brønsted acids on oriented metal oxide single crystals have allowed the testing of previously existing ideas regarding site requirements for reactions on oxide surfaces, and have led also to a number of interesting new discoveries. The site requirements for the dissociation of Brønsted acids have long been described as involving acid/base (i.e., cation/anion) site pairs. This principle is convincingly demonstrated by the reactivity differences of a variety of Brønsted acids on the Zn-terminated and O-terminated (0001) polar surfaces of ZnO [1-8]. These studies on ZnO single crystal surfaces have helped define the coordination requirements for surface cations and anions in the heterolytic dissociation of acids [9]. The critical requirements are coordinatively unsaturated surface cations, while the coordination environment of the participating oxygen anions apparently is much less critical [9]. These requirements are also consistent with the available data for MoO_3(010) [10,11], MgO(100) [12,13] and TiO_2(001) surfaces [14-16].

Besides the site requirements for the dissociation of Brønsted acids, the subsequent products formed by the reactions of the adsorbed conjugate base anions can also be affected by the extent of coordinative unsaturation of the surface cations. Several bimolecular coupling

reactions requiring two coordination vacancies on Ti^{4+} cations have been observed by Barteau and co-workers on the {114}-faceted TiO_2(001) surface. These reactions include the formation of ethers from surface alkoxides [15] and the formation of ketones from surface carboxylates [14,16]. Such observations have led to an interesting comparison of the TiO_2 surface chemistry to that of mononuclear metal complexes in solution [9]. Hence, the use of concepts from coordination chemistry to develop principles of surface reactivity for oxides has been recognized [9].

Like the previous work on faceted TiO_2(001) surfaces, SnO_2(110) provides an opportunity to study the effects of variations in surface cation and anion coordination number on oxide surface chemistry. However, unlike TiO_2(001) which allows one to access coordination differences via surface faceting, the SnO_2(110) surface may be manipulated by oxidation/reduction treatments to selectively introduce two types of crystallographically inequivalent oxygen vacancies (i.e., point defects) without a change in the surface periodicity [17].

2.2 Experimental

Gas exposures were performed by backfilling the chamber through a variable leak valve. Aldrich HPLC Grade methanol (99.9%) was degassed by repeated freeze-pump-thaw cycles prior to use. The reported formaldehyde desorption traces were obtained from the m/z 29 trace by subtracting the methanol contribution using the m/z 31 signal characteristic of methanol. All doses have been corrected for ion gauge sensitivity [22].

2.3 Results

2.3.1 Thermal Desorption Spectroscopy

Variations in the adsorption and reaction of methanol were examined by TDS for all the surface preparations described in Chapter 1. The only desorption products besides methanol observed in TDS were formaldehyde (H_2CO) and water. Other products tested for but not detected were formic acid, CH_4 (for evidence of CO bond breaking), dimethyl ether (CH_3OCH_3) and methyl formate ($HCOOCH_3$) (as possible products of bimolecular surface reactions), and CO and CO_2 (as non-selective oxidation products). Hence, methanol oxidation was completely selective to formaldehyde, but the conversion and kinetics of the rate-limiting surface reaction step were dependent on surface condition as shown below. Table 1 lists typical values for the conversion of methanol observed for the different surface conditions. Note that since formaldehyde is the only carbon-containing reaction product, the conversion gives a measure of the fractional yield of formaldehyde.

2.3.1.1 Stoichiometric Surface

Figure 2.1 shows the TDS data obtained following an 0.6 L dose of methanol on a stoichiometric SnO_2(110) surface at 170 K. Three features are apparent in the methanol desorption trace: a high-temperature shoulder near 450 K, a main desorption feature at 310 K, and a low-temperature feature near 215 K. Formaldehyde is evolved as a reaction-limited product at 450 K [24]. For the 0.6 L dose shown in Figure 2.1, the methanol

Table 1. Fractional Conversion of 0.6 L Doses at 170 K as a Function of Surface Condition.

Surface Condition	Conversion
Stoichiometric	10-20%
Reduced	40-50%
Less Defective	20-50%
Highly Defective	< 5%

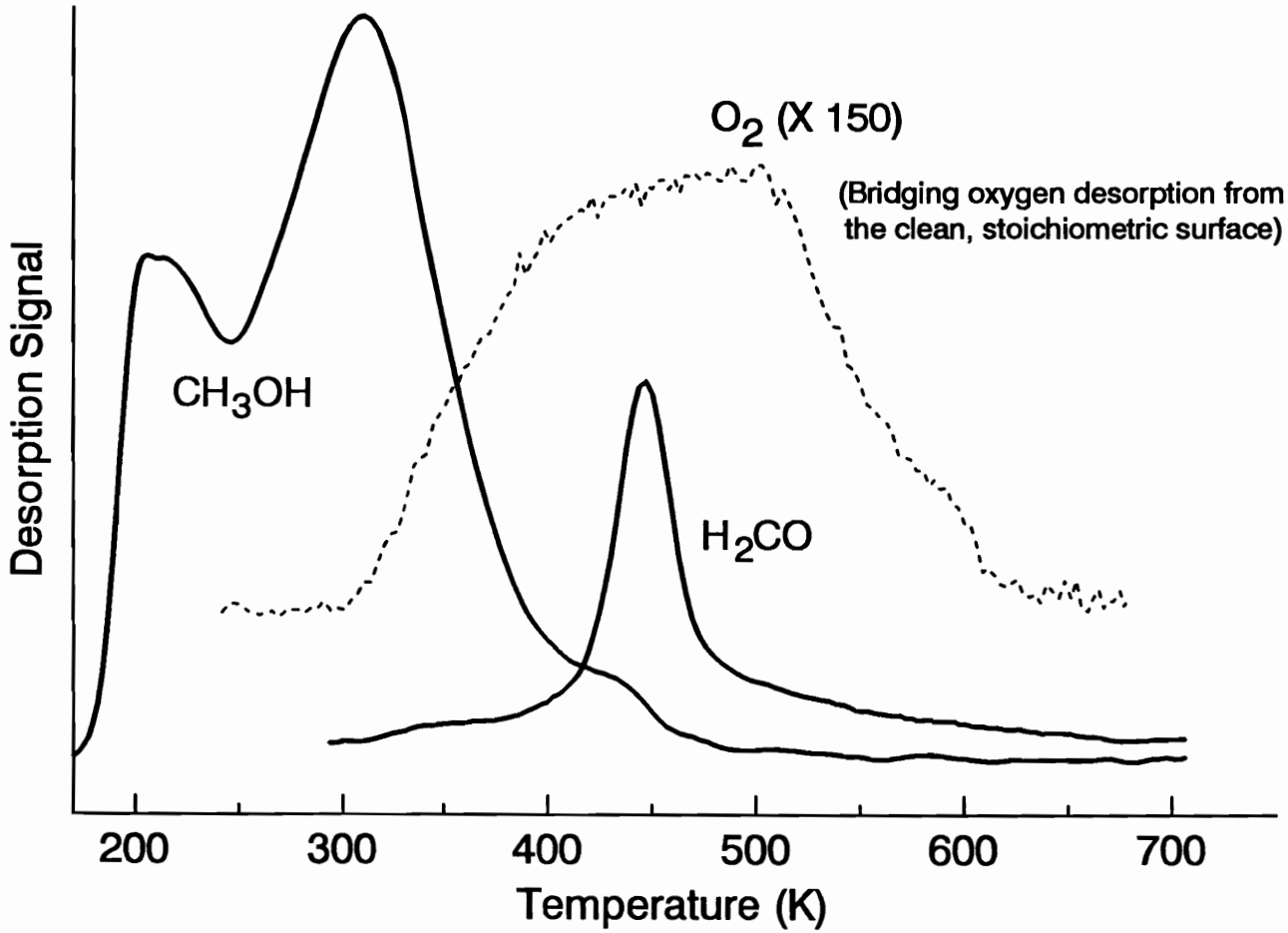

Fig. 2.1 Thermal desorption spectra following a 0.6 L dose on the stoichiometric surface at 170 K. The water desorption signal is not shown (see text for details). Also shown for comparison as a dashed line is O_2 desorption from a clean surface characteristic of the thermal removal of bridging oxygen anions.

conversion to formaldehyde is 11%, but run-to-run variations give conversions in a range of about 10% to 20%.

The simultaneous desorption of formaldehyde and methanol near 450 K is a characteristic fingerprint of a rate-limiting step for the decomposition of surface methoxide (CH_3O^-) via a unimolecular hydride elimination to form formaldehyde [25], $CH_3O^- \rightarrow H^- + CH_2O$. Using the Redhead equation [26] (see Appendix 1 for details) and assuming a normal first-order pre-exponential (10^{13} sec^{-1}) gives an activation energy of 28.5 kcal/mol for methoxide decomposition. The methanol feature at 215 K is attributed to the desorption of a molecular adsorbate (i.e., associatively adsorbed methanol) by virtue of the low desorption temperature, while the feature near 450 K is clearly associated with the recombination of methoxide and hydrogen (i.e., dissociatively adsorbed methanol) as described above, $CH_3O^- + H^+ \rightarrow CH_3OH$. The surface species associated with the intermediate (310 K) methanol desorption feature is more difficult to assign and falls in a temperature range attributed to methanol desorption from both molecular and dissociated species over other oxide surfaces. The assignment of the intermediate methanol desorption state will be addressed below with the aid of photoemission data.

Based on the relative maximum intensities of the methanol and formaldehyde desorption signals near 450 K in TDS, it is estimated that about 13% of the evolved C_1 products (methanol and formaldehyde) originate from methoxide in the 450 K desorption channel on the stoichiometric surface. For the two available pathways for methoxide

removal (H/methoxide recombination to methanol and methoxide decomposition to formaldehyde) it is estimated that a recombination to decomposition ratio of about 0.2 for the stoichiometric surface, again using the relative maximum intensities of the desorption signals near 450 K. In general, it would be better to use integrated intensities to evaluate such a ratio. Unfortunately, since the methanol recombination feature overlaps lower-temperature contributions such an approach is not practical.

Also shown in Figure 2.1, as a dashed line, is a representative O_2 desorption trace from a clean (no methanol dosed), oxidized, nearly-stoichiometric surface. The O_2 desorption below 700 K is characteristic of the thermal removal of bridging oxygen anions from the stoichiometric surface, and indicates that the surface condition changes during the course of a TDS run from a stoichiometric to a reduced surface as demonstrated in an earlier ISS investigation [17]. Note that the introduction of some bridging oxygen vacancies is anticipated before all the adsorbed methanol is removed. The O_2 signal from the clean surface is small, apparently indicating a significant angular dependence to the desorption. Hence, it is not possible to separate the small O_2 signal from the 32 amu signal for the parent mass of methanol in a methanol TDS run.

2.3.1.1 Reduced Surface (Oxidized, 700 K-Annealed)

TDS of methanol was also examined on the reduced surface (surface shown in Figure 1.1b) to investigate the effect on the surface chemistry of removing the bridging oxygen anions. As before, a 0.6 L

dose of methanol and a surface temperature of 170 K was used. Figure 2.2 shows two primary features for methanol: a feature near 310 K, and a high-temperature feature above 400 K. The total methanol uptakes for Figures 2.1 and 2.2 vary by less than 10%, hence the lack of a low-temperature desorption state (215 K) from the reduced surface indicates a significant difference in the interaction of methanol with this surface. This observation is confirmed by the intensity of the formaldehyde desorption signal, again at 450 K and associated with methoxide decomposition, which is indicative of a higher conversion of methanol to oxidation products. Typical values for the conversion of methanol on this starting surface fall in the range of 40-50%, significantly higher than from the stoichiometric surface. Some tailing of the formaldehyde desorption signal to higher temperatures is also observed. From the TDS data it is estimated that about 70% of the evolved C_1 products (methanol and formaldehyde) originate from methoxide in the 450 K desorption channel on the reduced surface compared to about 13% on the stoichiometric surface. Also, the branching ratio for the two reaction pathways for methoxide removal is different for the two surfaces. We estimate a recombination to decomposition ratio of about 0.5 for the reduced surface compared to about 0.2 for the stoichiometric surface.

2.3.1.1 Defective Surfaces

Figure 2.3 illustrates the methanol thermal desorption behavior from two different defective surfaces. The right panel in Figure 2.3 is characteristic of a surface prepared by oxidation followed by annealing to

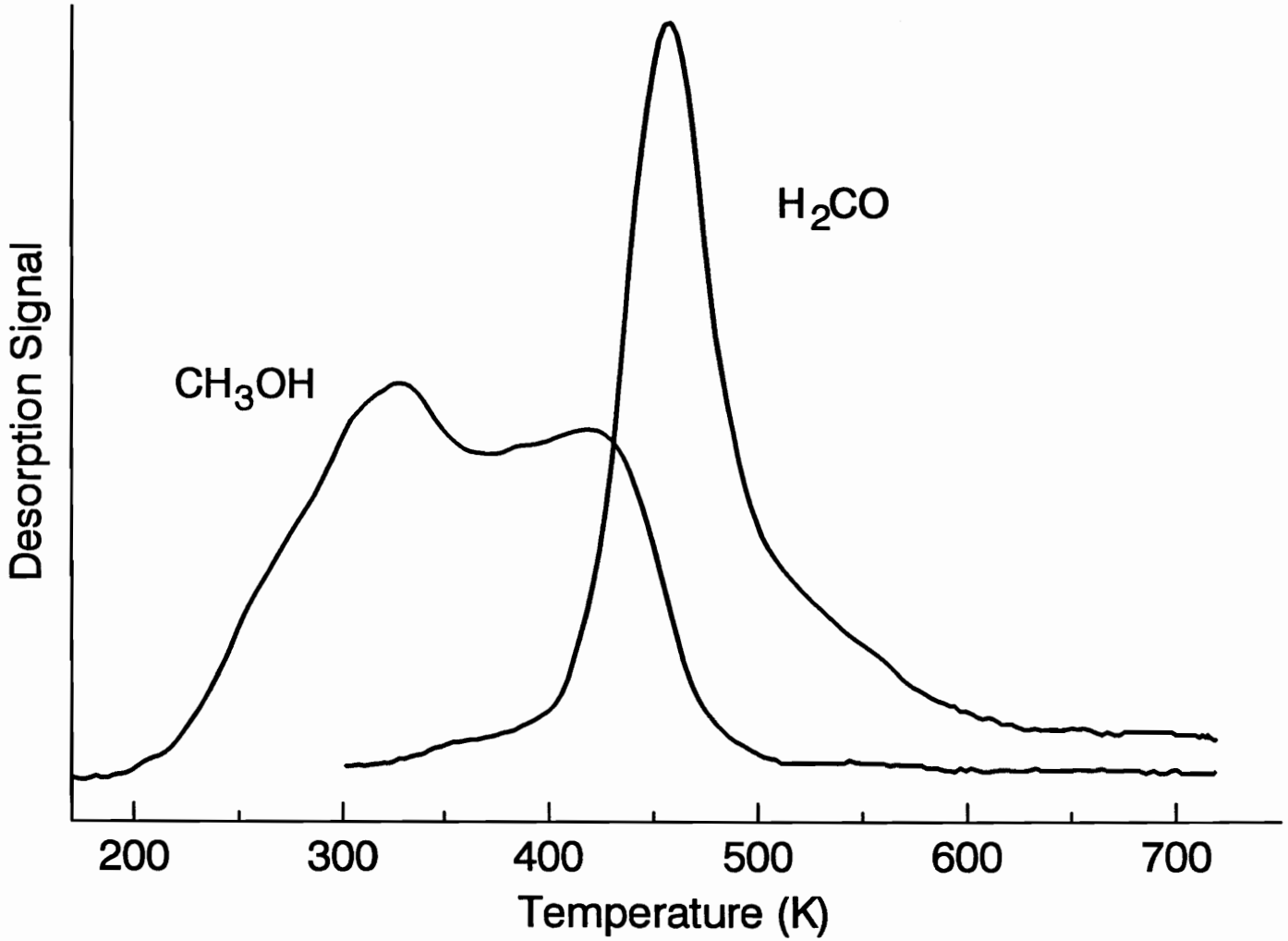

Fig. 2.2 TDS spectra following a 0.6 L dose on the "reduced" surface at 170 K.

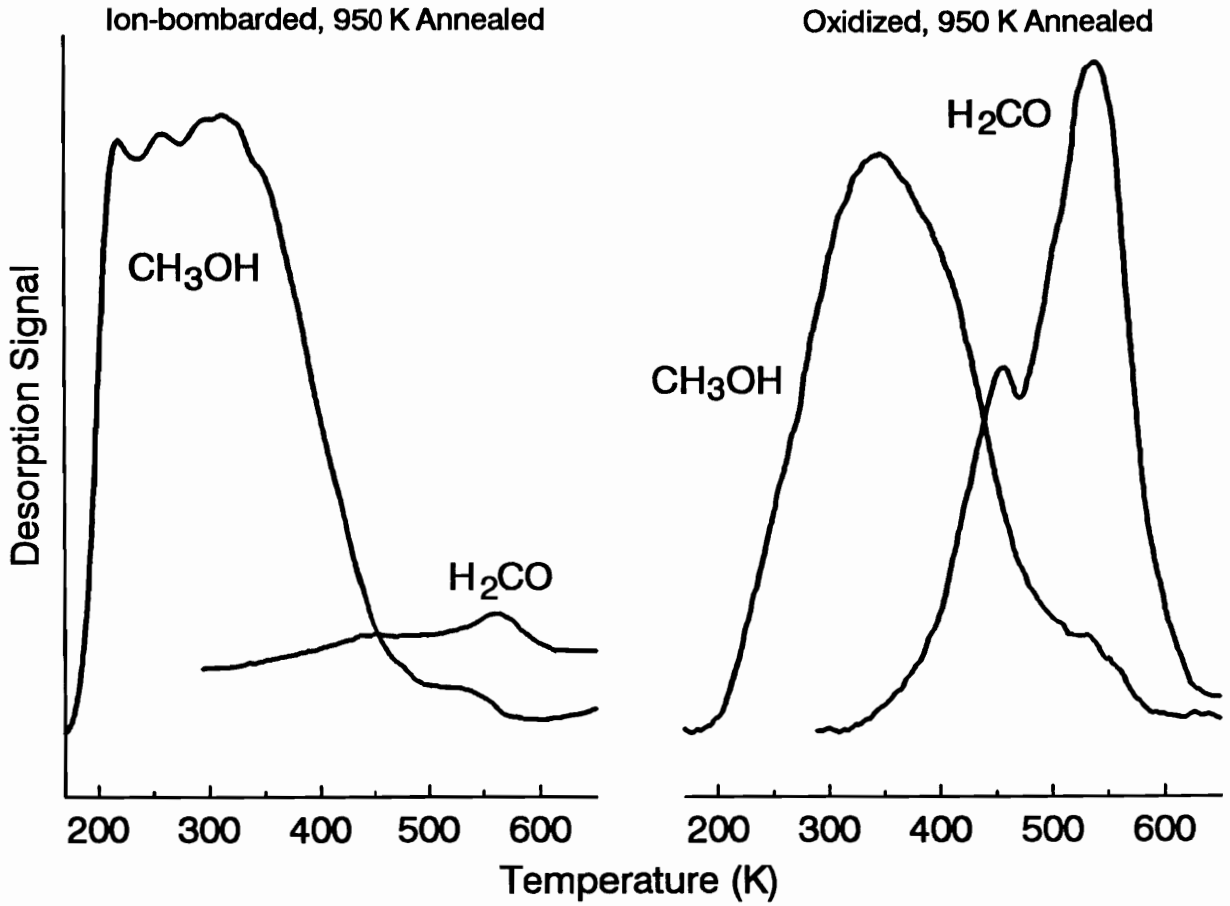

Fig. 2.3 TDS spectra following 0.6 L doses on the "defective" surface at 170 K. The panel on the right is characteristic of a slightly defective surface prepared by oxidation and annealing to 950 K. The panel on the left is characteristic of a highly-defective surface prepared by ion bombardment and annealing to 950 K. The relative scaling of the signal intensity for the two panels is arbitrary.

950 K to remove bridging oxygen anions and introduce in-plane oxygen vacancies. The left panel in Figure 2.3 is characteristic of a surface prepared by ion bombardment and annealing to 950 K. This second preparation gives a surface more oxygen deficient than the first [17,21]. In both cases, 0.6 L doses at 170 K surface temperatures were used.

For the less-defective surface (right panel), two features are observed in the methanol desorption trace: a broad feature centered near 350 K and a shoulder near 540 K. Formaldehyde is evolved as a reaction limited product in two temperature ranges: near 450 K (as on the stoichiometric and reduced surfaces) and also at 540 K. The simultaneous desorption of formaldehyde and methanol at 540 K is characteristic of the decomposition of surface methoxide, similar to the previous assignment for the 450 K desorption channel. Applying the Redhead equation gives a first-order activation energy of 34.2 kcal/mol assuming a normal first-order pre-exponential of 10^{13} sec^{-1} [26]. The conversion for the particular run in Figure 2.3 is 42%, but typical conversions for 0.6 L doses following this surface preparation vary between 20-50%.

For the more defective surface prepared by ion bombardment and annealing (left panel), the conversion of methanol following an 0.6 L dose at 170 K is significantly lower, less than 5%, indicating that a sufficiently high concentration of in-plane vacancies shuts down the oxidation chemistry. Broad, overlapping methanol desorption features are observed with components at temperatures less than 300 K and near 310 K. A small, high-temperature shoulder is also observed near 540 K. The small amount of reaction-limited formaldehyde is evolved at temperatures similar

to those observed on the less-defective surface: near 450 K and 550 K.

Since a reasonable method is not yet available for quantifying the number of in-plane oxygen vacancies produced by a given set of thermal treatments, the methanol oxidation reaction was used to introduce in-plane defects chemically. An estimate of the variation in the in-plane vacancy concentration is made by assuming that oxidation of one molecule of methanol produces one molecule of formaldehyde and one molecule of water by the extraction of in-plane lattice oxygen, O(I):

$$CH_3OH + O(I) \rightarrow CH_2O + H_2O$$

Starting with the surface initially in a reduced form (bridging oxygens removed, in-plane oxygens intact), the stoichiometric relationship above indicates that each molecule of methanol converted to formaldehyde extracts one in-plane oxygen anion to form one molecule of water. By assuming a unity sticking coefficient for methanol at 170 K, a surface unit cell density of 4.7×10^{14} cm^{-2} (based on the bulk lattice parameters) and noting the possibility of some undetected H_2 desorption, the conversion of methanol in successive TDS runs can be used to give an *upper limit* on the concentration of in-plane vacancies formed chemically.

Figure 2.4 illustrates the chemical introduction of in-plane defects via successive 0.6 L doses of methanol (2.16×10^{14} molecules/cm^2 assuming a unity sticking coefficient). The starting surface was produced by oxidation and subsequent annealing to 400 K. This treatment is expected to remove a significant fraction of bridging vacancies, but leave the in-plane anions intact. Only the formaldehyde production is illustrated in Figure 2.4. For the initial run the 450 K methoxide decomposition

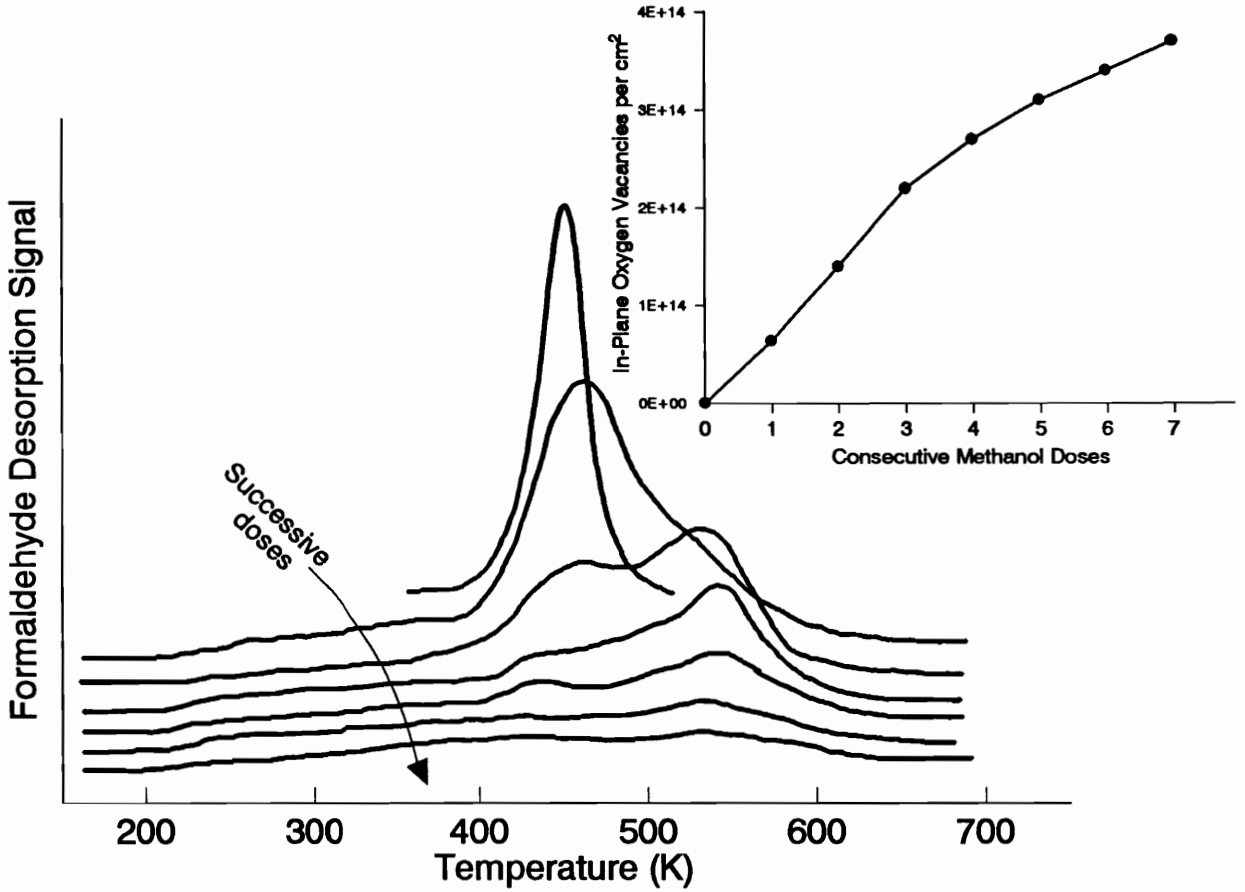

Fig. 2.4 Formaldehyde desorption following successive 0.6 L methanol doses on a reduced surface. The changing TDS signals illustrate the chemical introduction of in-plane oxygen vacancies using the selective oxidation of methanol to formaldehyde. The inset shows an upper-limit estimate of the number of in-plane oxygen vacancies formed with each successive dose.

channel associated with bridging oxygen vacancies (four-coordinate Sn^{2+} cations) is observed. In the second run the 450 K channel decreases, but the desorption feature is significantly broadened to higher temperatures. In successive doses, the 450 K channel continues to decrease, while the intensity of the 540 K channel first increases then decreases with successive doses. After the seventh successive dose shown in Figure 2.4, the methanol conversion is about 10-12%, not as low as the less than 5% conversions observed on the ion-bombarded and annealed surface, but approaching a similar value. The estimated in-plane oxygen vacancy density as a function of dose is shown as an inset in Figure 2.4. After the seventh dose, the total amount of formaldehyde produced in all seven runs suggests an in-plane oxygen vacancy concentration of about 3.7×10^{14} per cm^2. This concentration corresponds, on average, to about 0.7-0.8 in-plane oxygen vacancies per (110) surface unit cell. Hence, in-plane oxygen vacancy concentrations approaching about one per surface unit cell shut down the surface dehydrogenation chemistry for methanol in TDS.

A highly-defective surface prepared by ion-bombardment and 950 K annealing is the only starting condition which shows little or no variation in TDS behavior due to repeated doses. The experimental limit of about one oxidation treatment per day also makes this the only surface for which the coverage dependence in the desorption behavior can be examined conveniently. Figure 2.5 illustrates the coverage-dependent TDS behavior of methanol from this highly-defective and nearly unreactive surface following adsorption at 120 K. The right panel illustrates the low coverage

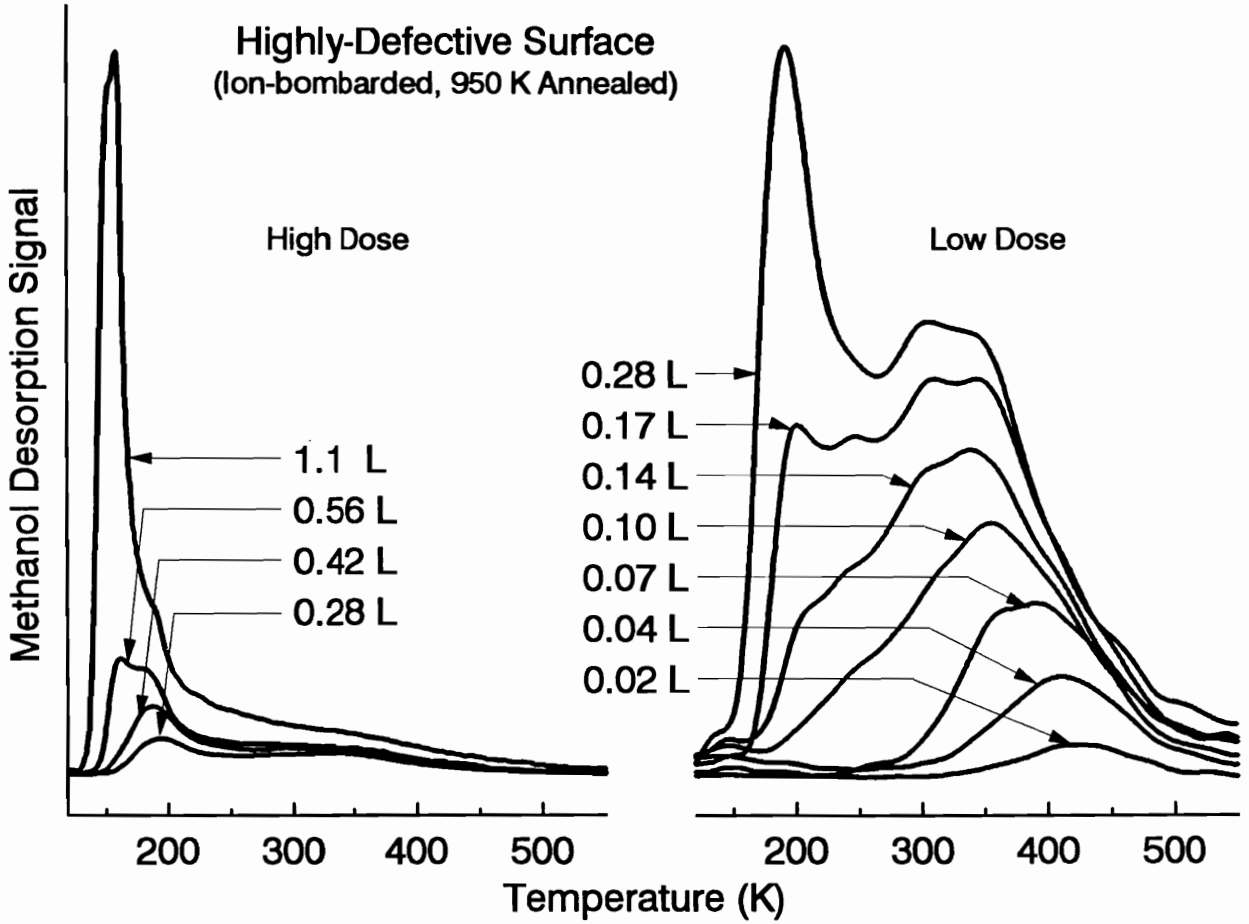

Fig. 2.5 Methanol TDS traces following adsorption on a highly-defective (nearly unreactive) surface at 120 K. The right panel shows the low dose range (0.02 to 0.3 L) while the left panel shows the higher dose range (0.3 to 1.1 L).

regime (doses less than 0.3 L) while the left panel illustrates the higher coverage regime (doses up to about 1 L). For the lowest dose (0.02 L), one desorption feature centered at 424 K is observed. This feature shifts down in temperature to 413 K for a dose of 0.04 L. Increasing doses result in additional, unresolved lower-temperature features, and the primary desorption temperature continues to decrease to about 335 K for a 0.14 L dose. For larger doses (0.17 L and above) a low-temperature feature is clearly apparent, initially at 200 K for a 0.17 L dose, and decreasing to about 185 K for a 0.42 L dose. For doses greater than 0.5 L an additional low-temperature feature appears at 160 K. With doses greater than about 1.1 L, a final desorption feature appears as a shoulder at about 155 K. This feature grows without saturation for increasingly higher doses, a characteristic of multilayer adsorption. The desorption temperature of 153 K for a 2.8 L dose compares favorably with the 150 K multilayer desorption temperature observed on Cu(100) [28].

A second-order kinetic analysis [26] was performed on the highest temperature desorption features associated with low coverages to test the kinetics associated with the 300 K to 325 K desorption features. If the intermediate temperature desorption feature were associated with the recombination of dissociated methanol, a second-order process would be expected. The analysis yields pre-exponentials on the order of 10^{-14} cm^2/sec *or less*, much too low to reasonably represent a second-order process [29]. Hence, because of the overlapping features, it is not possible to extract a reasonable order for the desorption kinetics in the 300 K to 325 K temperature range. Our inability to assign an order for the

desorption kinetics in this temperature range is likely due to the heterogeneity of the highly-defective surface which may preclude the use of coverage-invariant kinetic parameters.

2.3.2 Photoemission Measurements

XPS and UPS were used to monitor the adsorption and decomposition of methanol. The primary goal of these measurements was to determine the nature of the adsorbate responsible for methanol TDS features in the 300 K to 325 K temperature range.

Figure 2.6 shows C 1s XPS spectra following methanol adsorption on the highly-defective surface and on the reduced surface. These two surfaces were chosen because TDS indicates a significant concentration of methoxide on the reduced surface, while the TDS coverage series for the defective surface shows that a significant 300 - 325 K feature can be obtained at lower doses, with the molecular state (215 K desorption temperature and below) being readily accessed at higher doses. Spectrum a is representative of an 11 L dose of methanol on the highly-defective surface, a dose sufficient to produce a thick multilayer coverage as indicated by a strong attenuation of the Sn 3d features (not shown). This condensed molecular methanol spectrum appears at 287.1 eV with a full-width at half maximum (FWHM) of 1.6 eV. Heating the surface to 195 K for one minute to remove the clear molecular contributions seen in TDS leaves surface species primarily associated with the intermediate temperature desorption features (near 300 K). The result is shown as spectrum 7b. The C 1s feature is located at 286.6 eV and can be fitted

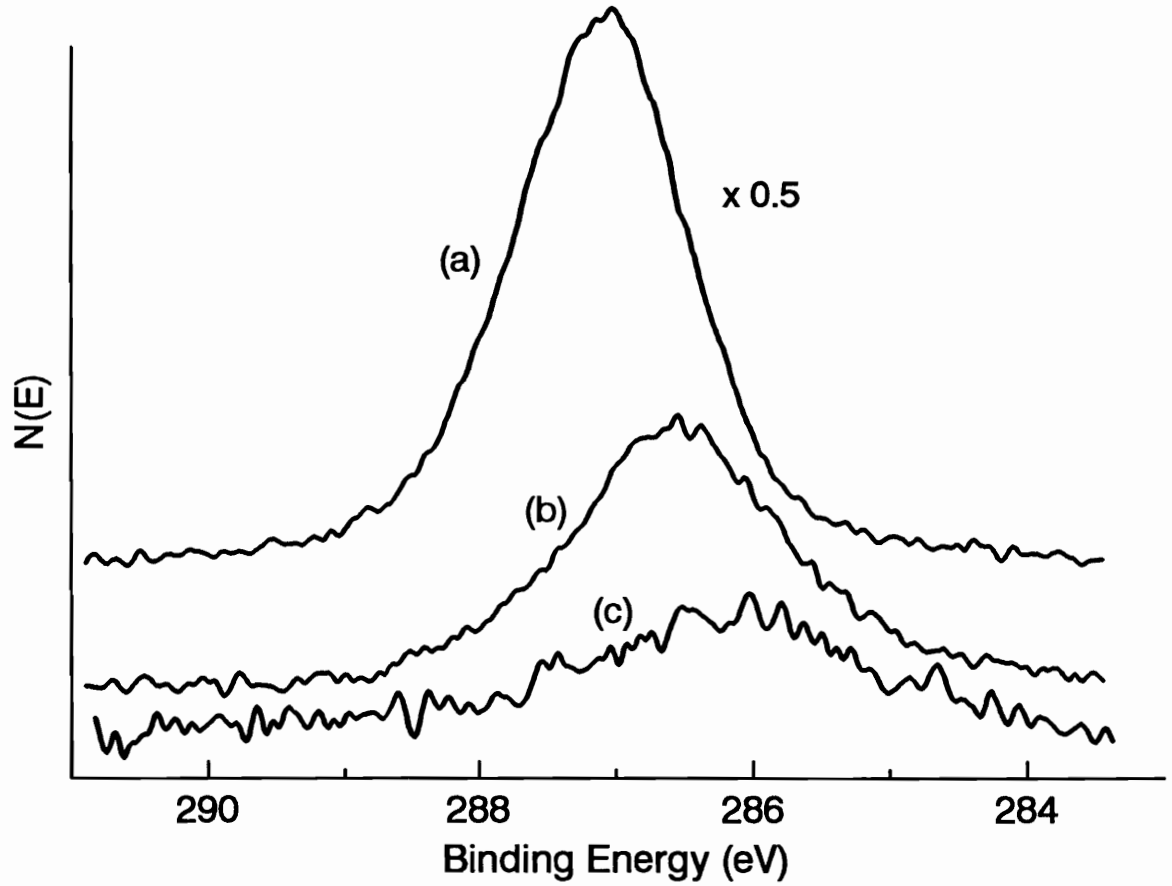

Fig. 2.6 Characteristic C1s XPS spectra following methanol adsorption. (a) methanol multilayer following an 11 L dose on the highly-defective surface. (b) surface in (a) heated to 195 K to remove the low-temperature TDS feature associated with molecularly adsorbed methanol. (c) reduced surface following a multilayer dose and heating to 210 K to remove the low-temperature methanol desorption state.

reasonably with a single Gaussian peak with a FWHM of 1.9 eV.

The 0.5 eV shift to lower binding energy from the multilayer to the chemisorbed layer on the defective surface is similar to that reported for the change from molecular methanol to methoxide on ZnO(0001)-Zn [3]. In this case, however, the majority of this shift (0.3 eV) can be easily accounted for by the change in work function associated with the thick multilayer. It is known that the binding energy of physisorbed multilayers tracks the work function rather than the Fermi level [31]. He I UPS data (not shown) indicate an 0.3 eV increase in the work function following the desorption (by heating to 160 K) of an even thinner multilayer from only a 3 L dose. Therefore, most of the 0.5 eV shift from a thick multilayer to a chemisorbed layer is not due to a difference in the chemical state of the adsorbate. Likewise, while a comparison of the 1.9 eV width of the C 1s feature of the chemisorbed layer is greater than that for a condensed molecular layer (1.6 eV), this increased width is not necessarily indicative of more than one chemisorbed species. A similar 0.2 eV increase in the width of the Sn $3d_{5/2}$ feature is also observed following methanol adsorption, hence the observed increase in line width is not specific to the C 1s feature.

Smaller initial doses have also been examined on the highly-defective surface (not shown). Doses of 0.3 L and 0.5 L were examined because the TDS measurements in Figure 2.5 indicate that a majority of adsorbed methanol appears in the 325 K desorption range for a 0.3 L dose, while the 0.5 L dose gives a majority of the adsorbate as molecular methanol (desorption temperature 215 K and below). C 1s

spectra for these two doses vary only in their absolute intensity, and are similar to that shown in Figure 2.6b (i.e., 286.4 eV and 1.9 eV FWHM). Thus, the low-temperature molecular adsorbate in the first monolayer (desorption temperature 215 K and below) cannot be distinguished from those species which desorb at intermediate temperatures (325 K) with XPS.

HeII UPS (not shown) for the defective surface with methanol coverages similar to those described by Figures 2.6a and 2.6b as well as the 0.3 L and 0.5 L doses described above show clear evidence of the molecular orbitals of methanol. Comparison to the gas-phase photoemission of methanol and the spectra for condensed multilayers on other surfaces [25,32-36] allows for the assignment of emission from the 2A" and 7A' molecular orbitals of methanol and a combination feature due to the 6A'(σ) and 1A"(π) MO's. The XPS and UPS results clearly indicate the presence of molecular surface species when the intermediate temperature (300 K to 325 K) desorption features are populated. These results together suggest the assignment of the intermediate temperature species to a molecular adsorbate.

Also shown as Figure 2.6c is the C 1s spectrum resulting from a multilayer coverage dose on the reduced surface (oxidized, then 700 K-annealed) followed by heating to 210 K to remove the low-temperature methanol associated with a molecular adsorbate. The resulting spectrum is adequately represented by a single Gaussian peak at 286.3 eV with a FWHM of 2.2 eV, 0.3 eV broader than that observed on the highly-defective surface. Spectra similar to 7c are observed also following

lower doses (0.6 L to 0.8 L) on the reduced surface.

For the reduced surface, the chemisorbed species give rise to a somewhat lower C 1s binding energy, but a significantly wider FWHM of 2.2 eV. For an 0.6 L dose which gives an XPS spectrum similar to 7c, the TDS data in Figure 2.2 suggest that about 75% of adsorbed methanol is present as methoxide associated with the 450 K desorption channel (desorbing either as formaldehyde or methanol) while the remainder is associated with the intermediate (310 K) desorption state. Previous XPS investigations of methanol adsorption on oxide single crystal surfaces with similar spectral resolutions have assigned C 1s line widths of 1.8 eV FWHM and lower to the presence of a single adsorbed species, and line widths of 1.9 eV and greater (typically greater than 2.0 eV) to the presence of two adsorbed species (i.e., molecular methanol and methoxide) [3,15]. Therefore, the 2.2 eV FWHM we observe on the reduced surface also appears to be indicative of at least two adsorbed species. The shift to lower binding energies (in comparison to the defective surface) is consistent with expectations for methanol dissociation to methoxide [3], and gives indirect but non-definitive evidence of a mixed monolayer of methanol and methoxide. Since the TDS data clearly indicate that methoxide is associated with the 450 K (and higher) reaction channels, the intermediate temperature desorption features (320 K) may be associated with the apparent molecular contribution in the mixed monolayer, similar to the XPS and UPS observations from the highly-defective surface. HeII UPS data for the reduced surface under similar conditions of coverage also indicate a mixed

monolayer, although the overlap of features makes it impossible to specifically identify methoxide.

The photoemission data taken *in toto* indicate the presence of molecular methanol when the intermediate temperature desorption states are populated, thus supporting an initial assignment of such states to a molecular adsorbate. However, the *definitive* assignment of the intermediate-temperature desorption features (300-325 K) to a molecular adsorbate is not possible since the photoemission data give an indirect identification of the surface species. A vibrational spectroscopy such as HREEL or IRAS, neither of which is yet widely practiced on metal oxide single crystal surfaces, may provide a much more direct identification of the adsorbed species. It is noted, however, that molecular adsorption of methanol at 300 K has been identified on the TiO_2(110) surface by Onishi *et al.* using UPS [37]. The TiO_2(110) surface has a composition (cation to anion ratio) and structure identical to that of the stoichiometric surface where the main desorption feature occurs at 310 K in TDS (Figure 2.1).

2.4 Discussion

The TDS and photoemission observations for the stoichiometric surface suggest that the major fraction (approximately 85%) of adsorbed methanol is removed by desorption of a molecular methanol surface species. For the reduced surface, the major fraction (approximately 70%) of adsorbed methanol is removed by either methoxide decomposition or methoxide recombination with surface hydrogen to form methanol. Hence, methanol is primarily adsorbed molecularly on the stoichiometric

surface and dissociatively adsorbed on the reduced surface. The higher conversion to formaldehyde observed on the reduced surface (50%, reduced vs. 10%, stoichiometric) is attributable to the ability of this surface to dissociate methanol. Likewise, the low conversions (< 5%) observed on the highly-defective surface are the result of molecular rather than dissociative adsorption.

It is instructive to consider first just the stoichiometric and reduced surfaces where the composition differences are related to the presence or absence, respectively, of bridging oxygen anions. Since site requirements for dissociative adsorption of Brønsted acids are typically described in terms of acid/base (cation/anion) site pairs, one can consider the enhancement in dissociation and reaction of methanol on the reduced surface in terms of surface acid/base properties. Considering first the "base" function performed by surface anions, one would expect the coordinately-*un*saturated bridging anions on the stoichiometric surface to be more reactive and capable of binding a proton than the coordinately-saturated in-plane anions available at the reduced surface. Hence, the stoichiometric surface is expected to be more "basic" than the reduced surface. It is concluded that the difference in the ability of these two surfaces to dissociate methanol is attributable primarily to the availability of different surface cations. The dissociation of methanol to methoxide is enhanced by the presence of the four-coordinate, Sn^{2+} cations associated with bridging oxygen vacancies on the reduced surface. The nature of the available lattice oxygen appears to be much less critical.

The results suggest that the dissociation of methanol occurs

preferentially at the four-coordinate Sn^{2+} sites, and that the dissociation probability at five-coordinate Sn^{4+} sites on the stoichiometric surface is low. The limited reactivity observed on the stoichiometric surface can be attributed to the removal of bridging anions during the course of the TDS run before all the molecular methanol is removed. A preliminary assignment of the 450 K methoxide decomposition channel is made to four-coordinate Sn^{2+} sites at bridging oxygen vacancies. It is noted that the possibility of methoxide diffusion to five-coordinate Sn^{4+} sites following methanol dissociation at four-coordinate Sn^{2+} sites has been considered. Saturation coverages of methanol following adsorption at 300 K show no evidence for increased methoxide coverages as would be expected if the surface diffusion of methoxide were an activated process.

The absolute values of the methoxide recombination/decomposition ratios should be viewed as rough approximations since they are based on maximum relative intensities in TDS. However, the *trends* in the reported ratios are significant indicators of differences in the surface chemistry associated with methoxide decomposition. The difference in the methoxide recombination/decomposition ratio for the stoichiometric surface (0.2) and reduced surface (0.5) appears to be related to the variance in oxygen anion concentration on the two different surfaces. Since the source of hydrogen for the methoxide/hydrogen recombination at 450 K is the rate-limiting unimolecular hydride elimination from methoxide, lower recombination/decomposition ratio for the stoichiometric surface suggests that the remaining coordinately-unsaturated bridging oxygen anions on the stoichiometric surface scavenge hydrogen more efficiently

than the reduced surface. It is noted, however, that the total amount of surface hydrogen scavenged on the reduced surface is actually greater than on the stoichiometric surface because of the higher conversion.

An interesting comparison can be made between the methanol surface chemistry of the reduced surface and that reported previously by Kim and Barteau for the TiO_2(001) surface [15]. The bimolecular coupling of surface methoxide to produce dimethyl ether was observed on the {114}-faceted TiO_2(001) surface which exposes four-coordinate Ti^{4+} cations. The proposed site requirement for this reaction is two coordination vacancies on a single cation capable of binding the two methoxides. On the reduced SnO_2(110) surface, four-coordinate Sn^{2+} cations are available, but no bimolecular coupling to dimethyl ether is observed. The one clear difference between these two cases is the oxidation state of the available four-coordinate cations. On TiO_2(001), the four-coordinate cations remain in a 4+ oxidation state, and are exposed as the result of surface faceting. On SnO_2(110), the removal of bridging oxygen anions to expose four-coordinate cations is accompanied by the requisite reduction of the cations from a 4+ to a 2+ oxidation state. If one examines the coordination chemistry of Sn^{2+} compounds, coordination numbers of three and four are typical. In the common blue-black form of SnO, shown in Figure 2.7, each Sn^{2+} cation has a bulk coordination number of four in a square-based pyrimidal configuration with a natural apparent coordination vacancy occupied by a stereochemically-active lone pair [38]. Hence, while the four-coordinate cations on the reduced surface appear to have two coordination vacancies

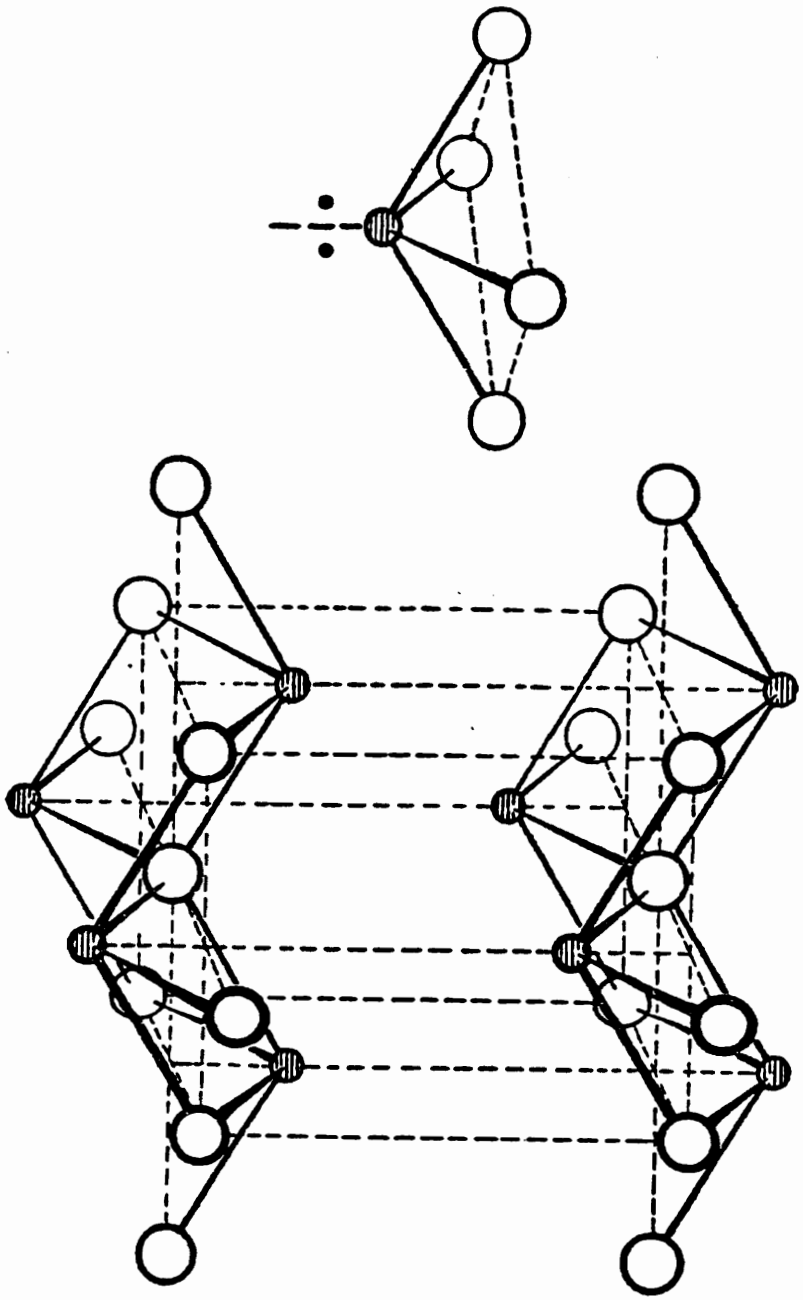

Figure 2.7 The crystal structure of tetragonal SnO. The small shaded circles represent metal atoms. The arrangement of bonds from a metal atom is shown at the right, where the 2 dots represent the "inert" pair of electrons. From Structural Inorganic Chemistry, 2nd ed., A. F. Wells, p. 368 (Clarendon Press, Oxford, 1950).

relative to Sn^{4+} cations at the stoichiometric surface, they are probably best thought of as having a single coordination vacancy, more in line with the expectations for Sn^{2+} compounds.

While the differences in methanol dissociation and oxidation chemistry on the stoichiometric and reduced surfaces can be attributed to the presence or absence of bridging oxygen anions, the chemical behavior of the defective surfaces is affected by the presence of in-plane oxygen vacancies. The higher-temperature methoxide decomposition channel observed at 540 K on the defective surface is clearly associated with the presence of these in-plane vacancies, and appears regardless of whether the in-plane vacancies are introduced thermally (950 K annealing) or chemically by methanol oxidation. The higher methoxide decomposition temperature associated with in-plane vacancies indicates that methoxide is stabilized significantly, by nearly 6 kcal/mol, at the low-coordination cations associated with these defects.

While cations associated with in-plane defects can more effectively stabilize surface methoxides, their introduction decreases the amount of methoxide formed by dissociative adsorption of methanol. For large in-plane oxygen vacancy concentrations approaching an average of one per surface unit cell, the dissociation and oxidation of methanol is nearly negligible. The observed variations in the extent of methanol dissociation and oxidation indicate a clear structure/composition dependence for the reaction of this weak Brønsted acid on SnO_2(110). Starting with the stoichiometric surface, the activity for methanol dissociation is low, but increases as the bridging oxygen anions are removed. The activity for

dissociation reaches a maximum as the surface reaches the reduced condition, then decreases with the removal of in-plane oxygen anions. Since all the surfaces investigated expose a significant concentration of surface anions and coordinately-unsaturated cations, it is clear that the site requirements for methanol dissociation involve more than just the availability of cation/anion pairs. Other studies have demonstrated clearly the importance of the availability of cation/anion pairs for the heterolytic dissociation of Brønsted acids on oxide surfaces [1-16]. The present work on SnO_2(110) indicates that while cation/anion site pairs may be a necessary condition for the dissociation of Brønsted acids, their availability is not a sufficient condition. Similarly, while the concepts of coordination chemistry have proven useful in understanding the surface chemistry of metal oxides, simple classifications based strictly on coordination numbers alone may be of limited value without the full details of local geometric and electronic structure. This point is most clearly illustrated by the lower reactivity of four-coordinate cations associated with in-plane oxygen vacancies on the defective surface compared to the most active four-coordinate Sn^{2+} cations associated with bridging oxygen vacancies on the reduced surface. Clearly, the local structure and composition can play a major role in defining the surface ensemble for the dissociation reaction.

2.5 Conclusions

The effect of local composition and cation coordination on the dissociation and oxidation of methanol over SnO_2(110) surfaces has been

investigated. The oxidation of methanol is completely selective to formaldehyde in TDS, with the conversion dependent on the surface composition. Starting with a stoichiometric surface, the conversion first increases then passes through a maximum as the surface becomes more oxygen deficient. The variable conversion for the oxidation reaction in TDS is related to variations in the ability of the surface to heterolytically dissociate this weak Brønsted acid. Two methoxide decomposition channels were observed, one at 450 K associated with four-coordinate Sn^{2+} cations at bridging oxygen vacancies, and the second at 540 K associated with lower-coordination cation sites at in-plane oxygen vacancies. The results demonstrate the importance of local surface properties in controlling the acid/base interaction of adsorbates on SnO_2 surface.

2.6 References

1. S. Akhter, K. Lui and H.H. Kung, *J. Phys. Chem.*, **89**(1984)1958.
2. G. Zwicker, K. Jacobi and J. Cunningham, *Intern. J. Mass Spectrosc. Ion Processes*, **60**(1984)213.
3. J.M. Vohs and M.A. Barteau, *Surf. Sci.*, **176**(1986)91.
4. J.M. Vohs and M.A. Barteau, *J. Phys. Chem.*, **91**(1987)4766.
5. J.M. Vohs and M.A. Barteau, *Surf. Sci.*, **201**(1988)481.
6. M.A. Barteau and J.M. Vohs, in Successful Design of Catalysts; Ed., T. Inui (Elsevier, Amsterdam, 1988) p. 89.
7. J.M. Vohs and M.A. Barteau, *Surf. Sci.*, **221**(1989)590.
8. J.M. Vohs and M.A. Barteau, *J. Phys. Chem.*, **95**(1991)297.
9. M.A. Barteau, *J. Vac. Sci. Technol. A*, **11**(1993)2162.

10. C.J. Machiels, W.H. Cheng, U. Chowdhry, W.E. Farneth, F. Hong, E.M. McCarron and A.W. Sleight, *Appl. Catal.*, **25**(1986)249.

11. W.E. Farneth, R.H. Staley and A.W. Sleight, *J. Am. Chem. Soc.*, **108**(1986)2327.

12. X.D. Peng and M.A. Barteau, *Langmuir*, **7**(1991)1426.

13. X.D. Peng and M.A. Barteau, *Catal. Lett.*, **7**(1990)395.

14. K.S. Kim and M.A. Barteau, *J. Catalysis*, **125**(1990)353.

15. K.S. Kim and M.A. Barteau, *Surf. Sci.*, **223**(1989)13.

16. H. Idriss, K.S. Kim and M.A. Barteau, in Structure-Activity and Selectivity Relationships in Heterogeneous Catalysis; Eds., R.K. Grasselli and A.W. Sleight (Elsevier, Amsterdam, 1991) p. 327.

17. D.F. Cox, T.B. Fryberger and S. Semancik, *Phys. Rev. B*, **38**(1988)2072.

18. P.A. Cox, R.G. Egdell, C. Harding, W.R. Patterson and P.J. Tavener, *Surf. Sci.*, **123**(1982)179.

19. J.M. Themlin, R. Sporken, J. Darville, R. Caudano, J.M. Gilles and R.L. Johnson, *Phys. Rev. B*, **42**(1990)11914.

20. T.J. Godin and J.P. LaFemina, *Phys. Rev. B*, **47**(1993)6518.

21. D.F. Cox, T.B. Fryberger and S. Semancik, *Surf. Sci.*, **224**(1989)121.

22. The ion gauge sensitivity for methanol was taken as 1.8, per the Inficon Quadrex 200 Mass Spectrometer manual.

23. B. Thiel and R. Helbig, *J. Cryst. Growth*, **32**(1976)259.

24. V.A. Gercher and D.F. Cox, **MANUSCRIPT IN PREPARATION.** The desorption of formaldehyde following formaldehyde adsorption occurs below 450 K on all preparations of the SnO_2(110) surface.

25. M. Bowker and R.J. Madix, *Surf. Sci.*, **116**(1982)549.

26. P.A. Redhead, *Vacuum*, **12**(1962)203.

27. V.A. Gercher and D.F. Cox, *Surf. Sci.,* SUBMITTED

28. R. Ryberg, *Phys. Rev. Lett.*, **49**(1982)1579.

29. See for example, R.L. Brainard and R.J. Madix, *J. Am. Chem. Soc.*, **111**(1989)3826 and references therein.

30. C.D. Wagner, W.M. Riggs, L.E. Davis, J.F. Moulder and G.E. Muilenburg, Handbook of X-Ray Photoelectron Spectroscopy (Perkin-Elmer, Eden Prairie, 1979).

31. K. Wandelt, J. Hulse, J. Küppers, *Surf. Sci.*, **104**(1981)212.

32. H. Lüth, G.W. Rubloff and W.D. Grobman, *Surf. Sci.*, **63**(1977)325.

33. J.W. Rogers, R.L. Hance and J.M. White, *Surf. Sci.*, **100**(1980)388.

34. T.E. Felter, W.H. Weinberg, G.Ya. Lastushkina, P.A. Zhdan, G.K. Boreskov, and J. Hrbek, *Appl. Surf. Sci.*, **16**(1983)351.

35. C.T. Au, W. Hirsch and W. Hirschwald, *Surf. Sci.*, **221**(1989)113.

36. N.D. Shinn, *Surf. Sci.*, **278**(1992)157.

37. H. Onishi, T. Aruga, C. Egawa and Y. Iwasawa, *Surf. Sci.*, **193**(1988)33.

38. P.G. Harrison, in Comprehensive Coordination Chemistry; Vol. 3; Ed., G. Wilkinson, (Pergamon Press, Oxford, 1987) p.186-188.

Chapter 3

Formic Acid Decomposition on $SnO_2(110)$

3.1 Introduction

The adsorption of Brønsted acids on single crystal metal oxides has been used to test a variety of ideas, such as reaction site requirements and acid-base properties of surfaces [1,2]. Both surface structure and the strength of the Brønsted acid can affect the reactivity on a particular surface. A series of Brønsted acids studied on MgO surfaces has shown a reactivity order relating to the acid strength in aqueous solution; stronger acids react more readily than weaker acids [1,3]. The site requirement of acid dissociation is recognized to be an acid-base site pair [1,3].

$SnO_2(110)$ readily allows the observation of reactions on surfaces with different atomic compositions since this surface can be manipulated by oxidation/reduction treatments to introduce two types of oxygen vacancies [4]. Methanol, a weak Brønsted acid, has previously been studied on various $SnO_2(110)$ surfaces by thermal desorption spectroscopy [5]. The dissociation and oxidation kinetics were found to be dependent on surface composition, indicating structure-sensitive dissociation and oxidation reactions. The primary factor controlling the surface reaction was the type of exposed surface cation.

Formic acid, a stronger Brønsted acid than methanol, has been studied to investigate the reactions of carboxylates on $SnO_2(110)$. CO_2, CO, and water are the main products formed, with trace amounts of formaldehyde observed on defective surfaces. Two formate reaction

pathways were observed, one producing CO preferentially and one producing CO_2 preferentially. A correlation between the density of in-plane anion vacancies and extent of dissociation is reported.

3.2 Experimental

Gas exposures were performed by backfilling the chamber through a variable leak valve. Aldrich (96%) formic acid was degassed by repeated freeze-pump-thaw cycles prior to use. All doses have been corrected for ion gauge sensitivity [9].

3.3 Results

3.3.1 Thermal Desorption Spectroscopy

Variations in the adsorption and reaction of formic acid were examined by TDS for all the surface preparations described in Chapter 1. The desorption products observed in TDS were formic acid, CO, CO_2, and water. Trace amounts of formaldehyde were observed on the defective surfaces. Other products tested for but not detected were CH_4, methanol, dimethyl ether (CH_3OCH_3) and methyl formate ($HCOOCH_3$). The conversion, selectivity, and kinetics of the rate-limiting surface reaction step are dependent on surface condition as shown below. Table 1 lists typical values for the conversion of formic acid and relative CO_2/CO yields observed for the various surface conditions.

3.3.1.1 Stoichiometric Surface

Figure 3.1 shows the TDS data obtained following a 0.4 L dose of

Table 1. Typical Fractional Conversion of 0.4 L Doses at 170 K as a Function of Surface Condition.

Surface Condition	**CO_2/CO**	**Conversion**
Stoichiometric	2.5	99%
Reduced	2.0	95-99%
Less Defective	1.0	80-90%
Highly Defective	1.0	50-60%

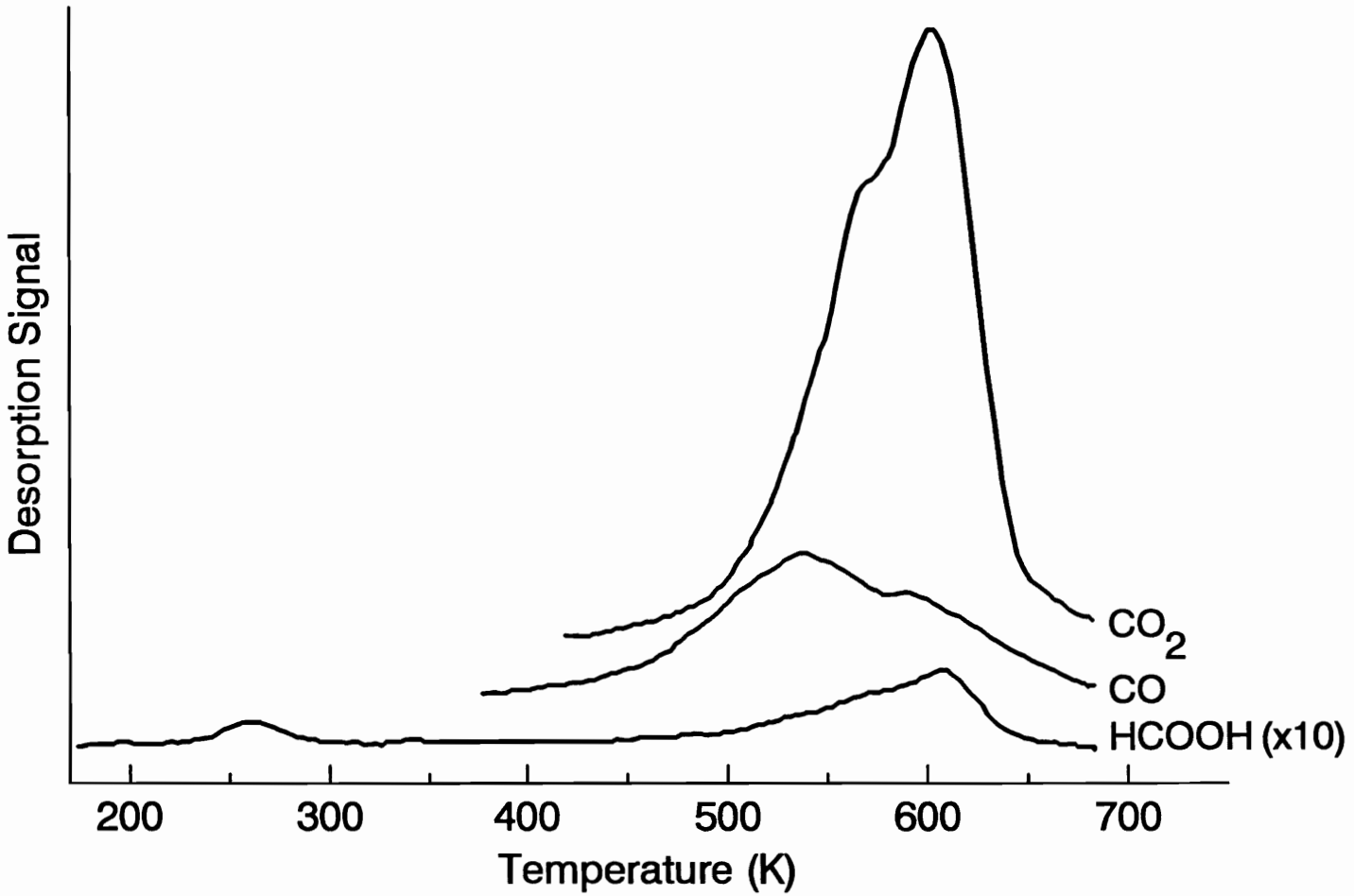

Fig. 3.1 Thermal desorption spectra for formic acid following a 0.4 L dose on the stoichiometric surface at 170 K.

formic acid on a stoichiometric surface (bridging oxygen anions and 5-coordinate Sn^{4+} present) at 170 K. The conversion is 99%. Trace HCOOH desorbs in a low temperature feature at 260 K and a broad high temperature feature at 605 K. CO desorption occurs with two broad features near 535 K and 600 K. CO_2 evolves as a feature centered at 605 K, with a shoulder at 560 K. Over the course of several experiments, the CO_2 shoulder at 560 K did not always appear, nor did the CO always show a definite feature near 535 K, but the majority of the data are consistent with this report. The probable explanation for this behavior is some small variation in the initial surface condition following the oxidation treatments of SnO_2(110). The CO_2/CO ratio on this surface is 2.5.

3.3.1.2 Reduced Surface

Formic acid TDS was also performed on the reduced surface (no bridging oxygen, exposed 4-coordinate Sn^{2+} and 5-coordinate Sn^{4+}). As before, a 0.4 L dose of formic acid at 170 K was used. Figure 3.2 shows two features for formic acid: a feature at 245 K, with a shoulder near 270 K, and a broad high temperature feature centered at 595 K. CO desorbs with one feature at 540 K and a shoulder at 600 K. CO_2 shows one feature at 605 K. Water desorbs near 420 K, and with a broad feature near 595 K. The total conversion for Figure 3.2 is 99% with a decreased CO_2/CO ratio of 2.0. Typical conversions of formic acid on this surface are in the range of 95-99%. A series of consecutive experiments on a reduced surface using 0.4 L doses of HCOOH shows evidence of a slow reactivity change: with each run, the conversion drops by about 2%,

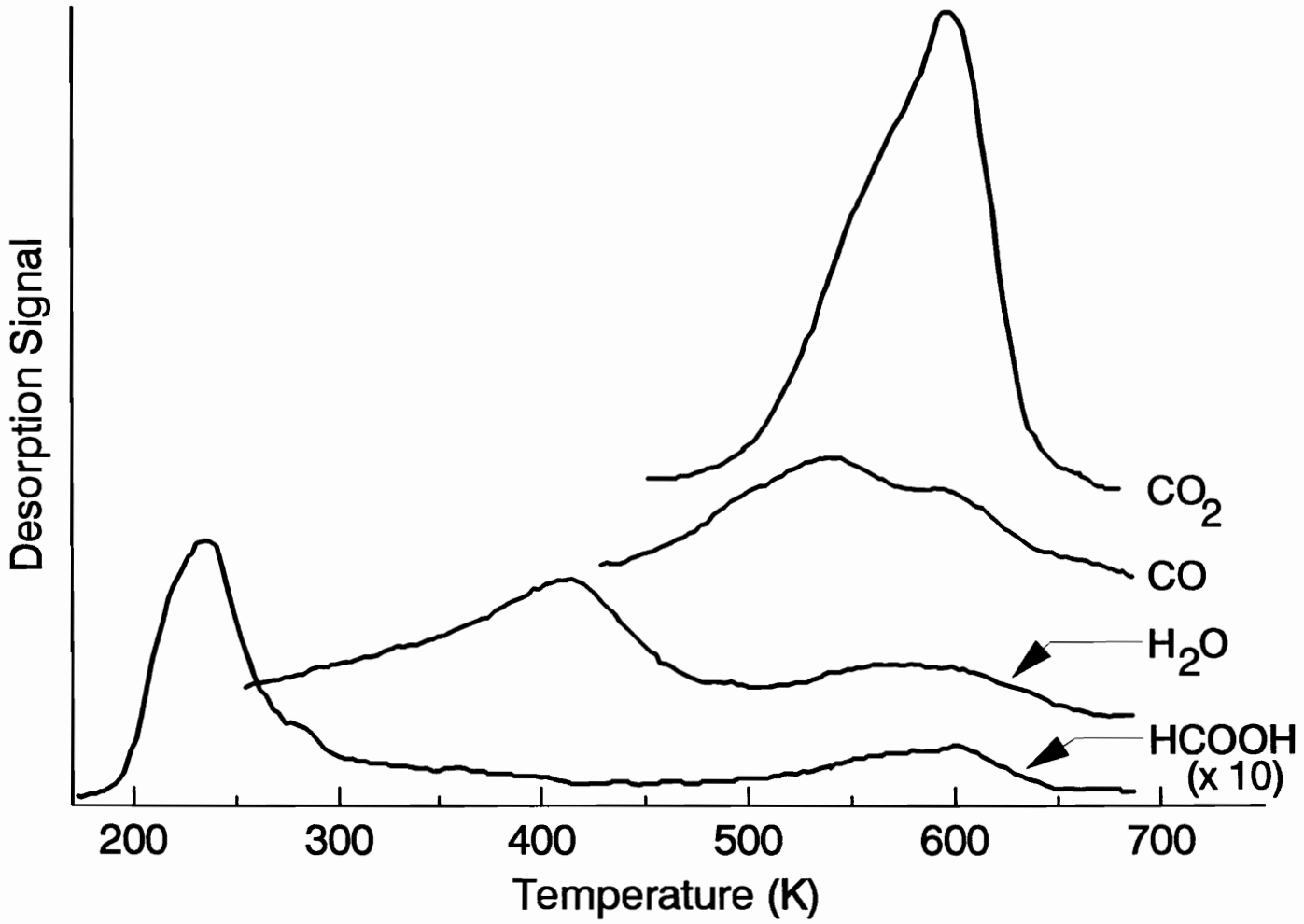

Fig. 3.2 TDS spectra following a 0.4 L dose on the reduced surface at 170 K.

and the CO_2/CO ratio changes from 2.0 towards the defective surfaces value of 1.0 (see below).

3.3.1.3 Defective Surfaces

Figure 3.3 shows the formic acid thermal desorption behavior from two defective surfaces. The right panel is characteristic of a surface prepared by oxidation followed by annealing to 950 K to remove bridging oxygen anions and introduce in-plane oxygen vacancies. The left panel is characteristic of a surface prepared by ion bombardment and annealing to 950 K. This second preparation gives a surface more oxygen deficient than the first [4,5,11]. In both cases, 0.4 L doses at 170 K were used.

For the less-defective surface (right panel), HCOOH desorbs in two broad overlapping peaks at 215 K and 300 K, with a trailing shoulder on the higher temperature side, and a high temperature feature at 595 K. CO desorption occurs with two overlapping features at 505 K and 590 K. CO_2 desorbs in a feature at 595 K. Water desorption occurs with one feature at 380 K and one at 595 K. Formaldehyde is also produced at 490 K. The total conversion for Figure 3.3 is 89%, but typical conversions for 0.4 L doses on this surface vary between 80 and 90%. The CO_2 to CO ratio drops to 1.0. The formaldehyde yield is only about 0.6% of the total conversion.

For the more defective surface (left panel), the conversion of formic acid following a 0.4 L dose at 170 K is even lower, about 59%. Typical conversions on this surface range from 50 to 60%. The CO_2 to CO ratio stays at 1.0. The formaldehyde production is about 1% of the total

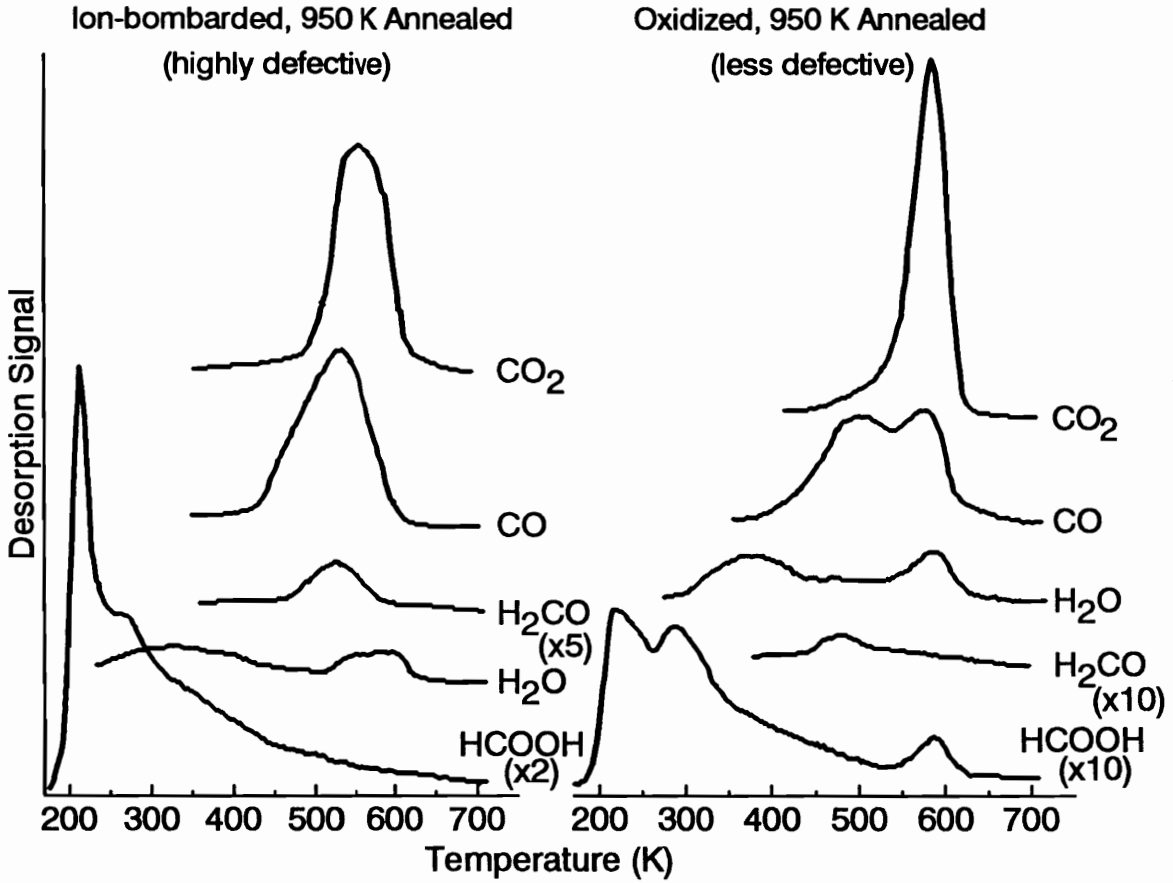

Fig. 3.3 TDS spectra following 0.4 L doses on the defective surfaces at 170 K. The panel on the right is characteristic of a less-defective surface prepared by oxidation and annealing to 950 K. The panel on the left is characteristic of a highly-defective surface prepared by ion bombardment and annealing to 950 K. The relative scaling of the signal intensity for the two panels is arbitrary.

conversion. Overlapping formic acid desorption features are observed at 215 K and 270 K, but with no significant high temperature component. A broad feature is observed for CO desorption at 530 K. CO_2 desorption occurs as one peak at 560 K, with a shoulder at 595 K. Water desorption occurs with a broad feature centered at 350 K and a broad, high temperature feature at 570 K. Formaldehyde desorption is observed at 520 K.

Figure 3.4 illustrates the coverage dependent TDS behavior of formic acid from this surface following adsorption at 120 K. The right panel shows the low coverage regime (doses less than 0.33 L) while the left panel shows the higher coverage regime (doses up to 2.2 L). For the lowest dose (0.03 L), a desorption feature is observed near 400 K. Increasing the dosage results in the primary desorption temperature decreasing to about 391 K for a 0.06 L dose. For a 0.11 L dose, two lower temperature features are clearly apparent, at 280 K and at 217 K. The feature at 217 K increases in intensity and decreases in temperature to 213 K for a 0.16 L dose. This feature continues to grow and decrease in temperature to 205 K for a 0.33 L dose. With 0.44 L doses and above, another feature grows in at 175 K. The low temperature feature appears at 177 K for a 2.2 L dose. This feature grows without saturation for increasingly higher doses, a characteristic of multilayer adsorption.

3.2.2 XPS Measurements

XPS was used to monitor the adsorption and decomposition of formic acid. Experiments were done on a highly-defective surface and a

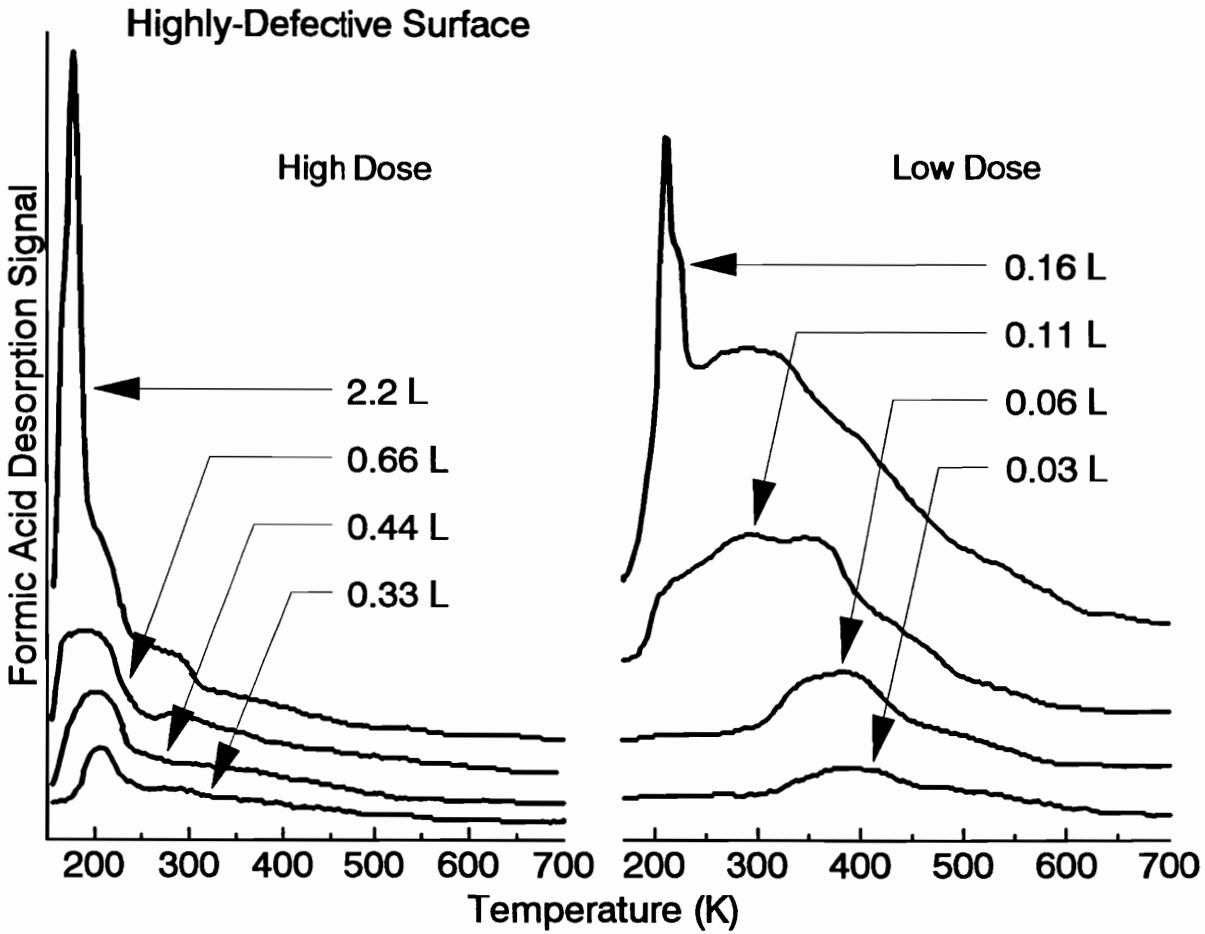

Fig 3.4 Formic acid TDS traces following adsorption on a highly-defective surface at 120 K. The right panel shows the low dose range (0.014 to 0.4 L) while the left panel shows the higher dose range (0.4 to 2.2 L).

reduced surface to compare surfaces in which TDS indicates a significant low-temperature contribution (below 300 K) and a predominant high-temperature contribution, respectively.

The C 1s spectrum (not shown) for a multilayer formic acid coverage resulting from a 2.2 L dose gives a symmetric peak at 289.3 eV with a full-width at half-maximum (FWHM) of 1.9 eV independent of the initial surface condition. For the highly-defective surface, heating to 215 K to remove the multilayer gives a single symmetric peak at 288.8 eV with a FWHM of 2.1 eV. A similar treatment for the reduced surface yields a peak at 288.9 eV with a FWHM of 2.5 eV. Hence, for monolayer coverages on the two surfaces showing different TDS behavior, the C 1s binding energies are essentially identical, but with a significant difference in line width.

3.4 Discussion

The TDS results demonstrate that the desorption temperature ranges for each product are dependent on the initial surface condition. Formic acid desorbs in three temperature ranges: 215-245 K, 260-300 K, and 595-605 K. CO_2 desorbs in two ranges: near 560 K and 595-605 K. CO desorbs in two ranges: 505-540 K and 590-600 K. Water also desorbs in two ranges: 350-420 K and 570-595 K. Formaldehyde desorbs from 490-520 K.

CO_2 is formed preferentially in the 590-605 K channel, along with some CO, H_2O and HCOOH. The simultaneous desorption of formic acid, CO_2, and CO on each surface at 590-605 K is evidence that they evolve

from a common surface intermediate with the same rate-limiting step. The most likely intermediate is formate since CO and CO_2 are typical formate decomposition products on metals and oxides [13-15]. Formate is formed by loss of the acidic proton from formic acid. The coincidence of CO_2 and HCOOH desorption is readily explained by a surface formate undergoing hydride elimination in the rate-limiting step to form CO_2, and recombination of surface hydrogen and formate to form HCOOH. These reactions are as follows: (1) $HCOOH \rightarrow HCOO^- + H^+$ (2) $HCOO^- \rightarrow CO_2 + H^-$ (3) $HCOO^- + H^+ \rightarrow HCOOH$. The rate-limiting step for CO_2 desorption is first order, as identified by the shape of the peak and the constant peak temperature for varying coverages [16]. The Redhead equation [16] can be used to determine an activation energy range for formate decomposition at 590-605 K. Assuming a normal first order pre-exponential of 10^{13} sec^{-1} gives an activation energy of 38.0 ± 0.5 kcal/mol for the unimolecular decomposition of surface formate to CO_2.

CO is formed preferentially in the 490-540 K range. The evolution of CO and H_2CO is reaction-limited [17,18]. Studies of CO and formaldehyde adsorption on similar SnO_2 surfaces show maximum CO and formaldehyde desorption peak temperatures of 350 K and 425 K, respectively. The simultaneous desorption of CO and H_2CO indicates a common intermediate, again most likely a formate species, where (1) $HCOO^- \rightarrow CO + H^- + O$ and (2) $HCOO^- + H \rightarrow H_2CO + O^-$. The rate-limiting step for CO desorption is first order, identified by the constant peak temperature with varying surface coverage [16]. Using the Redhead equation for the 490-540 K range of formate decomposition gives an

activation energy of 32.6 ± 1.2 kcal/mol, assuming a normal first order pre-exponential of 10^{13} sec^{-1}. It is noted that there is one other report of formate decomposition at two different temperatures on a ZrO_2(100)single crystal surface [19].

The formic acid desorption in the 215-245 K and 260-300 K ranges is attributed to molecular formic acid. This assignment is due to the low desorption temperature, and is consistent with the XPS data. The C 1s feature for multilayer formic acid gives a FWHM of 1.9 eV, and may be considered as characteristic of a single molecular species (i.e., formic acid). For the highly-defective surface which exhibits a large low-temperature TDS feature, a C 1s peak a line width of 2.1 eV is observed, slightly larger than observed for molecular formic acid. This observation is in contrast to the line width observed for the reduced surface which gives a TDS spectrum dominated by formate decomposition above 500 K. The C 1s peak is observed with a line width of 2.5 eV. This broader line can be considered as characteristic of more than one surface species, such as a mixed molecular acid/formate layer, or of a single formate species (reasonably identified with TDS) with an inherently broader line width. Hence, while XPS cannot clearly distinguish between the molecular formic acid and formate, it gives an indication of a surface species different than formate and similar to formic acid when the low-temperature formic acid TDS state is populated. Similarly, molecular formic acid desorption has been identified by TDS below 300 K on MgO films [20]. It is noted that for the 0.4 L doses shown in Figures 3.1-3 the low-temperature molecular formic acid contribution in TDS increases as

the conversion decreases, giving a nearly direct correlation between the extent of dissociation and the conversion.

As shown above, water formation occurs in two temperature ranges: 350-420 K and 570-595 K. In the 570-595 K range, the rate-limiting step for water formation is formate decomposition to release surface hydrogen. The oxygen involved in water production may originate from formate (when CO is formed as a product) or from lattice oxygen extracted from the surface. In the 350-420 K range, water must be formed by some other process since no evidence of formate decomposition is seen in this temperature range. The most reasonable explanation is that water is formed from the proton liberated by formic acid dissociation and oxygen is scavenged from the surface; the rate limiting step is most likely OH^- disproportionation [21], $2OH^- \rightarrow H_2O + O^-$. As the extent of dissociation decreases, the amount of water formed at this temperature also decreases. It is noted that the total amount of water formed is approximately equivalent to the amount of CO formed. It is not possible, however, close the hydrogen material balance. The water signals are difficult to quantify and the dihydrogen signal is unobservable because they both ride on large background signals.

One of the variables affecting the reactivity of formic acid is the density of in-plane oxygen vacancies. As the density of in-plane oxygen vacancies increases, the extent of dissociation and the conversion decrease. No significant difference is seen between the stoichiometric and reduced surfaces in the extent of dissociation and conversion, hence the presence or absence of bridging oxygen anions has little effect on the

dissociation of formic acid. The density of in-plane oxygen vacancies on these two surfaces is nominally the same: none. Also, the differences in exposed cations on these two surfaces have little effect on dissociation. There are 5-coordinate Sn^{4+} cations on the stoichiometric surface and 5-coordinate Sn^{4+} cations and 4-coordinate Sn^{2+} cations on the reduced surface.

However, moving from the reduced to defective surfaces, a significant difference is observed. As the density of in-plane oxygen vacancies increases (reduced < less defective < highly defective), the conversion decreases (95-99% to 80-90% to 50-60%, respectively). The fraction of in-plane oxygen vacancies on each surface has been estimated in a previous report [5]. An upper limit was determined by calculating the amount of lattice oxygen removed assuming the reaction of methanol to formaldehyde occurs with stoichiometry $CH_3OH + O(l) \rightarrow H_2CO + H_2O$ where O(l) is a lattice oxygen atom. The fraction of available in-plane oxygen anions was estimated to be ideally 100% on the stoichiometric and reduced surfaces, about 80% on the less-defective surface, and about 50% on the highly-defective surface. These fractions can be compared to the conversions observed for formic acid on each surface: about 99% on the stoichiometric and reduced surface, 80-90% on the less-defective surface, and 50-60% on the highly-defective surface. There appears to be a nearly linear dependence on the fraction of in-plane oxygen anions available on each surface and the conversion for that surface. Since conversion is directly related to the extent of dissociation, it appears that the in-plane oxygen anion density on the defective surfaces controls the

extent of dissociation.

As shown above, the in-plane oxygen vacancies have an effect on formic acid dissociation, or activity. They can also be shown to have an effect on formate decomposition kinetics and selectivity. The CO_2/CO ratio is observed to decrease with the increase in surface defects, both bridging and in-plane oxygen vacancies. The ratio is 2.5 on the stoichiometric surface, 2.0 on the reduced surface, and 1.0 on the defective surfaces. The amount of CO_2 formed decreases in this order as well, and is the main reason for the change. While the removal of bridging oxygen anions effects the selectivity slightly, the introduction of in-plane oxygen vacancies has the greatest effect for decreasing the CO_2/CO ratio.

One possible explanation for this difference in selectivity is based on the reducibility of each surface. It has been suggested [13] that more easily reduced oxides produce more CO_2: MgO (irreducible) produces only CO, while ZnO (easily reduced) produces more CO_2. The stoichiometric surface of SnO_2(110) is the most reducible of the four studied, followed by the reduced, the less-defective, and finally the highly-defective. CO production is preferred to CO_2 from formate decomposition in the 505-540 K temperature range. This reaction channel is most significant on surfaces with in-plane oxygen vacancies. Formate at the cations associated with in-plane vacancies can be deoxygenated by the surface to reoxidize in-plane oxygen vacancies, both the ones caused by water formation at lower temperatures (350-420 K) and those inherent to the starting condition of the surface. Hence, it appears that surface sites associated with in-plane oxygen vacancies are primarily responsible for CO

formation during formate decomposition.

Formaldehyde production occurs only in the presence of in-plane oxygen vacancies (i.e., on defective surfaces). The formate deoxygenation process described for the formation of CO is also consistent with the chemistry of formaldehyde production at the same temperature. The coincident desorption of CO with formaldehyde liberates hydrogen which is then available for formaldehyde production. Formate is hydrogenated and deoxygenated to form formaldehyde. The order of the steps is not clear from the TDS data, although a dioxymethylene species has been proposed over Cu and Ag surfaces [15,22,23], suggesting that hydrogenation may occur first. Like CO production, this process occurs near in-plane oxygen vacancies with formate decomposition as the rate-limiting step. However, very little formaldehyde is formed: the formaldehyde production on the defective surfaces was less than 1% of the total conversion.

Formaldehyde production has been detected in studies on other metal oxides and is said to be formed from formate in two different ways. Formaldehyde can be formed as a product of the reduction of formate by surface hydrogen, or of the bimolecular reaction of two formates. The former case has been observed on highly-defective (ion-bombarded) TiO_2 surfaces [24]. The latter was postulated for the {114}-faceted TiO_2(001) surface, as an analogous reaction to that observed with higher acids on this surface [2,25]. Acids such as acetic and propionic undergo bimolecular ketonization to acetone and 3-pentanone, respectively. Methanol was also seen to undergo a coupling reaction to form dimethyl

ether [26]. The site requirement proposed for these bimolecular reactions is two vacant coordination sites on a Ti^{4+} cation. The formaldehyde production on SnO_2(110) is thought to be a reduction reaction, rather than a coupling reaction, for two reasons: (1) coincident CO production demonstrates that formate decomposition is rate limiting, and liberates hydrogen then available for reduction; (2) no evidence of a coupling reaction is found for other reactants such as methanol [5]. In conclusion, formate decomposition at in-plane oxygen vacancies is the rate-limiting step for formaldehyde formation.

The decomposition of formic acid has been used in the past to determine the acid-base properties of other oxides [27]: basic surfaces are expected to dehydrogenate formic acid, forming CO_2, while acidic surfaces are expected to dehydrate formic acid, forming CO. While a description of specific sites as "acidic" or "basic" may depend on the particular probe reaction used, SnO_2 has been classified previously as both an acidic and a basic oxide [28] and therefore could be expected to form both CO_2 and CO, dependent on the specific acid-base properties of each surface site. The present results suggest that the most "acidic" (i.e., CO-producing) sites on SnO_2(110) are those associated with in-plane oxygen vacancies and the most "basic" are those associated with bridging oxygen anions.

Methanol, a weaker Brønsted acid, was previously studied on these surfaces [5], where formaldehyde from methoxide decomposition was the only observed carbon containing product. Methanol dissociated to methoxide most readily on the 4-coordinate Sn^{2+} cations which are

present in the highest abundance on the reduced surface. As the concentration of in-plane oxygen vacancies increased, the extent of dissociation decreased. However, the fraction dissociated decreased by a factor of ten while the fraction of in-plane anions decreased only by a factor of two. The conclusions reached were that the available cations were primarily responsible for controlling dissociation.

The results of the present study suggest that the increased molecular acidity of formic acid accounts for the higher extent of dissociation and conversion on each surface compared to that previously reported for methanol [5]. A comparison between conversions on the stoichiometric and reduced surfaces show that available cations have little effect on dissociation, unlike with methanol. Apparently, dissociation is not favored at a particular type of cation. However, the extent of dissociation depends directly on the in-plane anion density, as seen in a comparison of the reduced and defective surfaces. As the in-plane anion density decreases, the extent of dissociation also decreases. Hence, on the defective surfaces, the density of "basic" anions appears to control the extent of dissociation. However, the kinetics and selectivity of the subsequent formate decomposition are dependent on the available surface cations. Low coordination cations near in-plane oxygen vacancies form CO preferentially at 505-540 K, while more highly coordinated cations away from in-plane vacancies form CO_2 preferentially at 590-605 K.

3.5 Conclusions

Formic acid adsorption at 170 K on SnO_2(110) surfaces results in

both molecular adsorption and dissociation to formate. The acidic proton from formic acid dissociation reacts with lattice oxygen to form water near 400 K. Unimolecular formate decomposition is the rate-limiting step in the formation of all the other products. The extent of dissociation shows an apparent linear dependence on the density of in-plane oxygen anions. The types of available cations appear to have little effect on the extent of dissociation.

The selectivity is related to the reducibility of each surface. CO and H_2CO production near 530 K was determined to be due to formate decomposition at cations associated with in-plane oxygen vacancies. CO_2 production near 600 K, due to formate decomposition at cations away from in-plane oxygen vacancies, was seen to decrease with increasing surface defectiveness. Apparently, both types of oxygen vacancies affect the selectivity, with in-plane vacancies having the greatest effect.

3.6. References

1. X.D. Peng and M.A. Barteau, *Langmuir*, **7**(1991)1426.
2. H. Idriss, K.S. Kim, and M.A. Barteau, Structure-Activity and Selectivity Relationships in Heterogeneous Catalysis, (Elsevier Science Publishers, Amsterdam, 1991).
3. X.D. Peng and M.A. Barteau, *Catal. Lett.*, **12**(1992)245.
4. D.F. Cox, T.B. Fryberger, and S. Semancik, *Phys. Rev. B*, **38**(1988)199.
5. V.A. Gercher, D.F. Cox and J.-M. Themlin, *Surf. Sci.*, **306**(1994)279, also Chapter 2.
6. P.A. Cox, R.G. Egdell, C. Harding, and W.R. Patterson, and P.J. Tavener, *Surf. Sci.*, **123**(1982)179.

7. J.M. Themlin, R. Sporken, J. Darville, R. Caudano, J.M. Gilles and R.L. Johnson, *Phys. Rev. B*, **42**(1990)11914.

8. T.J. Godin and J.P. LaFemina, *Phys. Rev. B*, **47**(1993)6518.

9. The ion gauge sensitivity for formic acid was taken as 2.28, per the Inficon Quadrex 200 manual.

10. V.A. Gercher and D.F. Cox, *Surf. Sci.*, SUBMITTED.

11. D.F. Cox, T.B. Fryberger, and S. Semancik, *Surf. Sci.*, **224**(1989)121.

12. C.D. Wagner, W.M. Riggs, L.E. Davis, J.F. Moulder and G. Muilenburg, Handbook of X-ray Photoelectron Spectroscopy (Perkin-Elmer, Eden Prairie, 1979).

13. X.D. Peng and M.A. Barteau, *Surf. Sci.*, **224**(1989)327.

14. G. Zwicker, K. Jacobi and J. Cunningham, *International Journal of Mass Spectroscopy and Ion Processes*, **60**(1984)213.

15. M. Bowker and R.J. Madix, *Surf. Sci.*, **102**(1981)542.

16. P.A. Redhead, *Vacuum*, **12**(1962)203.

17. V.A. Gercher and D.F. Cox, unpublished CO TDS data for SnO_2(110).

18. V.A. Gercher and D.F. Cox, **MANUSCRIPT IN PREPARATION.**

19. P.A. Dilara and J.M. Vohs, *J. Phys. Chem.*, In Press.

20. K.S. Kim and M.A. Barteau, *Langmuir*, **6**(1990)1485.

21. V.E. Henrich, *Reports on Progress in Physics*, **48**(1985)1481.

22. I.E. Wachs and R.J. Madix, *Surf. Sci.*, **84**(1979)375.

23. M.A. Barteau, M. Bowker and R.J. Madix, *Surf. Sci.*, **94**(1980)303.

24. M.A. Barteau, private communication.

25. K.S. Kim and M.A. Barteau, *J. Catal.*, **125**(1990)353.

26. K.S. Kim and M.A. Barteau, *Surf. Sci.*, **223**(1989)13.

27. P. Mars, J.F. Scholten and P. Zwietering, *Advan. Catal.*, **14**(1963)35.

28. K. Tanabe, M. Misono, Y. Ono and H. Hattori, New Solid Acids and Bases (Elsevier, Amsterdam, 1989).

Chapter 4

Water Adsorption on Stoichiometric and Defective SnO_2(110) Surfaces

4.1 Introduction

Because the hydroxylation of oxides is a generally observed phenomenon, there is interest in understanding how water interacts with metal oxides surfaces [1,2], and under what conditions it adsorbs molecularly or dissociatively. Since water is a weak Brønsted acid , dissociation can be considered as a heterolytic acid-base dissociation reaction forming H^+ and OH^-. The site requirements for such heterolytic dissociation reactions are thought to be an available lattice oxygen anion (O^{2-}) to tie up H^+ as OH^-, and an available cation to coordinate the conjugate base anion [3], OH^- in the particular case of water.

A previous titration/displacement reaction study of surface acid-base properties by Barteau and co-workers [4] indicates that the relative acidity of adsorbed Brønsted acids *on oxides* tracks their solution phase acidities. Water (pKa = 15.7, [5,6]) is only slightly less acidic than methanol (pKa = 15.5, [6]) in solution. SnO_2(110) surfaces undergo significant changes in reactivity due to changes in surface condition as shown above in a study of methanol adsorption [7]. Since the acidities of these molecules are so close, any similarities or differences in the dissociation probability as a function of surface condition should suggest the extent to which molecular acidity/basicity can be used as an indicator of the site requirements for such reactions on SnO_2(110) surfaces.

In the present study, surface condition affects the dissociation of water and it is demonstrated that the dissociation is dependent on the type and concentration of oxygen vacancies present on the SnO_2(110) surfaces.

4.2 Experimental

Gas exposures were performed by backfilling the chamber through a variable leak valve. Aldrich HPLC grade water was degassed by repeated freeze-pump-thaw cycles prior to use.

4.3 Results

4.3.1 Thermal Desorption Spectroscopy

Variations in the adsorption of water were examined by TDS for all the surfaces described in Chapter 1. The only desorption product observed was water. No H_2 or O_2 desorption was observed. The desorption behavior is dependent on surface condition as shown below.

4.3.1.1 Stoichiometric and Reduced Surfaces

Figure 4.1a shows the TDS data from a 1.0 L dose of water on a stoichiometric surface at 170 K. Three features are apparent in the water desorption trace: a low temperature feature near 200 K, a broad, intermediate temperature feature near 305 K, and a high temperature feature centered near 435 K. Based on the relative areas of the water features, approximately $15 \pm 5\%$ of the water desorbing from this surface desorbs in the high temperature (435 K) channel.

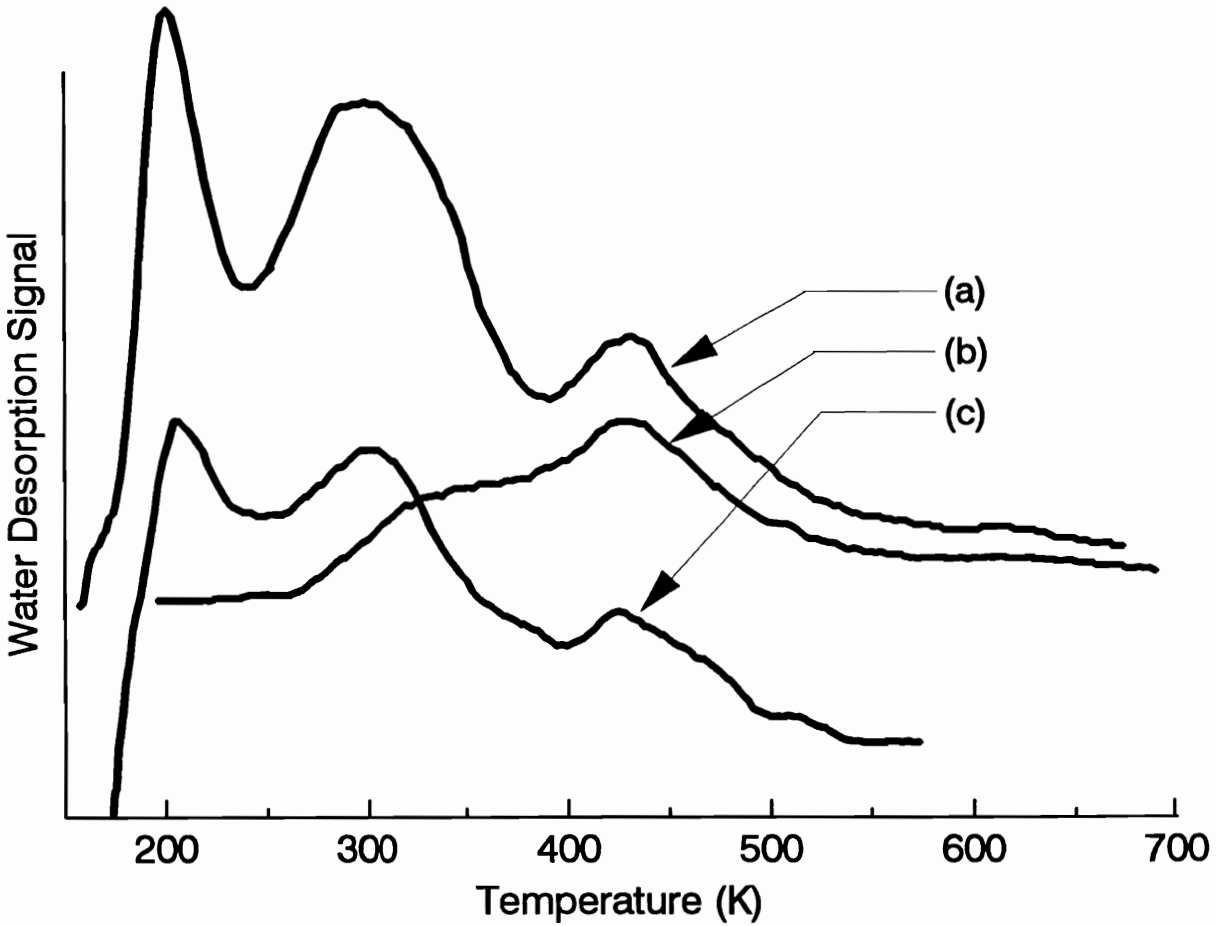

Fig. 4.1 Thermal desorption spectra following 1.0 L doses at 170 K on: (a) the stoichiometric surface and (c) the reduced surface. Fig. 4.1(b) is a TDS spectrum from a clean, stoichimetric surface, no dose at 170 K (see text for details).

Previous work [7,11] and Chapter 1 mentioned a concern with background water uptake on the stoichiometric surface. Figure 4.1b shows a representative water desorption trace from the "clean" (no dose) stoichiometric surface. The amount of background water is approximately equivalent to a 1/8 L water dose at 170 K; about 0.13 ML of water. The data in Fig. 4.1b indicate that approximately 23% of the desorption after a 1 L water dose on the stoichiometric surface is due to the uptake of background water during the initial cool-down period.

Figure 4.1c shows the TDS data from a 1.0 L dose of water on a reduced surface at 170 K. A comparison of Figure 4.1a and 4.1c shows that desorption from the reduced surface is similar to that on the stoichiometric surface. Desorption temperatures are the same and the amount of water desorbed in the high temperature channel is approximately the same ($15 \pm 5\%$). The coverage is lower on the reduced surface, but by an amount equivalent to the uptake of background water on the stoichiometric surface. The reduced surface does not show a significant uptake of background water, due to the heating (to 700 K) this surface undergoes prior to final cooling and dosing, which removes the adsorbed background water.

Room temperature (300 K) adsorption of water was also studied on the stoichiometric and reduced surfaces (Figure 4.2). On both surfaces, a 2.0 L dose was used. As the sample was heated, the signal increased until a broad peak centered at 390 K was formed. When compared with the desorption traces in Figure 4.1, these features track the higher temperature portion of the desorption traces obtained by adsorption at

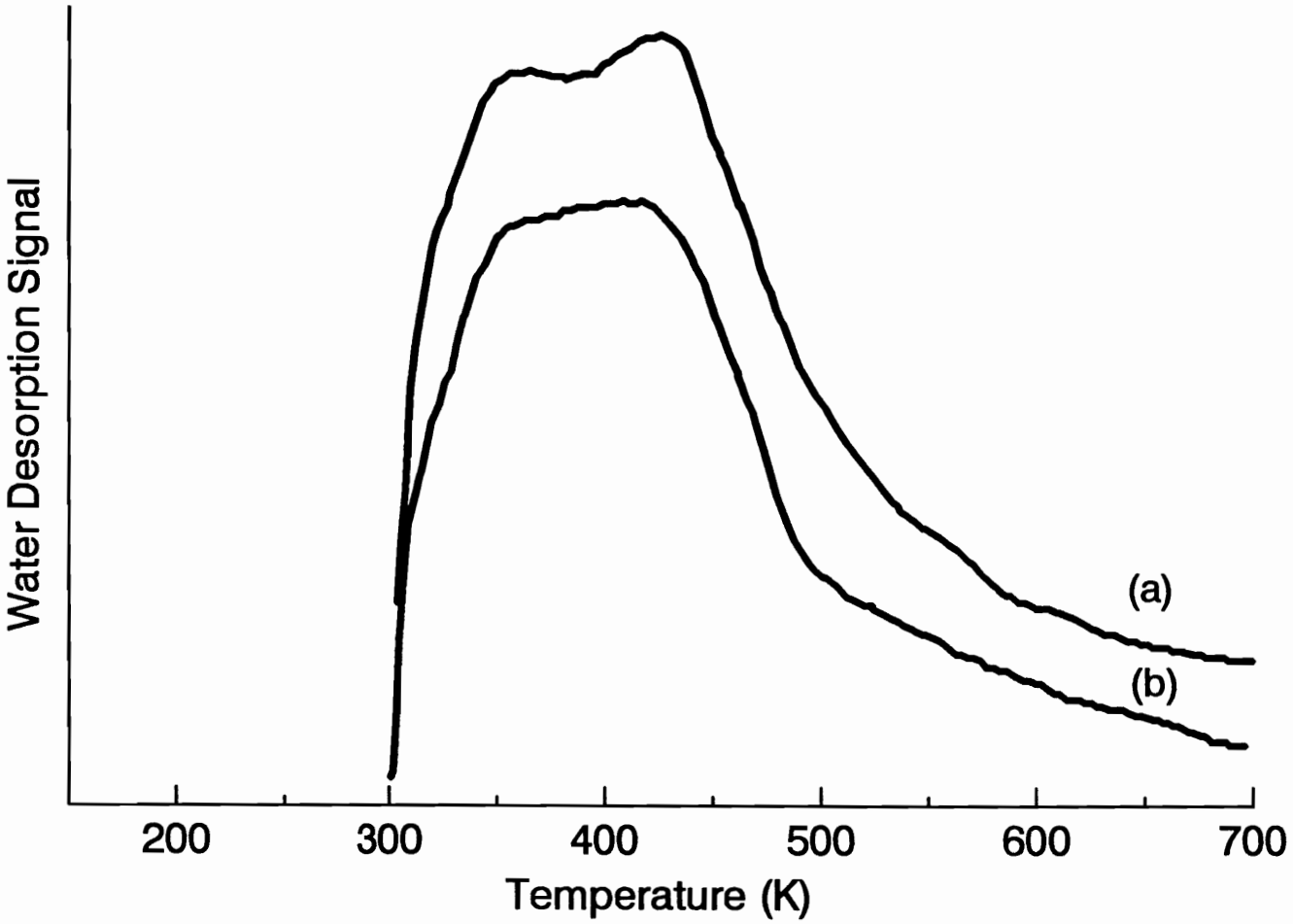

Fig. 4.2 TDS spectra following 2.0 L doses at 300 K on: (a) the stoichiometric surface, and (b) the reduced surface.

lower temperature.

4.3.1.1 Defective Surfaces

Figure 4.3 shows the water desorption data from two different defective surfaces. Figure 4.3a is representative of a less-defective surface prepared by oxidation followed by annealing to 950 K to remove bridging oxygen anions and introduce in-plane oxygen vacancies. This treatment is estimated to leave roughly 80% of the original in-plane oxygen anions intact [14]. Figure 4.3b is representative of a highly-defective surface prepared by ion bombardment and annealing to 1000 K. This second surface is more oxygen deficient than the first [9,10], with an estimated 50% of the original in-plane oxygen anions intact [14]. For Figure 4.3a and b, 1.0 L water doses at 170 K were used. Based on the integrated desorption signals, the total coverages are within about 8% for the two defective surfaces and the reduced surface.

The less-defective surface (Figure 4.3a) shows three features in the water desorption trace: a feature near 200 K, one near 280 K, and a high temperature feature near 450 K. Approximately $35 \pm 5\%$ of the water desorbs in the high temperature channel. The highly-defective surface (Figure 4.3b) has a low temperature feature at 220 K, with the signal tailing off at higher temperatures, and shoulders near 300 K and 435 K. Approximately $10 \pm 5\%$ of the water desorbs in the high temperature channel from the highly-defective surface.

Figure 4.4 illustrates the coverage dependence of TDS desorption behavior of water from the highly-defective surface at 120 K. The

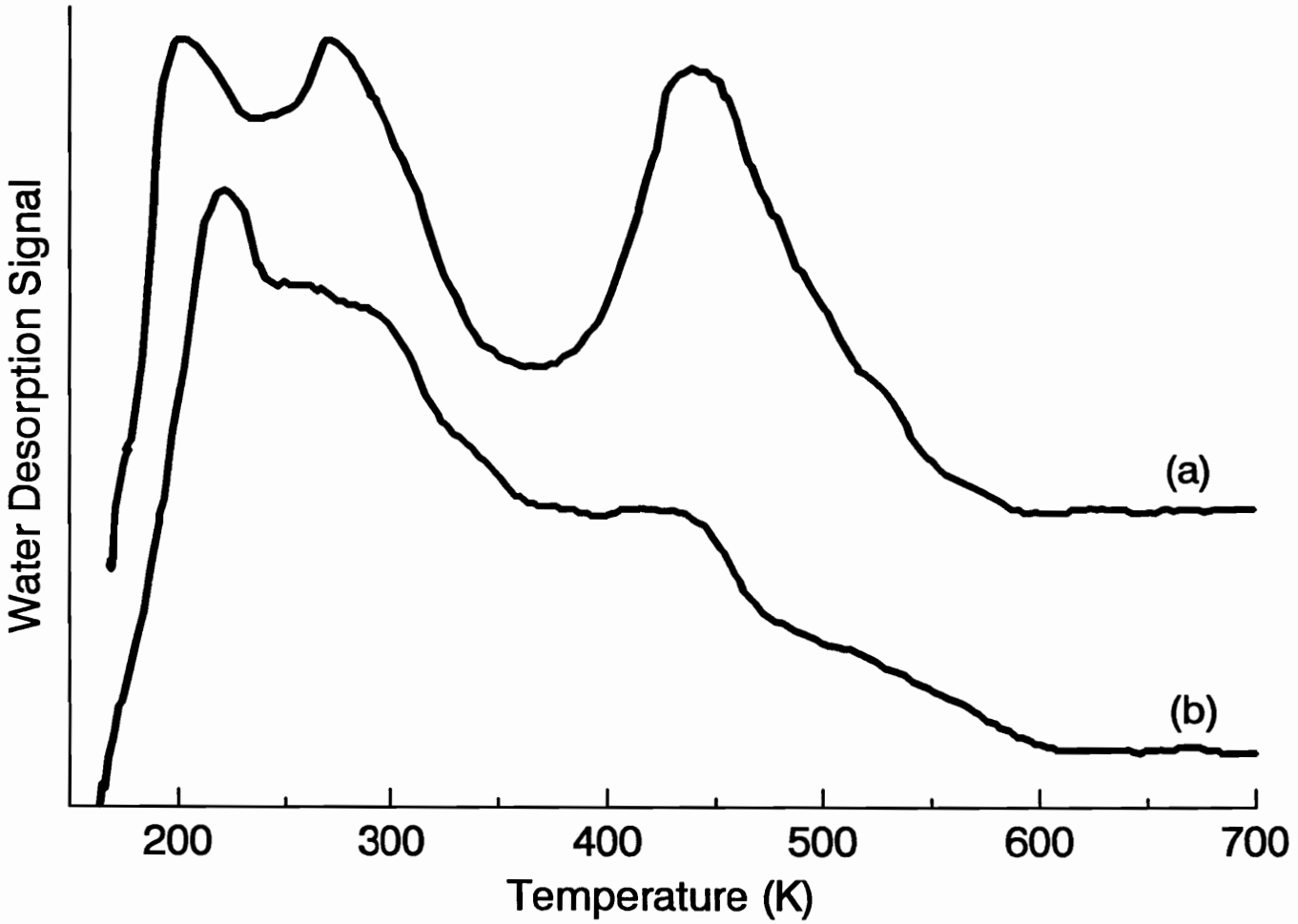

Fig. 4.3 TDS spectra following 1.0 L doses at 170 K on: (a) the less-defective surface, and (b) the highly-defective surface.

coverage for doses above 0.13 L is higher for the 120 K adsorption temperature than for 170 K, due to a higher sticking coefficient at lower dosing temperature. This results in the 1 L doses done at 170 K being equivalent in coverage to a 0.2 L dose at 120 K. The right panel shows the low coverage regime (doses less than 0.3 L) and the left panel shows the higher coverage regime (doses up to 2 L). For the lowest dose (0.03 L), one broad desorption feature centered at 410 K is observed. The broadness of the feature causes difficulty in separating the contributions from the high temperature feature seen at 435 K on other surfaces with those from lower temperature features on this surface. Larger doses result in additional lower temperature features. A feature grows in at about 300 K for a 0.06 dose. For larger doses (0.13 L and above), a lower temperature feature is apparent, initially at 200 K for a 0.13 L dose. This feature decreases to 180 K for a 0.25 L dose, and then increases to 184 K for a 0.5 L dose, 186 K for a 1.0 L dose, and 190 K for a 2.0 L dose. It continues growing without saturation, a characteristic of multilayer desorption. The shift to higher temperature with increasing coverage is also characteristic of zeroth order desorption of multilayer ice observed on metals [15]. The observation of water desorption at 180 K, at the sublimation temperature of multilayer ice [16] for clearly submonolayer coverages of water indicates that after approximately the first ¼ monolayer coverage [17], any additional water interacts as strongly with other water molecules as it does with the surface. A similar effect is observed with TDS on Ag surfaces where water only desorbs at the multilayer temperature regardless of coverage [18].

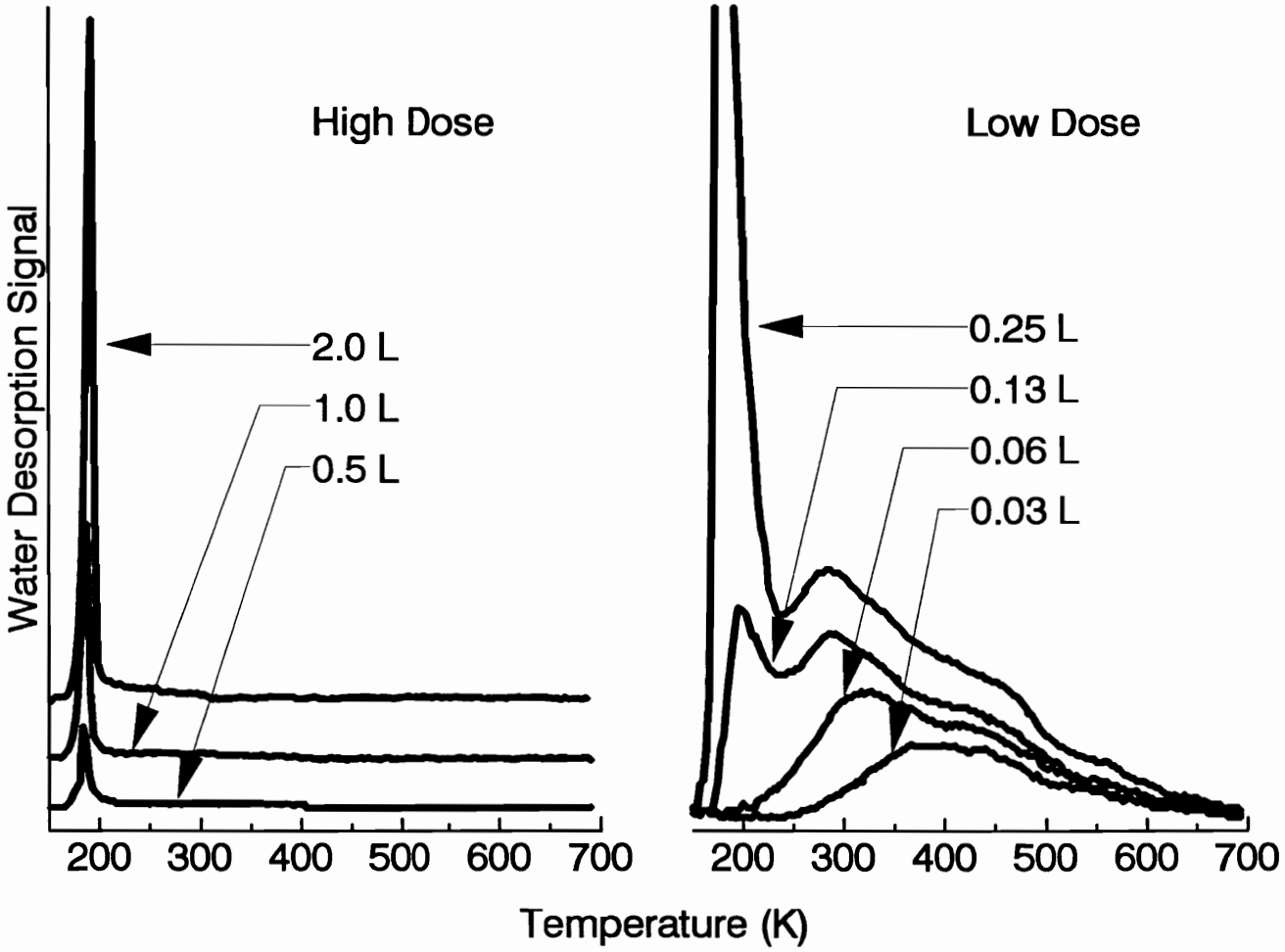

Fig. 4.4 TDS spectra following adsorption on a highly-defective surface at 120 K. The right panel shows the low dose range (0.03 to 0.25 L), while the left panel shows the higher dose range (0.5 to 2.0 L).

The feature near 300 K appears to be first order, identified by the constant peak temperature with changing coverage [19], though the overlap with the higher and lower temperature features makes a precise determination of peak temperature difficult. The Redhead equation [19] can be used to estimate a first-order activation energy for desorption associated with the feature near 300 K. Assuming a normal first-order pre-exponential of 10^{13} sec^{-1} gives an activation energy of 18.7 kcal/mol [16].

The TDS results demonstrate that water desorption shows three features, with peak temperatures mostly independent of the surface condition. A low temperature peak is found near 200 K, an intermediate temperature feature is seen near 300 K, and a high temperature feature can be found near 435 K. The main difference found between the surfaces is the amount of desorption in the high temperature channel: similar amounts on the stoichiometric and reduced surfaces ($15 \pm 5\%$), an increased amount on the less-defective surface ($35 \pm 5\%$), and the least on the highly-defective surface ($10 \pm 5\%$).

4.3.2 Photoemission Measurements

HeII UPS was used to monitor the adsorption of water. The sample was dosed at 120 K. Representative spectra are shown in Figure 4.5 for the highly-defective surface. This surface was used because of the ease of preparation and ability to cool quickly avoiding the uptake of significant amounts of background water. The results for this surface are characteristic of results for the other surfaces. A representative N(E)

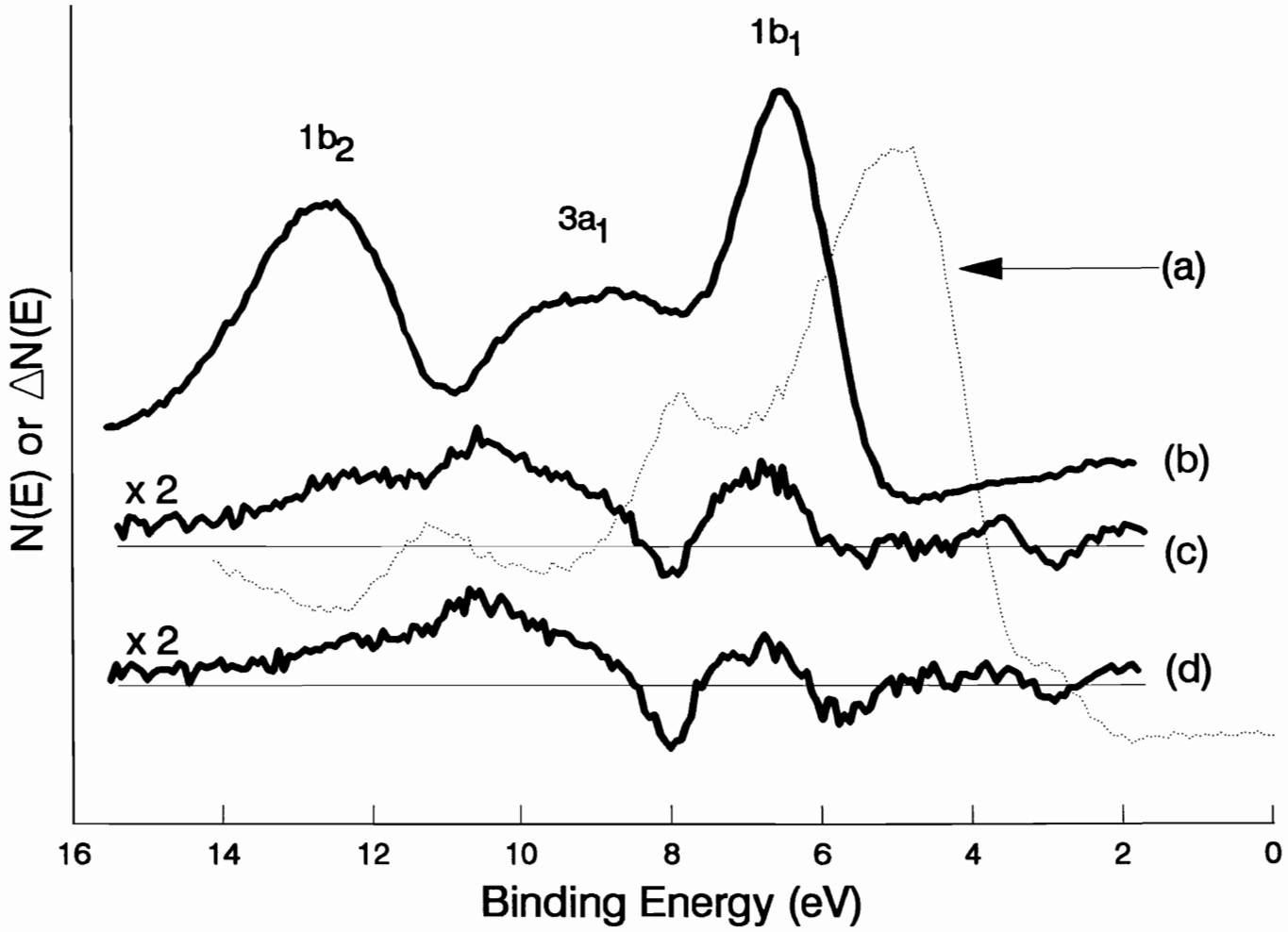

Fig. 4.5 UPS spectra following water adosrption. See text for details.

clean surface spectrum is included (Figure 4.5a) for comparison, and the binding energy is referenced to the Fermi level [20]. Spectra following water adsorption are reported as difference spectra, $\Delta N(E)$. Difference spectra were obtained by subtracting the corresponding clean surface spectrum from that of the dosed surface. Thin horizontal lines represent the zero levels in the difference spectra. Before generating the difference spectra, the spectra were normalized on the emission from the O 2p lone-pair valence band feature for SnO_2 at 4.8 eV, and shifted to align the valence band maximum to account for adsorbate-induced band bending. The difference spectra are referenced to the Fermi level of the clean surface.

Spectrum 4.5b is due to a large coverage of molecular water, formed by a 2.0 L dose at 120 K. Three features are apparent in the spectrum at 6.5 eV, 9.1 eV, and 12.6 eV. Spectrum 4.5b is similar to the gas-phase photoemission spectrum of H_2O [21] and spectra for condensed H_2O multilayers on other surfaces [22-24]. This similarity allows for the identification of molecular orbitals associated with the characteristic emission illustrated by spectrum 4.5b. The feature at 6.5 eV is due to emission from the $1b_1$ lone pair MO. The feature at 9.1 eV is due to emission from the $3a_1$ lone pair MO, and the feature at 12.6 eV is due to emission from the $1b_2$ (π_{OH_2}) MO. The $3a_1/1b_1$ separation for the molecular species, 2.6 eV, is similar to the separation for gas-phase H_2O of 2.2 eV [21], given the broadness of the features for the adsorbed species.

Spectrum 4.5c is the result of heating the surface in 4.5b to 190 K

to remove the large molecular water contribution. This treatment leaves a spectrum characteristic of the surface species associated with the 300 K and 435 K states observed in TDS. The emission at 6.5 eV has shifted down in energy to 6.8 eV, while the emission at 12.6 eV has shifted up in energy to 12.2 eV. The emission in the 9 eV range has broadened, and shows a maximum near 10.5 eV. When the surface is heated further to 300 K leaving surface species associated with the 435 K desorption state in TDS, spectrum 4.5d results. While the spectrum is similar to that of 4.5c, the emission at 12.2 eV due to the $1b_2$ MO of molecular water is attenuated considerably compared to the other features, indicating that little molecular water is present in this spectrum.

In spectrum 4.5c, the feature at 12.2 eV indicates the presence of a small amount of molecular water, possibly by readsorption. However, the broadening of the feature in the 9 eV range and the maximum at 10.5 eV indicates the presence of at least one additional surface species. Previous photoemission studies [1,23,25,26] indicate that the formation of OH^- results in two adsorbate MO's in UPS, the 1π and 3σ , with a separation ranging from 3.3 eV to 4.0 eV [1,25,26]. The maximum centered at 10.5 eV shows a 3.7 eV separation from the emission at 6.8 eV. Hence, the presence of OH^- is likely, with the emission at 10.5 eV due to the 3σ MO of OH^- and the 6.8 eV feature due to both the 1π MO of OH^- and a small contribution from the $1b_1$ MO of molecular water.

4.4 Discussion

The TDS spectra can be explained as follows. The feature seen

near 200 K is identified as molecular water based on the low TDS peak temperature and the predominance of molecular water in the UPS spectrum before this state is removed. The feature seen near 300 K can also be identified as primarily molecular water since UPS indicates the presence of the molecular water $1b_1$ MO. Molecular methanol and formic acid have been identified on this surface at comparable temperatures [7,11], and molecular water has recently been identified on TiO_2(110) in this same temperature range [27]. The desorption order of the feature, apparently first order, is also an indication that the 300 K desorption state is associated with molecular water. The activation energy of 18.7 kcal/mol for this feature can be compared to typical values of 12-17 kcal/mol for first-order desorption of molecular water surface species from metals [15].

The indication of OH^- groups on the SnO_2 surface by UPS after removal of molecular water leads to the conclusion that water dissociation forms surface hydroxyl groups. Disproportionation of OH^- to water and surface oxygen has been observed on various metal surfaces [28,29]. It is reasonable to consider that OH^- disproportionation can occur on oxides as well, as has been proposed for surfaces such as Cu_2O(100), where water desorption was observed at 465 K [30]. Therefore, the TDS desorption feature near 435 K on SnO_2 is assigned to the disproportionation of surface OH^- to form water, $2OH^- \rightarrow H_2O + O^-$.

Based on the TDS results for 1 L exposures at 170 K, there is no apparent difference in the extent of water dissociation (approximately 15% of the total water adsorbed) on the stoichiometric and reduced

surfaces. These two surfaces expose the same number of 5-coordinate Sn^{4+} cations. However, they differ in the removal of the bridging oxygen from the reduced surface, leading to the exposure of an equivalent number of 4-coordinate Sn^{2+} cations. It appears that the exposed 4-coordinate cations do not promote water dissociation, in contrast to the dominant role they play in the dissociation of methanol [7]. However, by the desorption temperature of the dissociated species (435 K), some bridging oxygen is thermally removed from the stoichiometric surface [7]. This allows access to a fraction of thermally-produced 4-coordinate cations during the TDS run even when starting with a stoichiometric surface. From the available data, there is no definitive way to distinguish at which cation sites on these two surfaces water dissociation occurs, though neither appears to be particularly active for the dissociation of water.

A significant increase in the extent of dissociation (up to 35% of the total water adsorbed) is observed on going from the reduced surface to the less-defective surface on which approximately 80% of the in-plane oxygen anions are intact. Apparently, the presence of a *limited* number of in-plane oxygen vacancies promotes dissociation. In an earlier UPS study [31], it was observed that the room temperature interaction of water with SnO_2(110) occurred primarily with electronic states low in the band gap associated with in-plane oxygen vacancies [8]. Both results demonstrate the importance of in-plane vacancies in the dissociative chemisorption of water.

On going from a less-defective surface to a highly-defective surface (approximately 50% in-plane oxygen intact), a decrease in the amount of

dissociation to 10% occurs. As observed with methanol [7] and formic acid [11], the increasing concentration of in-plane oxygen vacancies on the highly-defective surface decreases the dissociation probability. This lack of reactivity on the highly-defective surface is not understood.

Compared to formic acid on these surfaces where the amount of dissociation ranged from 100% on the stoichiometric surface down to 50% on the highly-defective surface, the total amount of water dissociation is low. This difference is attributed primarily to the difference in molecular acidities. Formic acid (pKa of 3.75 [5]) is much more acidic than water (pKa of 15.74 [5,6]) and gives up a proton via heterolytic dissociation much more readily than water, regardless of surface condition.

Molecular acidity does not explain the differences in the dissociation of water and methanol. If molecular acidity was the primary controlling factor, the dissociation of water and methanol would exhibit similar trends as a function of surface condition. However, the extent of methanol dissociation was observed to be greatest on the reduced surface, and declined with an increasing concentration of in-plane vacancies [7]. Details of the interaction of the specific adsorbate with the local defect environment have more effect on the site requirement and dissociation probability than the similar molecular acidity of these weak Brønsted acids would suggest.

The influence of defects on water adsorption has been studied on a variety of metal oxides. In general, defects seem to increase the ability of a surface to adsorb and/or dissociate water. The enhanced capability for

water dissociation can be seen when comparing defect-free and defective surfaces such as $Ti_2O_3(047)$, $TiO_2(100)$, $TiO_2(110)$ and MgO(100) [22,23,27,32]. Defect-free surfaces of these oxides do not dissociate water to a significant extent, while defective surfaces do. The defects considered were oxygen vacancies, leaving cations with vacant coordination sites available on the surfaces. In a study of water adsorption on $TiO_2(100)$ by Lo, *et al.* [22], it was postulated that the presence of the Ti^{3+} ions were required for water dissociation. However, a later study by Kurtz and Henrich on $Ti_2O_3(047)$ [23] demonstrated that the presence of Ti^{3+} cations is not in itself enough to cause dissociation. The local defect environment also has a great effect.

This work on $SnO_2(110)$ leads to a similar conclusion. The mere presence of a defect (oxygen vacancy) is not sufficient to dissociate water on $SnO_2(110)$. The large concentration of bridging oxygen vacancies on the reduced surface do little to increase the dissociation probability relative to the stoichiometric surface. Also, the highly-defective surface (approximately 50% in-plane anions intact) is less efficient than a surface with fewer in-plane vacancies (less-defective surface, approximately 80% intact) at dissociating water. It has been postulated [3] that the site requirement for dissociation of Brønsted acids on oxide surfaces is a vacant coordination site on a cation and an available anion. However, $SnO_2(110)$ surfaces indicate that while this site requirement may be a necessary condition for dissociation, it is not a sufficient condition. The local defect environment plays a considerable role in dissociation on $SnO_2(110)$ surfaces.

4.5 Conclusions

Adsorption of water on four types of SnO_2(110) surfaces was studied; water was the only product observed. Desorption of water occurred at three temperatures: molecular desorption at 200 K and 300 K, and desorption at 435 K attributed to disproportionation. The amount of dissociation was similar (10-15%) on the stoichiometric, reduced and highly-defective surfaces. Dissociation increased to 35% on the less-defective surface. The presence of a limited number of in-plane oxygen vacancies promotes dissociation, but further increasing the concentration of in-plane vacancies decreases the dissociation probability.

4.6 References

1. J.M. McKay and V.E. Henrich, *Phys. Rev. B,* **32**(1985)6764.
2. V.E. Henrich, *Reports on Progress in Physics,* **48**(1985)1481.
3. M.A. Barteau, *J. Vac. Sci. Technol.,* **11**(1993)2162.
4. R.N. Spitz, J.E. Barton, M.A. Barteau, R.H. Staley and A.W. Sleight, *J. Phys. Chem.,* **90**(1986)4067.
5. T.W.G. Solomons, Organic Chemistry, 3rd edition (John Wiley and Sons, New York, 1984), pp. 72 and 778.
6. A. Streitwieser, Jr. and C.H. Heathcock, Introduction to Organic Chemistry (Macmillan Publishing Co., Inc., New York, 1976), p. 215.
7. V.A. Gercher, D.F. Cox and J.-M. Themlin, *Surf. Sci.,* **306**(1994)279, also Chapter 2.
8. D.F. Cox, T.B. Fryberger and S. Semancik, *Phys. Rev. B,* **38**(1988) 2072.
9. P.A. Cox, R.G. Egdell, C. Harding, W.R. Patterson and P.J. Tavener, *Surf. Sci.,* **123**(1982)179.

10. J.M. Themlin, R. Sporken, J. Darville, R. Caudano, J.-M. Gilles and R.L. Johnson, *Phys. Rev. B,* **42**(1990)11914.

11. V.A. Gercher and D.F. Cox, *Surf. Sci.,* **312**(1994)106, also Chapter 3.

12. T.J. Godin and J.P. LaFemina, *Phys. Rev. B,* **47**(1993)6518.

13. D.F. Cox, T.B. Fryberger and S. Semancik, *Surf. Sci.,* **224**(1989) 121.

14. An upper-limit estimate of the in-plane oxygen vacancy density was made using the reaction $CH_3OH + O(l) \rightarrow CH_2O + H_2O$. This relationship indicates that each molecule of methanol converted to formaldehyde extracts one in-plane oxygen anion. Assuming a unity sticking coefficient for methanol, the density of in-plane oxygen defects introduced by successive 0.6 L doses of methanol was calculated. Formaldehyde desorption from each surface was compared to desorption from this experiment to estimate the defect density on each surface. Further details of the calculation can be found in [7].

15. P.A. Thiel and T.E. Madey, *Surf. Sci. Reports,* **7**(1987)211.

16. Our reported temperature is 20 K higher than the accepted value of 160 K for multilayer ice. Our sample and thermocouple mounting technique (see Ref. 7) generally give multilayer temperatures within 5 K of the accepted values in the literature. In this case we apparently get a contribution to our thermocouple reading from the metallic holder used as a support and heater for our SnO_2 sample. If this contribution is reasonably constant over the limited temperature range (up to about 300 K) where we wish to estimate first-order activation energies of desorption, our estimate should be high by less than 1.5 kcal/mol due to the temperature offset.

17. This upper limit estimate is made by assuming a unity sticking coefficient for H_2O at 120 K on the defective surface, and a monolayer coverage equivalent to 1 molecule per surface unit cell. The unit cell density on the (110) surface is about $4.x10^{14}$ cm^{-2}. Based on these assumptions, a 1 L dose of H_2O should produce a 1 monolayer coverage. The equivalent coverage of 1 molecule per surface unit cell as a monolayer is based on the recent estimate by Hugenschmidt *et al.* [Ref. 27] for water on stoichiometric $TiO_2(110)$, a surface with the same basic (cassiterite or rutile) structure as $SnO_2(110)$.

18. K. Bange, T.E. Madey, J.K. Sass and E.M. Stuve, *Surf. Sci.,* **183**(1987)334.

19. P.A. Redhead, *Vacuum,* **12**(1962)203.

20. The Fermi level was determined from the tantalum holder in electrical contact with the semiconducting SnO_2 sample.

21. D.W. Turner, C. Baker, A.D. Baker and C.R. Brundle, Molecular Photoelectron Spectroscopy (Wiley-Interscience, New York, 1970).

22. W.J. Lo, Y.W. Chung and G.A. Somorjai, *Surf. Sci.,* **71**(1978) 199.

23. R.L. Kurtz and V.E. Henrich, *Phys. Rev. B,* **26**(1982)6682.

24. R. Stockbauer, D.M. Hanson, S.A. Flodström and T.E. Madey, *Phys. Rev. B,* **26**(1982)1885.

25. R.L. Kurtz and V.E. Henrich, *Phys. Rev. B,* **28**(1983)6699.

26. J.A. Connor, M. Considine, I.H. Hillier and D. Briggs, *J. Electron Spectr.,* **12**(1977)143.

27. M.B. Hugenschmidt, L. Gamble and C.T. Campbell, *Surf. Sci.,* **302**(1994)329.

28. E.M. Stuve, S.W. Jorgensen and R.J. Madix, *Surf. Sci.,* **146**(1984) 179.

29. C. Benndorf, C. Nöbl and T.E. Madey, *Surf. Sci.,* **138**(1984)292.

30. D.F. Cox and K.H. Schulz, *Surf. Sci.,* **256**(1991)67.

31. D.F. Cox, T.B. Fryberger, J.W. Erickson and S. Semancik, *J. Vac. Sci. Technol. A,* **5**(1987)1170.

32. X.D. Peng and M.A. Barteau, *Surf. Sci.,* **233**(1990)283.

Chapter 5

Reaction of Isopropanol on SnO_2(110) Surfaces

5.1 Introduction

The adsorption of a variety of molecules has been studied on stoichiometric and reduced SnO_2(110) surfaces [1-7], in an attempt to understand the influence of defects on the reactivity of metal oxide surfaces. Two types of crystallographically inequivalent oxygen vacancies, bridging and in-plane, can be studied, and have been seen to have an effect on hydrocarbon oxygenate reactions.

Isopropanol was studied on SnO_2(110) surfaces for two reasons: to compare a secondary alcohol with the primary alcohol previous studied (methanol [2]), and as a reaction probe of acid/base properties of the surfaces. Isopropanol has traditionally been used as an acid/base probe for catalysts [8,9]. Dehydrogenation to acetone is thought to occur over basic sites, and dehydration to propene over acidic sites. Isopropanol adsorption has been studied over many metal oxide catalysts. The selectivity varies from mainly propene with a small amount of acetone on TiO_2 anatase powders [10] (an acidic oxide [8]), to mainly acetone on Co_3O_4 and Fe_2O_3 [11]. However, it has been observed that isopropoxide decomposition often leads to simultaneous acetone and propene desorption, indicating that one site may form both products [12-14].

The two types of oxygen vacancies present on SnO_2 surfaces affect the reactivity and selectivity of isopropanol reactions. Acetone and propene are formed from isopropoxide decomposition, with high C_3

dehydrogenation selectivity, at sites associated with both types of vacancies. Isopropoxide is stabilized by 2.6 kcal/mol at sites associated with in-plane oxygen vacancies compared to sites associated with bridging vacancies. Propene is also formed at sites not associated with vacancies, 5-coordinate Sn^{4+} cations. In contrast to behavior often seen on metals and other oxides, the most defective surface is the least active, the reactivity going through a maximum on the surface with only bridging oxygen vacancies. The acetone formation behavior of this secondary alcohol is similar to that seen for formaldehyde formation from methanol [2]. However, the propene formed has no analogy with methanol.

5.2 Experimental

Gas exposures were performed by backfilling the chamber through a variable leak valve. Aldrich HPLC grade isopropanol (99.5%) was degassed by repeated freeze-pump-thaw cycles prior to use. All doses have been corrected for ion gauge sensitivity [15].

5.3 Results

5.3.1 Thermal Desorption Spectroscopy

Variations in the adsorption and reaction of isopropanol were examined by TDS for all the surfaces described in Chapter 1. Isopropanol, acetone, propene and water were the only observed desorption products. Other products tested for but not observed were CO, CO_2, CH_4 and various C_2 and C_3 products. Evidence for propane formation, less than 1% of the total amount of desorption products, was observed with one

mass fragment at 41 m/z; however, due to the overlap of the major propane mass fragments with product mass fragments from acetone and isopropanol and the CO background, no definitive identification could be made. The total conversion, product distribution and kinetics of the rate-limiting surface reaction steps are dependent on surface condition as shown below.

5.3.1.1 Stoichiometric Surface

Figure 5.1 shows the TDS data obtained following a 0.2 L dose of isopropanol on a stoichiometric surface at a surface temperature of 170 K. Two features are apparent in the isopropanol desorption trace: a main desorption peak at 255 K and a shoulder near 330 K, trailing off above 400 K. Acetone desorbs as a reaction-limited product [4] at 410 K; propene evolves, also as a reaction-limited product [5], with a broad feature near 420 K coincident with acetone, and a larger feature centered near 560 K. The total conversion of isopropanol following the 0.2 L dose is about 50% on this surface. Table 5.1 lists typical values for the total conversion of isopropanol, the acetone and total propene (in both 400-470 K and 575 K ranges) yields and the acetone/propene ratio in the 400-470 K range observed for the various surface conditions.

The isopropanol feature at 255 K is attributed to the desorption of molecular isopropanol, due to the low desorption temperature. The identity of the other features are addressed below.

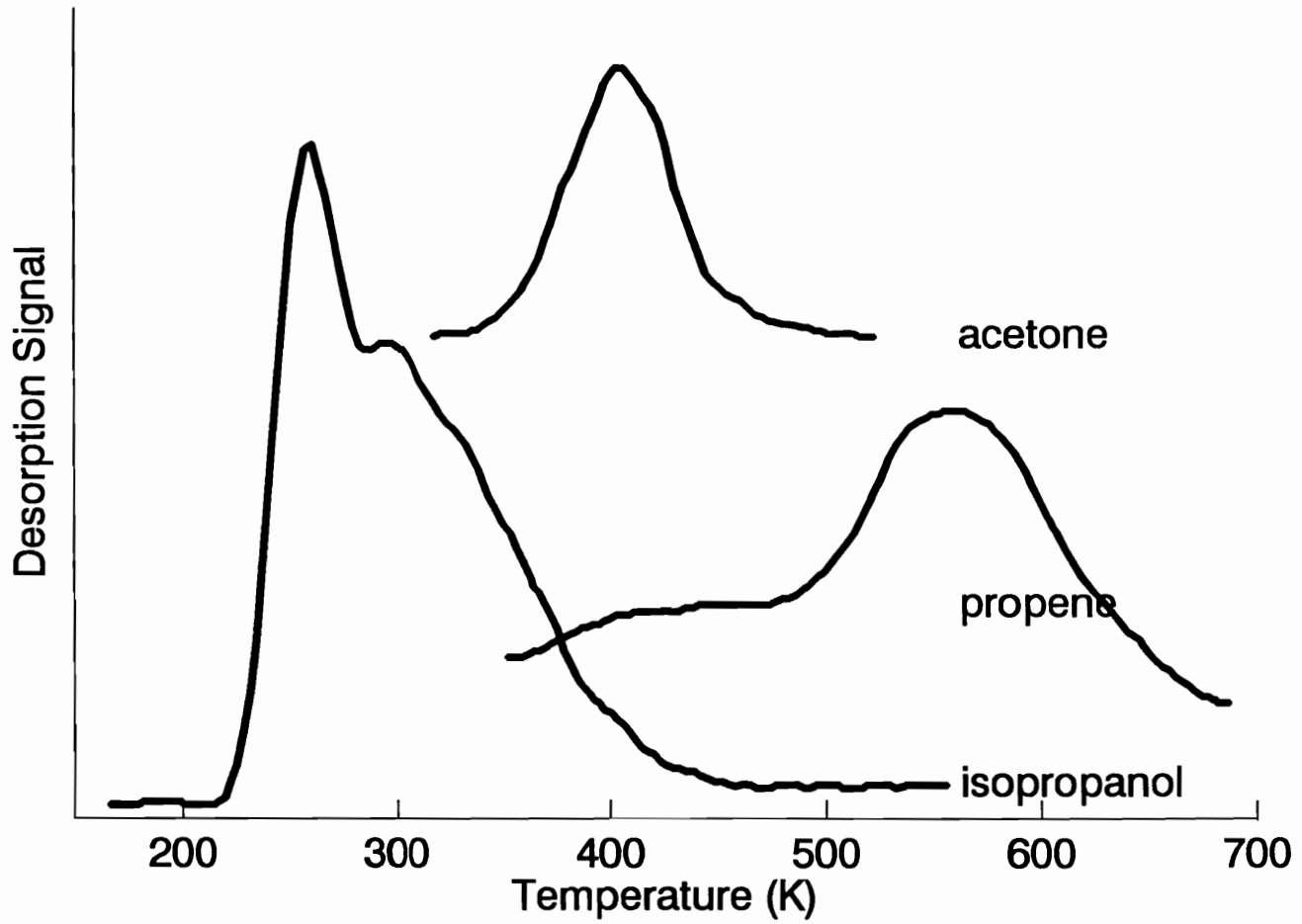

Fig. 5.1 Thermal desorption spectra following a 0.2 L isopropanol dose on the stoichiometric surface.

Table 1. Typical Conversion of 0.2 L Doses as a Function of Surface Condition

Surface Condition	Acetone Yield	Propene Yield	Total Conversion	400 K Acetone/ Propene
Stoichiometric	20%	30%	50%	2.9
Reduced	40%	25%	65%	2.9
Less Defective	15%	20%	35%	2.1
Highly Defective	25%	0	25%	

5.3.1.2 Reduced Surface

Isopropanol adsorbed on the reduced surface was also studied by TDS. As before, a 0.2 L dose was used at a surface temperature of 170 K. The initial total surface coverage following a 0.2 L dose at 170 K was within 15% on all the surfaces investigated. Figure 5.2 shows two features for isopropanol: a feature near 350 K and a shoulder above 400 K. Acetone desorbs in a first-order feature (determined by the peak shape and constant peak temperature as a function of coverage [16]) near 420 K, while propene desorbs in two broad features, one centered near 400 K, also a first-order peak, and one centered near 575 K. Water also desorbs with two broad features: one near 430 K and one near 580 K. The total conversion of isopropanol on this surface is about 65%.

The simultaneous desorption of isopropanol, acetone and propene at 420 K is characteristic of surface isopropoxide decomposition [13]; the rate-limiting step for acetone production is unimolecular hydride elimination from the carbon α to oxygen in isopropoxide: $CH_3CHOCH_3^- \rightarrow CH_3COCH_3 + H^-$. The activation energy for isopropoxide decomposition at 420 K, using the Redhead equation [16] and assuming a normal first-order pre-exponential of 10^{13} s^{-1}, is 26.4 kcal/mol.

Isopropanol desorbing above 300 K is assigned to recombination of a dissociated species, isopropoxide and hydrogen, as discussed below. The maximum amount of isopropoxide is formed on this surface, as evidenced by the maximum conversion, the maximum yield of acetone, and the lack of low temperature molecular isopropanol.

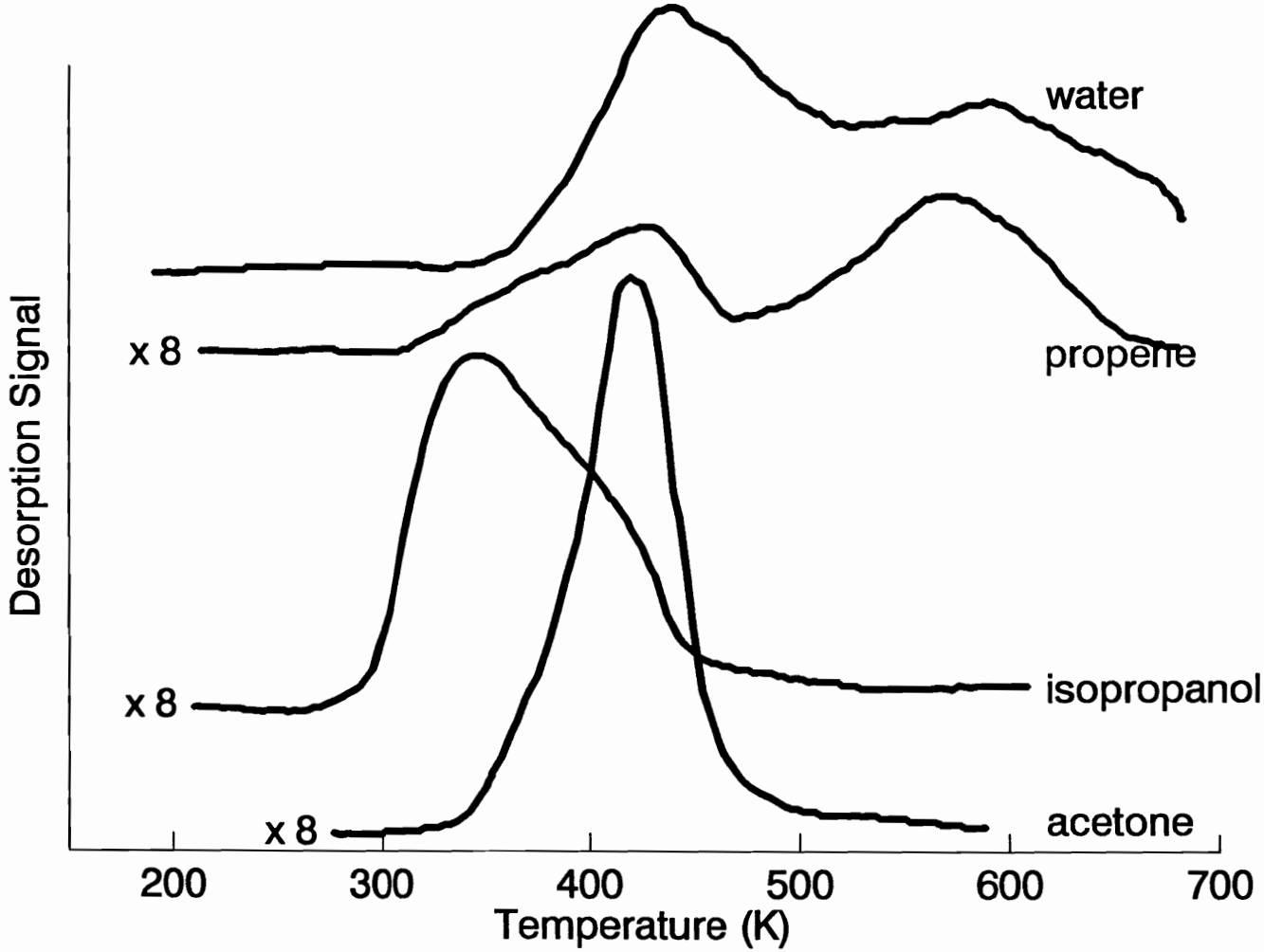

Fig 5.2 TDS following a 0.2 L dose on the reduced surface at 170 K.

5.3.1.3 Defective Surfaces

Figures 5.3 and 5.4 show the results of isopropanol TDS on two different defective surfaces. Figure 5.3 is characteristic of a less-defective surface prepared by oxidation followed by annealing to 950 K to remove bridging oxygen anions and introduce in-plane oxygen vacancies. This treatment is estimated to leave about 80% of the original in-plane oxygen anions intact [3,17]. Figure 5.4 is characteristic of a highly-defective surface prepared by ion bombardment and annealing to 1000 K. This second preparation is more oxygen deficient than the first [18,19], with an estimated 50% of the original in-plane oxygen anions intact [3,17]. In both cases, 0.2 L doses at 170 K surface temperatures were used.

For the less-defective surface (Fig. 5.3), two features can be seen in the isopropanol desorption trace: one feature near 240 K and a broad feature centered near 360 K. Acetone desorbs with a maximum near 410 K and a shoulder centered near 460 K. Propene desorption is seen to evolve with two broad features centered near 470 K and 580 K. The simultaneous acetone and propene desorption again indicate isopropoxide decomposition, with the rate-limiting step unimolecular hydride elimination from the carbon α to oxygen in isopropoxide. The activation energy for isopropoxide decomposition at 460 K, using the Redhead equation [21] and assuming a normal first-order pre-exponential of 10^{13} s^{-1}, is 29.0 kcal/mol. Water desorption occurs with a broad feature having a maximum near 475 K. The total conversion of isopropanol on this surface is 35%.

For the highly-defective surface (Fig. 5.4), three isopropanol

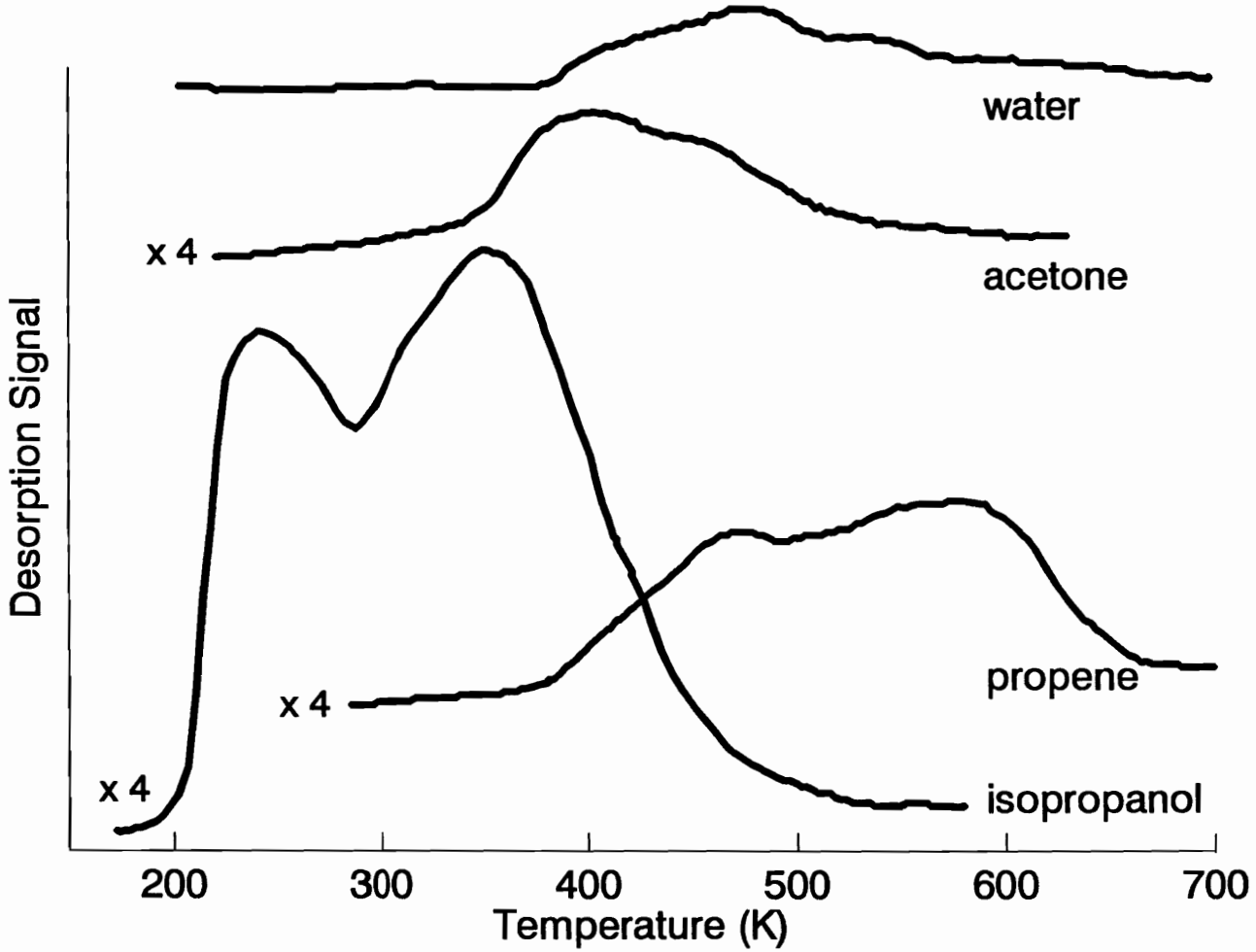

Fig. 5.3 TDS following a 0.2 L dose on the less-defective surface at 170 K.

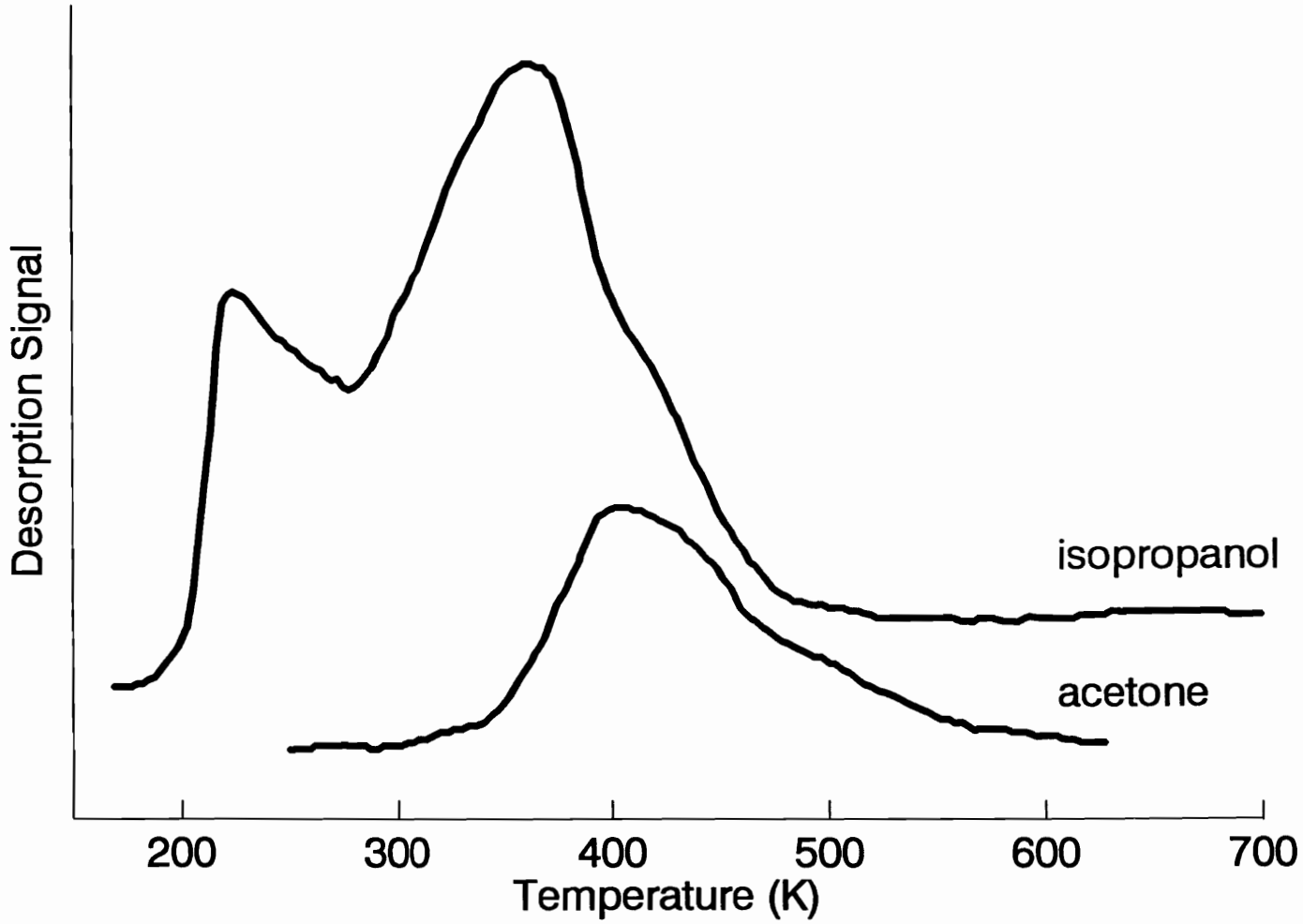

Fig. 5.4 TDS following a 0.2 L dose on the highly-defective surface at 170 K.

features are apparent: one near 230 K, one near 370 K and a shoulder near 420 K. Acetone is the only carbon-containing product observed, desorbing via a first-order process (determined by the constant peak temperature with varying coverage [16]) near 420 K with a broad feature extending to above 500 K. The conversion on this surface is 25%.

The amount of isopropoxide formed is decreased on the defective surfaces compared to the reduced surface. This is evidenced by the decreased conversions and increased low temperature molecular contributions to the isopropanol signals.

In-plane oxygen vacancies can also be introduced chemically. Starting with the reduced surface, it is assumed that the oxidation of isopropanol produces acetone and water, extracting in-plane lattice oxygen anions and having a net reductive effect on the surface: $CH_3CHOHCH_3$ + O(l) → CH_3COCH_3 + H_2O. Isopropanol can also produce propene and water (dehydration); this process results in no net reduction or oxidation: $CH_3CHOHCH_3$ → $CH_3CH{=}CH_2$ + H_2O. A series of experiments (not shown) on a reduced surface using successive 0.2 L doses of isopropanol shows a broadening in the acetone desorption signal from a single first-order peak at 420 K to a feature having contributions from 420 K to above 500 K. The broadening is accompanied by a decrease in reactivity due to chemical reduction of the surface, similar to that observed due to the thermal reduction of the surface described above. No surface carbon buildup was observed.

Figure 5.5 illustrates the coverage-dependent TDS behavior of isopropanol from a highly-defective surface dosed at 120 K. The right

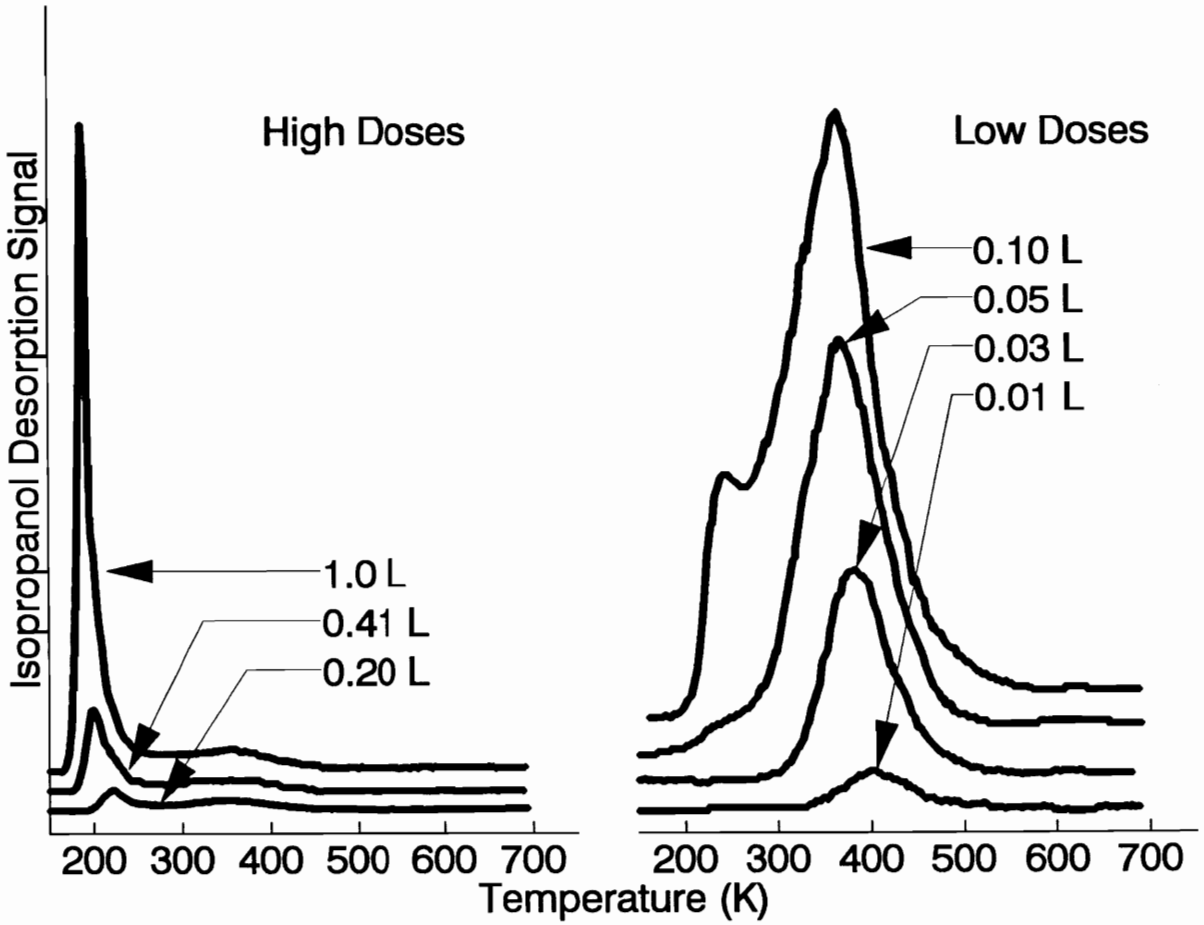

Fig. 5.5 TDS traces following adsorption on a highly-defective surface at 120 K. The right panel shows the low dose range (0.01 to 0.1 L) while the left panel shows the high dose range (0.2 to 1.0 L).

panel shows the low coverage regime (doses from 0.01 L to 0.10 L), while the left panel shows the high coverage regime (doses above 0.10 L). For the lowest dose (0.01 L), one desorption feature centered at 405 K is observed. This feature shifts down in temperature to 387 K for a 0.03 L dose, and further to 369 K for a 0.05 L dose. For the 0.05 L dose, a second feature starts to grow in at 240 K, and continues to grow for a 0.10 L dose. This peak shifts to 222 K for a 0.20 L dose. For doses of 0.41 L and greater a feature appears at 200 K. With doses greater than 1.0 L a final feature appears at 188 K.

A second-order kinetic analysis [16] was done on the feature above 300 K associated with low coverages on the highly-defective surface to test its kinetics. A second-order process would be expected if this feature is associated with the recombination of isopropoxide and hydrogen, as indicated by the high temperature of the feature. The analysis yields a pre-exponential of $2.3 \times 10^{-5} cm^2/s$, reasonable for a second-order process [20], and an activation energy of 16.2 kcal/mol.

5.3.2 XPS Measurements

XPS was used to monitor the adsorption and decomposition of isopropanol. Experiments were done on a highly-defective surface and a stoichiometric surface to compare surfaces in which TDS indicates a significant low temperature molecular isopropanol contribution (below 300 K) and a notable high temperature propene contribution, respectively.

The C 1s spectrum, shown in Figure 5.6(a), for multilayer isopropanol coverages resulting from a 4.1 L dose on the highly-defective

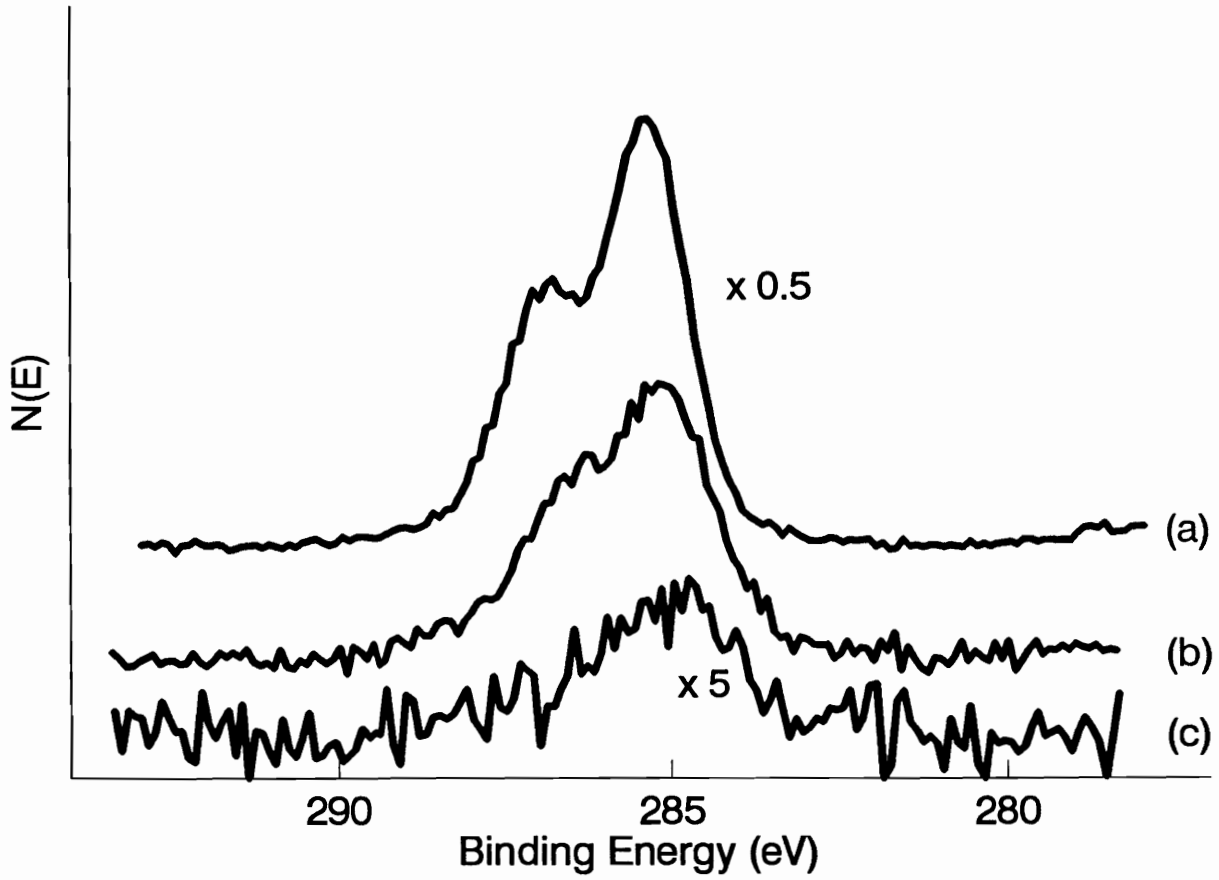

Fig. 5.6 Characteristic C1s XPS spectra following isopropanol adsorption. (a) isopropanol multilayer following a 4.1 L dose on the highly-defective surface at 120 K. (b) surface in (a) heated to 195 K to remove the low-temperature TDS feature associated with molecularly adsorbed isopropanol. (c) stoichiometric surface following a 1.0 L dose and heating to 195 K.

surface is a spectrum which can be resolved into two symmetric Gaussian peaks. A peak at 285.3 eV with a full-width at half-maximum (FWHM) of 1.45 eV is due to the methyl carbons of isopropanol, and the peak at 286.9 eV with a FWHM of 1.35 eV is due to the oxygenated carbon of isopropanol [21]. The methyl carbon/oxygen carbon area ratio is about 1.9, close to that expected for isopropanol. Heating the surface to 195 K to remove the multilayer coverage results in a spectrum, shown in Fig. 5.6(b), in which the two contributions were lowered in energy by approximately 0.4 eV. The methyl carbon/oxygen carbon ratio of this spectrum is about 1.7. This spectrum is typical of isopropoxide species. This assignment is consistent with that made on {011}-faceted TiO_2(001) [22], on which was observed binding energies of 285.7 eV and 287.3 eV for isopropanol; these peaks shifted to 285.4 eV and 286.9 eV for isopropoxide species. Dosing 1.0 L on a stoichiometric surface and then heating to 195 K results in the spectrum shown in Fig. 5.6(c). No distinct isopropoxide peaks can be observed in this spectrum. However, isopropoxide is known to be present on this surface above 195 K, due to isopropoxide decomposition occurring at 400-470 K observed in TDS. The methyl carbon/oxygen carbon ratio for this spectrum is about 3. The width and shape of the feature observed in XPS and the carbon/carbon ratio is consistent with a decrease in the signal from the oxygenated carbon relative to the signal from the methyl carbons, which indicates a second contribution to the signal at 285.3 other than that of isopropoxide. The binding energy of this second contribution is consistent with an isopropyl species [21], though isopropyl cannot be definitively identified

using the XPS data.

5.4 Discussion

The TDS results demonstrate the dependence of the isopropanol reaction behavior on the surface condition. The reactivity goes through a maximum on the reduced surface and is the lowest on the highly-defective surface. The dehydrogenation/dehydration ratio increases as the surface becomes more oxygen-deficient. No non-selective oxidation products were observed.

Isopropanol desorbs in two ranges on all surfaces: below 300 K and above 300 K, and the features can be identified as follows. Isopropanol desorbing between 230 K and 255 K in TDS is due to molecularly adsorbed isopropanol. This assignment is made because of the low temperature of the features and because it is consistent with the XPS data. It is also consistent with assignments made for molecular adsorbates for MeOH [2], HCOOH [3] and H_2O [1] features below 300 K on these surfaces, as well as isopropanol desorption from other metal oxide surfaces. Vohs and Barteau observed molecularly adsorbed isopropanol desorb below 300 K on the (0001)-O polar ZnO surface [12], while Kim and Barteau saw molecular isopropanol desorb at 260 K on the {011}-faceted TiO_2(001) surface [22].

Isopropanol desorbing above 300 K does not originate from a molecular surface species, and may be assigned to two different rate-limiting steps. The first is recombination of isopropoxide and surface hydrogen, occurring between 300 and 400 K, below the isopropoxide

decomposition temperature range from 400-470 K: $CH_3CHOCH_3^-$ + H^+ → $CH_3CHOHCH_3$. Surface hydrogen is traditionally considered to be bound to a surface oxygen anion [23]. The process is second-order as most clearly observed on the highly-defective surface where the conversion is lowest. The second rate-limiting step for isopropanol formation occurs above 400 K, simultaneously with acetone and propene production. This rate-limiting step is the first-order, unimolecular hydride elimination described above, which is followed by isopropoxide and surface hydrogen recombination to form isopropanol. All isopropanol desorbing above 300 K is due the recombination of isopropoxide and hydrogen.

Acetone desorbs at two temperatures, dependent on the surface condition. The simultaneous desorption of acetone, isopropanol, water and propene at 420 K and 460 K is an indication that they evolve from an isopropoxide intermediate, and that the rate-limiting step is unimolecular isopropoxide decomposition. Acetone is a dehydrogenation product from isopropoxide, formed by hydride elimination from the carbon α to oxygen in isopropoxide. Acetone is a reaction-limited product in both temperature ranges [4].

One of the motivations for this work is trying to understand the effect of introducing two types of oxygen vacancies, bridging and in-plane, on the interaction of molecules with the SnO_2(110) surface. Both types of vacancies affect the reactivity of isopropanol and the kinetics of isopropoxide decomposition.

The effect of introducing bridging oxygen vacancies can be studied

by comparing the stoichiometric and reduced surfaces. The stoichiometric surface ideally has no bridging vacancies, though a limited number are formed thermally during a TDS run. The reduced surface ideally has only bridging vacancies. Isopropoxide decomposition occurs only at 420 K on both surfaces. The molecular contribution in TDS decreases as conversion increases; the amount of dissociation changes from surface to surface. The maximum amount of isopropoxide is formed on the reduced surface, indicating that dissociation to isopropoxide is promoted by 4-coordinate Sn^{2+} cations exposed on the reduced surface. Therefore, the dissociation of isopropanol and decomposition of isopropoxide to form acetone at 420 K is dependent on the presence of the 4-coordinate Sn^{2+} cations. The limited reactivity observed for this process on the stoichiometric surface is attributed to the thermal removal of bridging oxygen during the course of the TDS run. A similar conclusion was reached for MeOH [2] reacting to produce formaldehyde on these surfaces. The introduction of bridging vacancies also increases the selectivity for the dehydrogenation process and decreases the amount of high temperature propene formed.

The effect of in-plane oxygen vacancies can be seen by comparing the reduced and defective surfaces. The reduced surface ideally has no in-plane vacancies, while the less-defective surface has a maximum of 20% in-plane vacancy density and the highly-defective surface has a maximum of 50% in-plane vacancy density [17]. The desorption of acetone at 460 K, also a result of isopropoxide decomposition, occurs only on defective surfaces. Therefore, it is associated with in-plane oxygen

vacancies. Isopropanol decomposition to form acetone at two temperatures is similar to methanol decomposition behavior [2]; methoxide decomposed to form formaldehyde at 450 K and 540 K. There is a 2.6 kcal/mol stabilization of isopropoxide at cations associated with lower coordination sites at in-plane vacancies compared with those associated with bridging vacancies. However, as the density of in-plane defects increases, the alcohol dissociation probability decreases, which in turn decreases the overall reactivity. The overall dehydrogenation/dehydration ratio continues to increase as the surface becomes more oxygen deficient.

Propene desorbs in two temperature ranges: 400-470 K and near 575 K. Propene is the dehydration product from isopropanol and is formed when the alcohol undergoes C-O bond cleavage and hydrogen elimination It is a reaction-limited product in both temperatures ranges [5].

Propene in the 400-470 K range is produced by alkoxide decomposition with a first-order rate-limiting step, unimolecular isopropoxide decomposition, suggested by the simultaneous desorption with acetone. Simultaneous propene and acetone desorption has been observed previously on ZnO single crystal surfaces [13]. The amount of propene formed in this temperature range is proportional to the amount of acetone formed on all surfaces except the highly-defective surface (which forms no propene), with an propene/acetone ratio of approximately 0.4.

Propene desorbing at 575 K is formed by a rate-limiting step other than isopropoxide decomposition (as observed at 400-470 K), since no acetone is formed. The preferred site at which propene in the 575 K channel is formed is not the 4-coordinate Sn^{2+} cations, because if this

process were competing with acetone formation, the amount of propene formed would increase on going from the stoichiometric to the reduced surface as noted for acetone production. Also, the site is not associated with in-plane vacancies, because if it were, propene in this channel would not be formed on the stoichiometric surface which has no in-plane defects initially present, and propene production would increase on going to the defective surfaces, the opposite of the observed trend. Therefore, the proposed site for this propene formation process is the 5-coordinate Sn^{4+} cation. This is the only site initially present on the stoichiometric surface, still present in an equal density on the reduced surface and with a decreased concentration as the surface becomes more defective.

Olefin formation from primary and secondary alcohols is thought to require alkoxide formation and deoxygenation accompanied by ß-hydride elimination [10,22]. C-H bond activation from surface hydrocarbon fragments has been observed on $Cu_2O(100)$ [24,25], causing water formation between 500 K and 600 K, above alkoxide decomposition temperatures. C-H bond activation of methyl groups was also observed at 600 K for t-butoxide formed from t-butanol adsorbed on Cu(110) [26], which dehydrogenated to produce isobutylene. Water desorbs between 500 K and 600 K after isopropanol adsorption on SnO_2 surfaces which form propene, a reasonable temperature range to expect C-H bond activation from isopropyl, above the isopropoxide decomposition temperatures. C-H bond activation from isopropyl is a possible rate-limiting step for propene formation at 575 K and water formation between 500 and 600 K. It is thought that propene formed at 575 K is

not due to alkoxide decomposition similar to that occurring at 400-470 K because if so, acetone would be observed desorbing at 575 K in an analogous process. A preliminary assignment of the intermediate leading to propene at 575 K is an isopropyl species. There is no direct spectroscopic evidence for an isopropyl intermediate, but the XPS data does not contradict the idea. The process suggested is as follows: (1) $CH_3CHCH_3^- \rightarrow CH_3CHCH_2 + H^-$. The data give no insight into the number or order of elemental steps required to form the isopropyl species.

It can be seen that the amount of propene formed at 575 K is dependent on the surface condition. On the stoichiometric surface, the propene yield in the 575 K channel is 22%, while on the reduced surface it is about 9% and on the less-defective surfaces it is about 14%. No propene is formed on the highly-defective surface. Apparently, the 4-coordinate alkoxide decomposition sites compete successfully for isopropoxide when they are formed on the reduced surface, while Sn^{4+} sites are present in decreasing numbers on the defective surfaces, with few or none on the highly-defective surface.

Water is observed desorbing between 400 and 500 K (in addition to that observed between 500-600 K). The source of hydrogen for water formed in the 400-500 K range is the acidic proton lost by alcohol dissociation and hydride elimination during alkoxide decomposition. The source of the oxygen may be either oxygen from propene formation or surface lattice oxygen. There are two possible contributions to the water signal in this temperature range involving desorption-limited and reaction-limited kinetics. A previous water adsorption study on SnO_2(110)

surfaces [1] attributed water desorption near 435-450 K to OH disproportionation as the rate-limiting step, which can be associated with the lower temperature water desorption following isopropanol adsorption: $2OH^- \rightarrow H_2O + O^{2-}$. Any water desorbing above 450 K (but below 500 K) must be reaction-limited with isopropoxide decomposition as the rate-limiting step. The two contributions cannot be separated due to overlapping water signals.

Isopropanol has traditionally been used to probe acid/base sites on oxide catalyst surfaces [8,9]. Dehydrogenation is considered a base-catalyzed process, while dehydration is considered an acid-catalyzed process. Acetone formation, however, is very often accompanied by propene. On the (0001)-Zn polar surface of ZnO, Vohs and Barteau [12] observed that acetone and propene form at similar temperatures from isopropanol adsorbed at 300 K, with a dehydrogenation/dehydration selectivity of order unity. Lui *et al.* observed simultaneous acetone and propene formation from Zn-polar, O-polar and non-polar ZnO surfaces [13], with increasing dehydrogenation/dehydration selectivity from Zn- to O-polar to non-polar. Both groups assigned acetone and propene formation to alkoxide decomposition at a single site. Even substances with very strong basic sites which form predominantly acetone, such as CsNaY zeolites and MgO powders [27], form some propene from isopropoxide. On SnO_2(110), both acetone and propene were formed as well, at Sn^{2+} cations associated with bridging and in-plane oxygen vacancy sites, and while two different sites are suggested, both products form at each site. The individual selectivities at each site cannot be

determined due to overlapping signals, but the overall dehydrogenation/dehydration ratio from alkoxide decomposition is approximately 2.5 on all surfaces except the highly-defective surface. Both ZnO [8] and SnO_2 [28] are considered amphoteric oxides with both basic and acidic properties as determined using indicator tests which test average surface properties and not specific sites. There may be some correlation between the dehydrogenation/dehydration selectivity and the acid/base properties of a surface site, but it is unknown what controls the isopropanol reaction selectivity at a given site.

Isopropanol decomposition has also been studied on the {011}-faceted TiO_2(001) surface [22]. This facet exposes only Ti^{4+} cations with one coordination vacancy. The reaction of isopropanol with other facets of the TiO_2(001) crystal has not been reported. TiO_2 is considered an acidic oxide [8]. Only propene, H_2O and H_2 were formed from isopropoxide decomposition on this surface, although primary alcohols adsorbed on the same surface did form small amounts of dehydrogenation products. The TiO_2 results can be compared to propene formation at 575 on SnO_2(110), which was attributed to Sn^{4+} cations with one coordination vacancy. Both Sn^{4+} and Ti^{4+} are considered hard acids [29]. In comparison, the Sn^{2+} cation at which acetone and propene are formed simultaneously is considered a borderline (between hard and soft) acid [28], which would lead one to expect that, of the two sites, the Sn^{4+} site would form propene preferentially. On the other hand, while acid/base considerations may be useful for rationalizing Sn^{4+} as a preferred site for dehydration, they do not offer any insight into the

predominantly "basic" dehydrogenation channel observed at "acidic" Sn^{2+} sites and in-plane oxygen vacancies.

The overall selectivity trend, that the selectivity for dehydrogenation increases as the surface becomes more oxygen-deficient, seems to indicate that basicity of the surfaces increases with oxygen-deficiency. This is consistent with acid/base concepts, which suggest that cations in lower oxidation states are less acidic than those in higher oxidation states. However, the opposite trend was observed for HCOOH [3], another traditional probe of acid/base behavior [30]. HCOOH showed the highest dehydrogenation selectivity on the stoichiometric surface, and the dehydrogenation/dehydration ratio decreased as the surface became more oxygen deficient; low coordination sites that are highly reduced readily deoxygenate surface formate species to reoxidize themselves, while higher coordination sites do not. The most "acidic" sites (those associated with dehydrogenation) are those associated with in-plane vacancies. These results are consistent with oxidation/reduction concepts, in that easily reducible surfaces form greater amounts of the dehydrogenation product, while less reducible surfaces form lesser amounts of the dehydrogenation product. Formic acid may be probing the acid/base nature of the anions, while isopropanol probes the nature of the cations. The contradictory nature of these results shows that the application of traditional acid/base, redox concepts and probe molecules to oxide surfaces are not always straightforward.

As shown above, isopropanol dissociates to isopropoxide most readily on the 4-coordinate Sn^{2+} cations present in the largest amount on

the reduced surface. Acetone formed at these cations desorbed at 420 K. As in-plane vacancies are introduced, acetone is also produced at 460 K, a stabilization of the isopropoxide of 2.6 kcal/mol. As the density of in-plane vacancies increased, isopropanol dissociation to isopropoxide and acetone production decreased. Methanol [2] on these surfaces shows a lower conversion to formaldehyde on the highly-defective surface (< 5%) and more stabilization of methoxide by in-plane vacancies (nearly 6 kcal/mol) than isopropoxide. Otherwise the trend of aldehyde and ketone production from surface to surface was the same for the two alcohols and is due to the extent of dissociation to alkoxide by each surface. The conclusion for methanol was that the available cations controlled dissociation. A similar conclusion can be drawn for isopropanol dissociation leading to isopropoxide decomposition in the 400 K temperature range.

Isopropanol decomposition leading to propene formation at 575 K also depends on the available cations due to the fact that this process appears to occur only on 5-coordinate Sn^{4+} cations. The type of available oxygen anion seems to be of less importance to the decomposition of isopropanol at all temperatures.

The results of the present study confirm the conclusion reached by others [12,22] that the use of isopropanol as an acid/base probe molecule is not straightforward. It also confirms previous work on SnO_2 [1-3] which showed that reactivity and selectivity of oxygenate reactions are surface dependent, and that reactivity is lowest on the most defective surface. Again, the local defect environment appears to have more

significance on reactivity and selectivity than the mere presence of a defect.

5.5 Conclusions

Isopropanol adsorption was studied on four SnO_2(110) surfaces with varying densities of oxygen anion vacancies. Molecular isopropanol is observed to desorb below 300 K, similar to methanol [2] and formic acid [3] studied previously on these surfaces. Isopropanol dissociates to isopropoxide, which further reacts to form acetone, propene, isopropanol and water at 420 K and 460 K. Isopropoxide decomposition as the rate-limiting step at 420 K is associated with bridging oxygen anion vacancies, while isopropoxide decomposition at 460 K is associated with in-plane oxygen anion vacancies. The propene/acetone selectivity in the 400 K range was about 0.4 on all surfaces except the highly-defective surface.

Isopropanol also undergoes another reaction, to form propene and water at 575 K on all surfaces but the highly-defective surface. The proposed site for this reaction is the 5-coordinate Sn^{4+} cation, and while there is no direct evidence for the intermediate resulting in propene formation at this temperature, an isopropyl intermediate is suggested.

The overall activity goes through a maximum on the reduced surface, and is lowest on the highly-defective surface. The overall dehydrogenation/dehydration ratio increases as the surface becomes more oxygen deficient.

5.6 References

1. V.A. Gercher and D.F. Cox, *Surf. Sci.*, **SUBMITTED**, also Chapter 4.

2. V.A. Gercher, D.F. Cox and J.-M. Themlin, *Surf. Sci.*, **306**(1994)279, also Chapter 2.

3. V.A. Gercher and D.F. Cox, *Surf. Sci.*, **312**(1994)106, also Chapter 3.

4. V.A. Gercher and D.F. Cox, unpublished acetone TDS data from SnO_2(110).

5. V.A. Gercher and D.F. Cox, unpublished propene TDS data from SnO_2(110), also Chapter 6.

6. V.A. Gercher and D.F. Cox, unpublished CO TDS data from SnO_2(110).

7. V.A. Gercher and D.F. Cox, **MANUSCRIPT IN PREPARATION.**

8. K. Tanabe, Solid Acids and Bases (Academic Press, New York, 1970).

9. M. Ai, *Bull. Chem. Soc. Jpn.*, **50**(1977)2579.

10. K.S. Kim, M.A. Barteau and W.E. Farneth, *Langmuir*, **4**(1988)533.

11. C. Daniel, M. Subrahmanyam and J.C. Kuriacose, *Indian J. Chem.*, **13**(1974)419.

12. J.M. Vohs and M.A. Barteau, *J. Phys. Chem.*, **95**(1991)297.

13. K. Lui, S. Akhter and H.H. Kung, *Solid St. Chem. Catal.*, **12**(1985)206.

14. M. Bowker, R.W. Petts and K.C. Waugh, *J. Catal.*, **99**(1986)53.

15. The ion gauge sensitivity for isopropanol was taken as 4.91. This ion gauge sensitivity was calculated using a correlation by S. George for hydrocarbons and alkyl chlorides reported in R.L. Brainard and R.J. Madix, *J. Am. Chem. Soc.*, **111**(1989)3826.

16. P. A. Redhead, *Vacuum*, **12**(1962)203.

17. An upper limit estimate of the in-plane oxygen vacancy density was made using the reaction $CH_3OH + O(l) \rightarrow CH_2O + H_2O$. This relationship assumes that each molecule of methanol converted to formaldehyde extracts one in-plane oxygen anion. Assuming a unity sticking coefficient for methanol, the density of in-plane oxygen defects introduced by successive 0.6 L doses of methanol was calculated and used as a reference. Formaldehyde desorption from the reaction of methanol with the less-defective and highly-defective surfaces were compared to desorption from the reference experiments to estimate the defect density on each surface. Further details of the calculation can be found in Ref. 2.

18. D.F. Cox, T.B. Fryberger and S. Semancik, *Phys. Rev. B*, **38**(1988)2072.

19. D.F. Cox, T.B. Fryberger and S. Semancik, *Surf. Sci.*, **224**(1989)121.

20. See for example, R.L. Brainard and R.J. Madix, *J. Am. Chem. Soc.*, **111**(1989)3826, and references therein.

21. J.F. Moulder, W.F. Stickle, P.E. Sobol and K.D. Bomben, Handbook of X-ray Photoelectron Spectroscopy (Perkin-Elmer, Eden Prairie, 1992).

22. K.S. Kim and M.A. Barteau, *J. Molec. Catal.*, **63**(1990)103.

23. M.A. Barteau, *J. Vac. Sci. Technol.*, **11**(1993)2162.

24. K.H. Schulz and D.F. Cox, *J. Phys. Chem.*, **97**(1993)3555.

25. K.H. Schulz and D.F. Cox, *J. Phys. Chem.*, **97**(1993)647.

26. R.L. Brainard and R.J. Madix, *Surf. Sci.*, **214**(1989)396.

27. P.E. Hathaway, Ph.D. Dissertation, Virginia Tech, 1989.

28. K. Tanabe, *et al.*, New Solid Acids and Bases, (Elsevier, New York, 1989).

29. J.E. Huheey, E.A. Keiter and R.L. Keiter, Inorganic Chemistry, (HarperCollins College Publishers, New York, 1993), p. 347.

30. P. Mars, J.F. Scholten and P. Zwietering, *Advan. Catal.*, **14**(1963)35.

Chapter 6

Propene Adsorption

6.1 Introduction

Propene oxidation is a much studied process over metal and metal oxide catalysts [1,2] due to the need for oxygenated chemicals in the petrochemical industry. The selective oxidation of propene to products such as acrolein, propylene oxide, acrylonitrile and acrylic acid over a variety of catalysts has been seen. Copper (I) oxide [3] and bismuth molybdate [4-6] catalysts have proven useful for acrolein formation, while propylene oxide formation occurs over a wide variety of catalysts [7-10]. Propene adsorption studies have been done on a few single crystal metal and metal oxide surfaces. On metal oxides, Schulz and Cox [11] studied propene oxidation to acrolein on Cu_2O surfaces, while Lui *et al.* [12] studied propene adsorption (no reaction) on ZnO surfaces. On metal surfaces, Barteau and Madix [13] saw no reaction on clean Ag(110) and only complete oxidation of propene on Ag(110) with pre-adsorbed oxygen. The most commonly proposed initial reaction intermediate in the selective oxidation of propene is a symmetric π-allyl intermediate [11,12,14-16] formed by the loss of a methyl (allylic) hydrogen.

As a single component catalyst, SnO_2 shows low activity and selectivity for the selective oxidation of propene [1,17,18]; in general, most of the products are complete oxidation products, CO and CO_2. Fattore *et al.* [17] suggested that this is a result of the rapid use of surface oxygen and slow diffusion of oxygen from the bulk. However, SnO_2 used

as a component in mixed oxide catalysts works much more effectively [1], increasing both selectivity and activity, such as with SnO_2/MoO_3 catalysts [18-20].

A preliminary propene adsorption study has been carried out on SnO_2(110) single crystal surfaces with varying amounts and types of surface oxygen vacancies using thermal desorption spectroscopy (TDS), to find the desorption-limited behavior of propene to compare to propene desorbing as a product from isopropanol reaction. Propene desorbs in several temperature ranges dependent on the surface condition, with a high temperature desorption state associated with in-plane oxygen vacancies.

6.2 Experimental

Gas exposures were performed by backfilling the chamber through a variable lead valve. Matheson polymer grade propene (99.5%) was used as received. All doses have been corrected for ion gauge sensitivity [21].

6.3 Results

6.3.1 Thermal Desorption Spectroscopy

Variations in the adsorption of propene were examined by TDS for all the surfaces described in Chapter 1. Propene was the only desorption product observed on all the surfaces. CO, CO_2 and H_2O were observed desorbing from the stoichiometric and reduced surfaces; however, much of the CO, CO_2 and H_2O data cannot be distinguished from background CO, CO_2 and H_2O formed on the sample hardware which desorbs at

similar temperatures to that observed after propene adsorption. A new preparation technique must be developed to eliminate the hardware signals so it may determined whether oxidation products are observed coming from SnO_2(110) surfaces. No selective oxidation products were observed. Products tested for but not observed included acrolein, CH_4, formaldehyde, propane, 1,5-hexadiene, various C_2 products and propylene oxide. Coverages are apparently surface dependent and are very sensitive to dosing temperature.

6.3.1.1 Stoichiometric Surface

Figure 6.1a shows the TDS data obtained following a 0.3 L dose of propene on a stoichiometric surface at 170 K. Three features are apparent in the propene desorption trace: a main desorption peak at 210 K, a shoulder near 250 K, a broad feature centered near 360 K.

6.3.1.2 Reduced Surface

Propene adsorbed on the reduced surface at 170 K was also studied by TDS, again using a 0.3 L dose. Figure 6.1b shows three features for propene: the main desorption peak at 217 K, a feature with a maximum near 325 K and a small, broad feature extending from 400 K to 550 K.

6.3.1.3 Defective Surfaces

Figure 6.1c and d shows the results of propene TDS on two different defective surfaces. Figure 6.1c is characteristic of a less-defective surface prepared by oxidation followed by annealing to 950

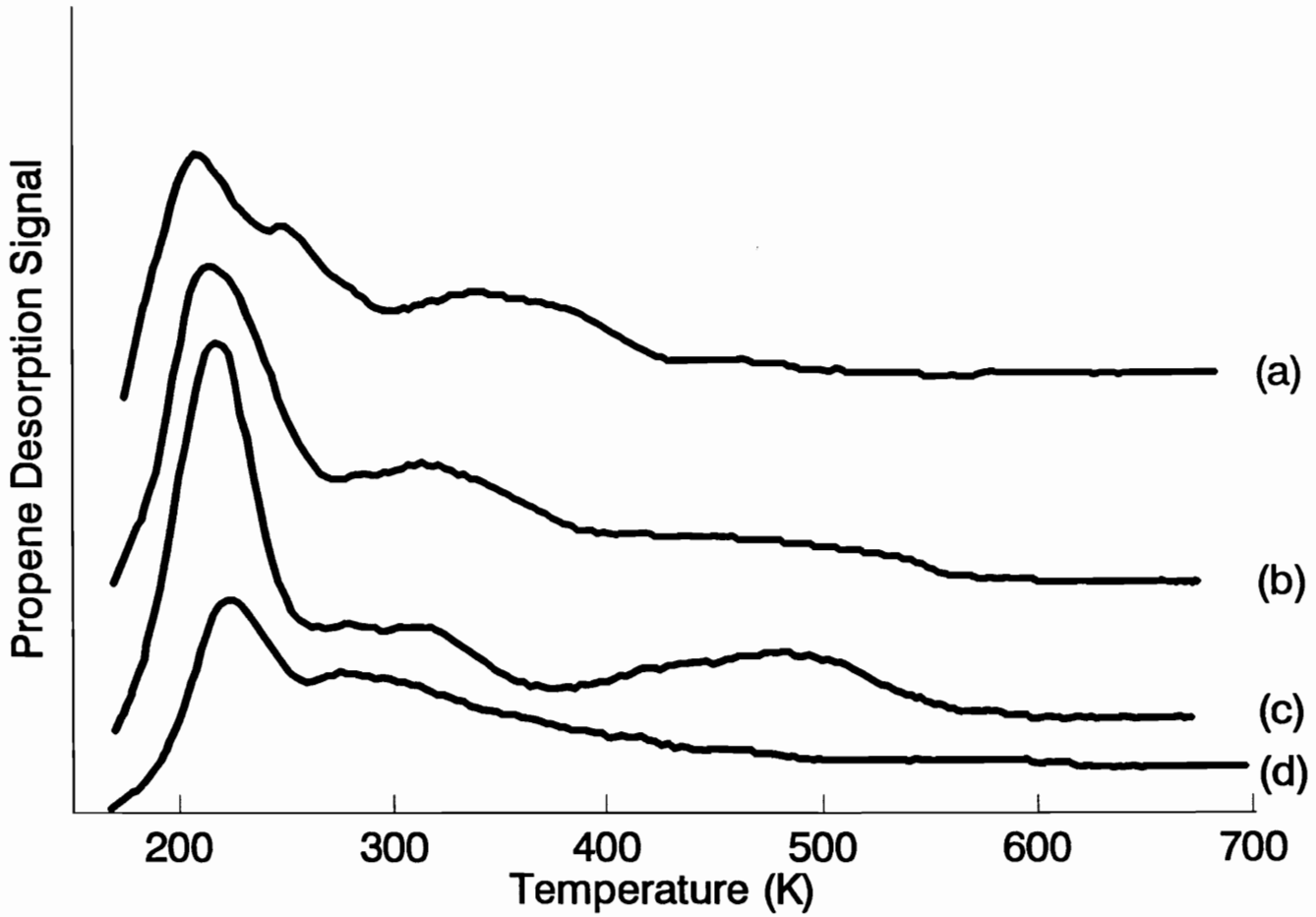

Fig. 6.1 Thermal desorption spectra following 0.3 L propene doses at 170 K on: (a) the stoichiometric surface, (b) the reduced surface, (c) the less-defective surface and (d) the highly-defective surface.

K to remove bridging oxygen anions and introduce in-plane oxygen vacancies. This treatment is estimated to leave about 80% of the original in-plane oxygen anions intact [22]. Figure 6.1d is characteristic of a highly-defective surface prepared by ion bombardment and annealing to 1000 K. This second preparation gives a surface which is more oxygen deficient than the first [23,24], and is estimated to leave about 50% of the original oxygen anions intact [22]. In both cases, 0.3 L doses at 170 K surface temperatures were used.

For the less-defective surface, three features can be seen in the propene desorption trace (Fig. 6.1c): a main peak at 220 K, a feature near 320 K and a broad feature centered at 465 K.

For the highly-defective surface (Fig. 6.1d), two features are apparent in the propene trace (Fig. 6.1d): one at 225 K and one with a maximum at 290 K, extending to about 450 K.

6.4 Discussion

Propene TDS shows clear surface dependent behavior. Propene seen desorbing at 210-225 K on all the surfaces is assigned to a molecular species due to the low temperature. Schulz and Cox [11] noted molecular propene desorption on the Cu_2O(111) surface at 150 K and on the (100) surface at 190 K, while Barteau and Madix [13] observed molecular propene desorption at 190 K and 205 K on the oxygen pre-dosed Ag(110) surface. Propene desorbing at 465 K on the less-defective surface and over the range 400-550 K on the reduced surface is assigned to desorption of a dissociated and recombined species based on the high

temperature. The high temperature propene state is largest on the less-defective surface. One dissociated intermediate suggested is an allylic surface species. This appears to be a common dissociated propene species reported [11,12,14-16,25,26]; however, there is no evidence supporting a particular intermediate leading to the feature above 400 K. Due to the small amount of propene uptake on SnO_2(110) surfaces at the adsorption temperature which can be reached, available spectroscopies are not sensitive enough to use to determine the intermediate.

There is no evidence to determine whether propene desorbing between 250 K and 365 K is the result of molecular adsorption or dissociative adsorption. However, on Cu_2O(111) [11], propene desorbing at 260 K and 325 K was identified using D_2 co-adsorption as the result of a dissociated species undergoing recombination, while propene desorbing at 370 K on ZnO surfaces was attributed to recombination of an allyl and surface hydrogen. It is suggested tentatively that propene desorbing between 250 K and 365 K on SnO_2(110) is due to dissociative adsorption, but further study is needed.

The influence of the two types of oxygen vacancies which can be formed has been studied. The effect of bridging oxygen vacancies on the adsorption of propene with SnO_2(110) can be seen by comparing the stoichiometric and reduced surfaces. The stoichiometric surface ideally has no bridging oxygen vacancies, while the reduced surface ideally has no bridging oxygen available. The effect of the loss of bridging oxygen is to cause a decrease in the amount of propene desorbing at 250 K, and a decrease in the 365 K feature on the stoichiometric surface with a

corresponding increase in the 325 K on the reduced surface. It cannot be determined if this is due to one feature moving down in temperature or two features. The loss of bridging oxygen also causes some propene to dissociate, desorbing above 400 K.

A significant increase in the extent of dissociation at 465 K is seen on going from the reduced surface to the less-defective surface. Apparently, the presence of a *limited* number of in-plane oxygen vacancies promotes dissociation and the propene desorption state at 465 K can be associated with low coordination cations near in-plane oxygen vacancies. A very similar effect was seen for H_2O dissociation [29]. On going from a less-defective surface to a highly-defective surface, a considerable decrease in the amount of high temperature propene is seen. The increasing concentration of in-plane oxygen vacancies on the highly-defective surface decreases the dissociation probability, as observed with other adsorbates on SnO_2 [27-30].

These preliminary results were undertaken to provide desorption-limited behavior to compare to isopropanol reaction products [30], to test the defect sensitivity of propene adsorption and because of the general interest in oxidation processes on SnO_2(110). Propene oxidation has undergone considerable study. The search for a catalyst with high activity and selectivity for selective oxidation products has taken researchers through many metal/metal oxide combinations. Tin oxide as a single component has both low activity and low selectivity [17], though when used in a mixture of otherwise fairly inactive metal oxides [1], the activity and selectivity increase dramatically.

Single crystal studies of propene adsorption are few in number. In one study done by Barteau and Madix [13], propene only adsorbed molecularly on clean Ag(110), but with pre-adsorbed oxygen on the surface [13], propene was oxidized to CO_2, water and surface carbon. An allylic intermediate was proposed, but there was no direct spectroscopic evidence for the formation of this intermediate. Propene oxidation was also studied on Cu_2O(100) and (111) surfaces [11]. Only molecular adsorption was observed on Cu_2O(100), while on Cu_2O(111), CO was formed; propene dissociation occurred around oxygen vacancies, similar to what is observed for SnO_2. Propene adsorbed on ZnO single crystal surfaces [12] desorbed at 370 K, with no reaction observed, though this desorption feature was assigned to recombination of a surface allyl and hydrogen.

6.5 Conclusions

The desorption behavior of propene on SnO_2(110) surfaces is dependent on the surface condition. Molecular propene desorption occurs at 210-225 K, while propene desorption attributed to recombination of a dissociated species and surface hydrogen occurs at 465 K. No identification of a surface species could be made for propene desorbing from 250 K to 365 K, though it is suggested that it is also due to recombination.

6.6. References

1. D.J. Hucknall, Selective Oxidation of Hydrocarbons, (Academic Press, New York, 1974).

2. G.W. Keulks, L.D. Krenze and T.M. Notermann, *Adv. Catal.*, **27**(1978)183.

3. G.W. Hearne and M.L. Adams, U.S. Patent 2,451,485 (1948).

4. C.R. Adams, *Chemy Ind.*, **52**(1970)1644.

5. J.D. Idol, Jr., U.S. Patent 2,904,580 (1959).

6. J.L. Callahan, R.W. Foreman and F. Veatch, U.S. Patent 3,044,966 (1962).

7. T. Honda, H. Tanaka and I. Watanabe, Japan Patent 72 19,770 (1972).

8. P. Centola, C. Mazzocchia, G. Terzaghi and I. Pasquon, *Chimica Ind., Milano,* **54**(1972)859.

9. R. Hiatt, *Oxidation* **2**, R.L. Augustine, ed., (M. Dekker, New York, 1971) p. 113.

10. D.I. Metelitsa, *Usp. Khim.*, **41**(1972)1737.

11. K.H. Schulz and D.F. Cox, *Surf. Sci.*, **262**(1992)318.

12. K. Lui, S. Akhter and H.H. Kung, *Solid State Chemistry in Catalysis,* **12**(1985)206.

13. M.A. Barteau and R.J. Madix, *J. Am. Chem. Soc.*, **105**(1983)344.

14. S.T. Oyama, *Bull. Chem. Soc. Jpn.*, **61**(1988)2595.

15. A.L. Dent and R.J. Kokes, *J. Am. Chem. Soc.*, **92**(1970)6709,6718.

16. B.L. Kugler and R.J. Kokes, *J. Catal.*, **32**(1974)170.

17. V. Fattore, Z.A. Fuhrman, G. Manara and B. Notari, *J. Catal.*, **37**(1975)215.

18. S. Tan, Y. Moro-oka and A. Ozaki, *J. Catal.*, **17**(1970)125,132.

19. J. Buiten, *J. Catal.*, **10**(1968)188.

20. V.I. Lazukin, M.Y. Rubanik, Y.V. Zhigailo, A.A. Kurganov and Z.F. Buteiko, *Katal. Katal., Akad. Nauk. SSR, Resp. Mezhvedom. Sb.*, **No. 2**(1966)50.

21. The ion gauge sensitivity for propene was taken as 3.28. This ion gauge sensitivity was calculated using a correlation by S. George for hydrocarbons and alkyl chlorides reported in R.L. Brainard and R.J. Madix, *J. Am. Chem. Soc.,* **111**(1989)3826.

22. An upper limit estimate of the in-plane oxygen vacancy density was made using the reaction $CH_3OH + O(l) \rightarrow CH_2O + H_2O$. This relationship assumes that each molecule of methanol converted to formaldehyde extracts one in-plane oxygen anion. Assuming a unity sticking coefficient for methanol, the density of in-plane oxygen defects introduced by successive 0.6 L doses of methanol was calculated and used as a reference. Formaldehyde desorption from the reaction of methanol with the less-defective and highly-defective surfaces were compared to desorption from the reference experiments to estimate the defect density on each surface. Further details of the calculation can be found in Ref. 29.

23. D.F. Cox, T.B. Fryberger and S. Semancik, *Phys. Rev. B,* **38**(1988)2072.

24. D.F. Cox, T.B. Fryberger and S. Semancik, *Surf. Sci.,* **224**(1989)121.

25. J.T. Roberts, R.J. Madix and W.W. Crew, *J. Catal.,* **141**(1993)300.

26. A.A. Davydov, V.G. Mikhaltchenko, V.D. Sokolovskii and G.K. Boreskov, *J. Catal.,* **55**(1978)299.

27. V.A. Gercher, D.F. Cox and J.-M. Themlin, *Surf. Sci.,* **306**(1994)279.

28. V.A. Gercher and D.F. Cox, *Surf. Sci.,* **312**(1994)106.

29. V.A. Gercher and D.F. Cox, *Surf. Sci.,* **SUBMITTED.**

30. V.A. Gercher and D.F. Cox, *J. Phys. Chem.,* **MANUSCRIPT IN PREPARATION.**

Chapter 7

Summary and Recommendations for Future Work

7.1 Summary

The reactions of a variety of molecules have been studied on SnO_2(110) stoichiometric and defective surfaces. The methanol study showed that the oxidation of methanol is completely selective to formaldehyde in TDS. Starting with a stoichiometric surface, the conversion first increases then passes through a maximum as the surface becomes more oxygen deficient. Two methoxide decomposition channels were observed, one associated with four-coordinate Sn^{2+} cations at bridging oxygen vacancies, and the second associated with lower-coordination cations sites at in-plane oxygen vacancies.

The formic acid study showed that the extent of dissociation to formate had an apparent linear dependence on the density of in-plane oxygen anions. The activity was a maximum on the stoichiometric surface and decreased as the surface became more oxygen deficient. Two formate decomposition channels were observed, one producing CO and H_2CO at cations associated with in-plane oxygen vacancies, and the second producing CO_2 at cations away from in-plane oxygen vacancies.

The adsorption of water resulted in water desorption from molecular species and recombination of dissociated species (due to OH disproportionation). The amount of dissociation was similar on all surfaces except the less-defective surface, which showed a significant increase in dissociation. Dissociation appeared was promoted in the presence of a

limited number of in-plane defects. No conclusion was reached as to which type of cation caused dissociation on the stoichiometric and reduced surfaces.

The isopropanol study showed that isopropanol reacted in three channels. Two channels were isopropoxide decomposition channels, forming acetone and propene in a ratio of about 2.5. The reactivity and kinetics showed similar trends as those observed with methanol oxidation to formaldehyde. Again, one channel was associated with Sn^{2+} cations at bridging oxygen vacancies, and the second was associated with lower-coordination cations at in-plane oxygen vacancies. A third isopropanol reaction channel was observed to form propene; isopropyl was the suggested intermediate, reacting at five-coordinate Sn^{4+} cations. The overall activity went through a maximum on the reduced surface, and was lowest on the highly-defective surface. No propene was observed desorbing from the highly-defective surface.

The preliminary propene adsorption study indicated that propene desorbed from molecular and recombined dissociated species. The high temperature dissociated species appeared to be associated with cations at in-plane oxygen vacancies, though dissociation decreased as the in-plane vacancy concentration increased.

Several overall conclusions can be drawn from the work presented in this dissertation. Much of the work done utilized acid/base concepts to explain the results. It can be seen that the reactions of adsorbates on SnO_2(110) surfaces can be correlated to a certain extent with the adsorbate acid strength in aqueous solution. The site requirement for

Brønsted acid dissociation is considered to be an acid/base site pair. The extent of dissociation of Brønsted acids on SnO_2(110) is dependent on the strength of the acid and also on the surface being considered. The conclusion reached was that the conversion observed for each molecule was dependent on the extent of dissociation on each surface.

While the most active surface varied from molecule to molecule, the least active surface was always the highly-defective surface. While studies from other researchers have shown that defects generally increase reactivity significantly [1], no other studies are known where the most defective surface which can be prepared is the least active. What causes this behavior of the highly-defective surface is not understood. However, most other single crystal studies have been performed on transition metal oxides, while Sn has a d^{10} configuration.

The hard/soft acid/base idea was used to try to understand isopropanol reactivity on SnO_2(110), and can be applied to the general reaction of oxygenates on these surfaces. The Sn^{4+} cation is considered a hard acid, while the Sn^{2+} cation is considered a borderline (between hard and soft) acid. Oxygenated hydrocarbons anions such as alkoxides and formates are considered hard bases, as are aldehydes, ketones and hydroxyl groups. From this, it would be expected that oxygenates would react preferentially with Sn^{4+} cations. The results for propene formation from isopropanol and the reaction of formic acid were consistent with this idea, but the results for alkoxide decomposition and water and propene adsorption contradicted it. Alkoxides do not react with Sn^{4+} preferentially; their decomposition appears to be the result of interaction

with Sn^{2+} cations. The formation of propene from isopropanol (dehydration - considered an acid-catalyzed process) at Sn^{4+} sites is consistent with these sites being fairly acidic. However, acetone (major product) and propene were both formed at Sn^{2+} sites with a dehydrogenation/dehydration ratio of 2.5. Sn^{2+} sites are less acidic than the Sn^{4+} sites, but they are still acidic. Generally, what causes the dehydrogenation/dehydration selectivity for a given site is not understood.

The interaction of formic acid with SnO_2(110) was explained using oxidation/reduction concepts; reduced surface sites near in-plane oxygen vacancies tend to dehydrogenate and deoxygenate formate to form CO and H_2CO to reoxidize themselves rather than merely dehydrogenating formate to form CO_2 as less reduced sites do. However, the trend observed for formate decomposition, that the dehydrogenation/dehydration ratio decreased as the surface became more oxygen deficient, is the opposite seen for isopropanol, and the opposite expected using acid/base concepts.

Several general conclusions can be drawn from this work. The two types of oxygen vacancies that can be introduced do influence surface reactions, by decreasing the density of oxygen available to interact with adsorbates and by decreasing associated cation coordination. For the strong Brønsted acid formic acid, introducing in-plane oxygen vacancies causes a decrease in reactivity, while for weaker Brønsted acids, a given density of vacancies (dependent on the adsorbate being considered) increases reactivity up to a certain point after which increasing densities decrease reactivity (again dependent on the adsorbate). This results in the

highly-defective surface being the least active.

An important idea in understanding reactions of adsorbates on surfaces is the necessary site requirements for dissociation of molecules. The generally accepted site requirement is a coordinatively-unsaturated cation and an available anion [2]. All the work done so far on SnO_2(110) surfaces indicates that while this site requirement may be a necessary condition for the dissociation of Brønsted acids , it is not a sufficient condition, as illustrated by the relative lack of activity on the highly-defective surface. Other factors such as the local defect environment and the adsorbate being studied also influence activity of the surfaces.

7.2 Recommendations for Future Work

Further work with propene adsorption to clarify the presence or absence of oxidation products is necessary. A new preparation and oxidation procedure must be developed in order to distinguish between CO and CO_2 being formed on the sample and on the hardware. Co-adsorption of propene with atomic deuterium would be useful to determine at what temperatures dissociated propene desorbs.

Repetition of these experiments using IR to characterize the surface intermediates would be useful. Also suggested is the use of labelled oxygen to oxidize the surface so that the source of oxygen in products can be determined, which would also strengthen the identification of rate-limiting steps.

These studies suggest several possibilities for future adsorbates.

Adsorption of another primary alcohol such as ethanol would provide a comparison to the methanol data. Adsorption of a tertiary alcohol such as t-butanol would provide more information on reaction pathways that do not involve hydride elimination from carbon α to oxygen in alkoxides, such as that suggested for propene formation from an isopropyl species after isopropanol adsorption. Further study of acetone adsorption is also indicated. And as most of the work so far has been done with Brønsted acids, studies using bases would provide additional information about the acid/base properties of the surfaces.

7.3 References

1. V.E. Henrich, *Reports on Progress in Physics,* **48**(1985) 1481.
2. M.A. Barteau, *J. Vac. Sci. Technol,* **11**(1993) 2162.

Appendix 1 Mass Spectrometer Sensitivity

All desorption traces have been corrected for the mass spectrometer sensitivity. This appendix describes the methods used to calculate the sensitivity factors for each mass fragment and the mass fragments used for each molecule. The Redhead equation [1] used to calculate activation energies is also described. The TDS data is reported as desorption signal vs. temperature, but the signals all have been corrected, making them proportional to the number of molecules.

The mass spectrometer sensitivity factor was calculated using two methods. The first method uses an equation described in the Inficon Quadrex 200 manual [2], where the partial pressure of substance "A" indicated by the amplitude (I) of signal at mass "B" is:

$$PP_A = (I_{AB} \times FF_{N28})/(FF_{AB} \times IGS \times TF_B \times DF_{AB} \times S) = I_{AB} \times (mssf).$$

PP_A = partial pressure of a given substance "A" in a gas mixture in mTorr

I_{AB} = current output of the Quadrex 200 sensor, signal amplitude of a mass peak "B" resulting from substance "A"

FF_{N28} = fragmentation factor for N_2^+ ions from nitrogen (typically .90 to .95, often taken as 1)

FF_{AB} = fragmentation factor, fraction of total ions from substance "A" having mass "B" (from Table 4.1 of manual)

IGS = ion gauge sensitivity, relative yield of ions from substance "A" compared to nitrogen at the same partial pressure (from Table 4.2 of manual)

TF_B = transmission factor, the number of ions of mass "B" that pass through the analyzer, relative to ions of mass 28 = 28/mass "B"

(nominal)

DF_{AB} = detection factor, the relative current per ion at mass "B" compared to nitrogen ions at mass 28 ≅ 1 for Quadrex 200

S = sensitivity for nitrogen, output current (at mass 28) per unit absolute pressure for pure nitrogen in amp/Torr ≅ 1 for Quadrex 200

Therefore, mssf = $1/(FF_{AB}$xIGSx28/mass"B"). This method was used to find the mssf for methanol (using mass fragment 31, mssf = 1.43), formaldehyde (using mass fragment 29, mssf = 1.41), CO (using mass fragment 28, mssf = 1.05), CO_2 (using mass fragment 44, mssf = 1.32) and water (using mass fragment 18, mssf = 0.857). The 29 m/z mass fragment for formaldehyde has a contribution from methanol, which was subtracted before applying the mssf.

A second method was used to calculate the mssf, both to check the factors found by the first method, and because fragmentation data was not available for some of the molecules studied. The second method used was as follows. The pressure dependence of the amplitude of a given mass fragment for each substance was found. The amplitude of the mass fragment was then plotted vs. the corrected pressure (corrected for IGS). Then, the slope of the plotted line was found. The mssf = 1/slope. For some of the molecules, the fragmentation patterns used in this method were pressure dependent, resulting in non-linear plots; therefore, a range of mssf's was calculated. These values were compared to those calculated by the first method when available; the range encompassed the values calculated by the first method. When mssf's were not available

through the first method, the mssf was chosen using an mssf which corresponded to the range of dosing pressures used. This method was used for formic acid (using mass fragment 46, mssf = 3.52), isopropanol (using mass fragment 45, mssf = 0.55), acetone (using mass fragment 58, mssf = 2.4) and propene (using mass fragment 41, mssf = 1.7). The 58 m/z mass fragment for acetone and the 41 m/z mass fragment for propene both have a contribution from isopropanol, which was subtracted before applying the mssf.

The Redhead equation [1] is used to find the activation energy of first- and second-order processes. These equations are derived from a material balance done on a desorption system in which gas is leaked in at a constant rate and is pumped out at a constant speed, to find an equation describing the desorption rate from a sample as dependent on pressure, time and the characteristic pumping time. When either the desorption cycle is short compared to the characteristic pumping time, or the pumping speed is very high, the desorption rate as a function of sample temperature is proportional to the desorption signals. This assumes that no re-adsorption on the sample occurs during the desorption cycle, a valid assumption for the pumping speed and desorption cycle length used in the TDS experiments. Then, the temperature at which the maximum desorption rate occurs can be used to solve for the activation energy. The equation for first-order processes is as follows:

$$E = R \times T_p \times [\ln(v_1 \times T_p / \beta) - 3.64]$$

R = gas constant

T_p = temperature at which the desorption rate is a maximum

v_1 = pre-exponential

ß = sample heating rate = 2 K/s.

The equation assumes that E and T_p are independent of coverage and fixed. v_1 can be found by varying ß and plotting log T_p vs. log ß ; however, the low value of ß necessary to avoid fracturing the sample does not allow much variation, so a value of 10^{13}/sec is assumed for v_1 (as in the Redhead paper).

The process to calculate second-order activation energies is as follows: plot log (σ_o xT_p^2) vs. $1/T_p$, where σ_o = coverage = the area under the desorption curve. If a straight line is found, the process is second-order and the slope = E/R. It is assumed that E is independent of coverage and fixed.

References

1. P.A. Redhead, *Vacuum,* **12**(1962)203.

2. Inficon Quadrex 200 manual

VITA

Victoria Ann Gercher, daughter of John W. and Katherine Gercher, was born on March 15, 1968, in Northridge, CA. She graduated as valedictorian from Ligonier Valley Senior High School, Ligonier, PA, in 1986, and *cum laude* with a B.S. in Chemical Engineering from the University of Pittsburgh, Pittsburgh, PA, in 1990. She then started work on a Ph.D. in Chemical Engineering at Virginia Polytechnic Institute and State University, which she finished in August, 1994.